Experimental properties of superfluid ^{3}He *

John C. Wheatley

Department of Physics, University of California at San Diego, La Jolla, California 92037

This paper presents a summary and evaluation of the experimental properties of superfluid ^{3}He as they were known in the fall of 1974. Subjects having thermodynamic significance, including specific heat, static magnetism, phase equilibria, and superfluid density, are discussed first. Then known flow properties are treated. After a brief discussion of the theoretical ideas which motivated some of the later experiments, the subject of dynamic magnetism is reviewed. Closely related work in a magnetic field in the immediate temperature region of the critical temperature is discussed, as are the propagation of ultrasound, the phenomena of supercooling and superheating, precise indication of the critical temperature, and the effects of certain restrictive geometries. The article concludes with a brief discussion of some new developments which appeared after the main text was finished. Appendices on thermometry and on parameters of the normal Fermi liquid are included.

CONTENTS

I. INTRODUCTION TO THE NEW PHASES OF LIQUID ^{3}He

Experimental work on liquid ^{3}He as a substance possibly described by Landau's (1956) theory of a Fermi liquid was still in its infancy when it was suggested by Pitaevski (1959); Brueckner, Soda, Anderson, and Morel (1960); and Emery and Sessler (1960) that a BCS-like pairing transition to an ordered state might take place in ^{3}He. Estimates of the critical temperature T_c for this transition placed it somewhat below the lower limt (≈ 0.1 K) of then existing experimental data. If the transition occurred at all it was suggested that the ordered pairs would be in states of relative orbital angular momentum greater than zero; a relative D state was suggested from detailed calculations. The fluid might then be expected to exhibit anisotropic properties. Some of the properties of such fluids were

worked out by Anderson and Morel (1961); and, for pairs in a relative P wave, by Balian and Werthamer (1963).

All of these exciting new theoretical ideas, starting with those of Landau on the normal rather than the superfluid Fermi liquid, proved to be a fine motivation for experimental work. The technology for achieving lower and lower ^{3}He temperatures through multistage adiabatic demagnetizational cooling improved rather rapidly. The lower temperature limit of measurements decreased substantially while the number, diversity, and quality of these measurements increased. Then Peshkov (1964) performed heat capacity experiments on a mixture of powdered CMN (Cerous Magnesium Nitrate) and low pressure liquid ^{3}He from which he derived a ^{3}He heat capacity that had a rather broad bump at near 5 mK, *on a magnetic temperature scale*, and then decreased rather rapidly at lower temperatures. Although Peshkov suggested that he had observed the superfluid transition, this conclusion was contested by the author and his colleagues, who had recently completed similar measurements and had not observed any extraordinary effects. Subsequently (Wheatley, 1966) it was suggested that Peshkov's effect was a manifestation of a not uncommon defect of specific heat measurements in which some of the heat Q added in a measurement escapes the sample so that the measured temperature difference ΔT is too small. The *calculated* heat capacity $Q/\Delta T$ is then too high. If the spuriously lost heat has a maximum at some temperature, then this will be reflected as a maximum in calculated heat capacity. The possibility of such a maximum does exist as a result of an unexpected minimum as a function of temperature in the thermal diffusivity of a CMN–^{3}He mixture, reflecting a linear temperature dependence of the thermal resistance coupling the CMN and liquid ^{3}He. It was not until later (Wheatley, 1968; Leggett and Vuorio, 1970) that it was realized that this linear thermal resistance was not the ^{3}He itself but rather a surface magnetic thermal resistance coupling the electronic moments in the CMN to the nuclear moments in the ^{3}He. So although Peshkov had not found superfluidity in liquid ^{3}He he had in fact discovered one of the most important very low temperature phenomena: an effective means of establishing thermal equilibrium between a magnetic substrate and liquid ^{3}He.

After Peshkov's work there was still a high level of activity in liquid ^{3}He but the lower temperature limit of the experi-

ments had bottomed out at several millikelvin. In the late sixties and early seventies scientific measurements on pure ^{3}He and dilute solutions of ^{3}He in superfluid ^{4}He at very low temperatures went on in parallel with very significant technical developments in dilution refrigeration, in the adiabatic compressional cooling method, in nuclear refrigeration, in thermometry, and in new methods of measurement. The dilution refrigerator provided a thermal reservoir at 10 to 15 mK which served as a base for further reduction of temperature by the other cooling methods, which now could be applied much more effectively. The stage was thus set for the discovery by Osheroff, Richardson, and Lee (1972a) of two distinctive features, called "A" and "B" and occurring below 3 mK, on the pressurization curve (pressure vs time) of liquid ^{3}He in equilibrium with solid ^{3}He at nearly 34.4 bar in a compressional cooling cell. Although they originally interpreted these features in terms of effects in the solid, where nuclear spin ordering had been expected, they soon performed nuclear magnetic resonance experiments (Osheroff, Gully, Richardson, and Lee, 1972b) showing that the A and B features were associated with dynamic magnetic effects in the *liquid*. Johnson, Paulson, Pierce, and Wheatley (1973) showed that the A feature was *not* due to thermal changes in the solid; Webb, Greytak, Johnson, and Wheatley (1973b) found a line in the P–T plane of Ehrenfest type second-order transitions in the bulk liquid off the melting curve; and Alvesalo, Anufriyev, Collan, Lounasmaa, and Wennerstrom (1973) showed in experiments at melting pressure that the motion of a vibrating wire was dramatically altered at both the A and B features, indicating major changes in flow properties. These and subsequent experimental developments over the past two years are the subject of the present article. Prior experimental reviews have been given by Wheatley (1973) and Lounasmaa (1974).

Since the companion article by A. J. Leggett covers theoretical matters, the present point of view will be primarily experimental. Such subjects as specific heat and static magnetism will be introduced without detailed theoretical discussion. On the other hand, where the *motivation* for the experiments or the interpretation of the measurements draws heavily on theoretical concepts, as is particularly true in the case of dynamic magnetism, enough theoretical background will be given to assist in comprehension of the experiments.

The organization of this article is as follows. Subjects having thermodynamic significance, where little new theoretical motivation was needed, will be discussed first. These include specific heat, static magnetism, phase equilibria, and superfluid density. Then, known flow properties, closely related to the concepts of superfluid and normal fluid density, will be treated. Next, including a brief discussion of theoretical ideas which motivated some of the later experiments, the subject of dynamic magnetism, which is so important for building a microscopic understanding of the new phases, will be reviewed. This will be followed by discussion of closely related work in a magnetic field in the immediate temperature region of the critical temperature and of such subjects as the propagation of ultrasound, the phenomena of supercooling and superheating, the precise indication of the critical temperature, and the effects of certain restrictive geometries. The article is concluded by a brief discussion of some new developments which appeared after the main text was finished and by a critical summary of what the experiments have established to date. Appendices on thermometry and on parameters of the normal Fermi liquid are included.

Insofar as it is currently known the phase diagram of liquid ^{3}He on a pressure–temperature plane is shown in Fig. 1 (Greytak, Johnson, Paulson, and Wheatley, 1973; Ahonen, Haikala, Krusius, and Lounasmaa, 1974b; Halperin, Rasmussen, Archie, and Richardson, 1974b). The temperature scale is a provisional absolute scale (see Appendix A). Since ^{3}He has nuclear spin 1/2 and a magnetic moment, it is not surprising that the phase diagram is affected by a magnetic field. What is surprising is that the phase diagram is profoundly influenced by a magnetic field, particularly near the point labeled PCP. In zero field the line T_c is a line of second-order transitions in the Ehrenfest sense: there is a discontinuity but not a divergence in the specific heat (Webb, Greytak, Johnson, and Wheatley, 1973b). This line presumably intersects the melting curve at the temperature of the A feature discovered by Osheroff, Richardson, and Lee (1972a). In a magnetic field the transition T_c is split into two transitions with temperatures T_{c1} and T_{c2} (Gully, Osheroff, Lawson, Richardson, and Lee, 1973) and with splitting $T_{c1} - T_{c2}$ proportional to the field. In zero field $T_{c1} = T_{c2} = T_c$. The line T_{AB} is a line of first-order transitions presumably terminating in zero field on the line of second-order transitions T_c at a polycritical point (Greytak, Johnson, Paulson, and Wheatley, 1973; Paulson, Johnson, and Wheatley, 1973b). But in a moderate magnetic field the line T_{AB} does not intersect the T_c line (Paulson, Kojima, and Wheatley, 1974a). Even in small magnetic fields details of the T_{AB} line are not known near the PCP (Kleinberg, Paulson, Webb, and Wheatley, 1974). It is thought that the AB line intersects the melting curve at the location of the B' transition of Osheroff, Richardson, and Lee (1972a).

For temperatures above T_{c1}, ^{3}He is a normal Fermi liquid. Between T_{c1} and T_{c2} the fluid is called ^{3}He-A_1. Between the lines T_{c2} and T_{AB} is a phase called ^{3}He-A. For a field of 378 G it is not possible to distinguish T_{c1} and T_{c2} on the scale of this diagram. The ^{3}He-A phase is superfluid with superfluid density increasing from zero as T falls below T_c (Kojima, Paulson, and Wheatley, 1974; Alvesalo, Anufriyev, Collan, Lounasmaa, and Wennerström, 1973; Alvesalo, Collan, Loponen, and Veuro, 1974a; Yanof and Reppy, 1974). The normal viscosity drops precipitously with decreasing T below T_c and then becomes relatively temperature-independent (Alvesalo *et al.*, 1974a,b). The attenuation of zero sound suddenly increases at T_c, rises to a peak, and then falls rapidly as T decreases (Lawson, Gully, Goldstein, Richardson, and Lee, 1973; Paulson, Johnson, and Wheatley, 1973a). Furthermore, heat flows hydrodynamically as for a two-fluid model but with low critical velocity (Greytak, Johnson, Paulson, and Wheatley, 1973). The magnetic properties of ^{3}He-A are particularly interesting. The perpendicular nuclear magnetic resonance frequency is shifted by a temperature-dependent amount (Osheroff, Gully, Richardson, and Lee, 1972b). Both parallel NMR (Osheroff and Brinkman, 1974; Bozler, Bernier, Gully, Richardson, and Lee, 1974) and its analog in the time domain, parallel ringing (Webb, Kleinberg, and Wheatley, 1974a), have been observed. However, parallel NMR is not observed while perpendicular NMR is altered in the ^{3}He-A_1 phase (Osheroff and Anderson, 1974).
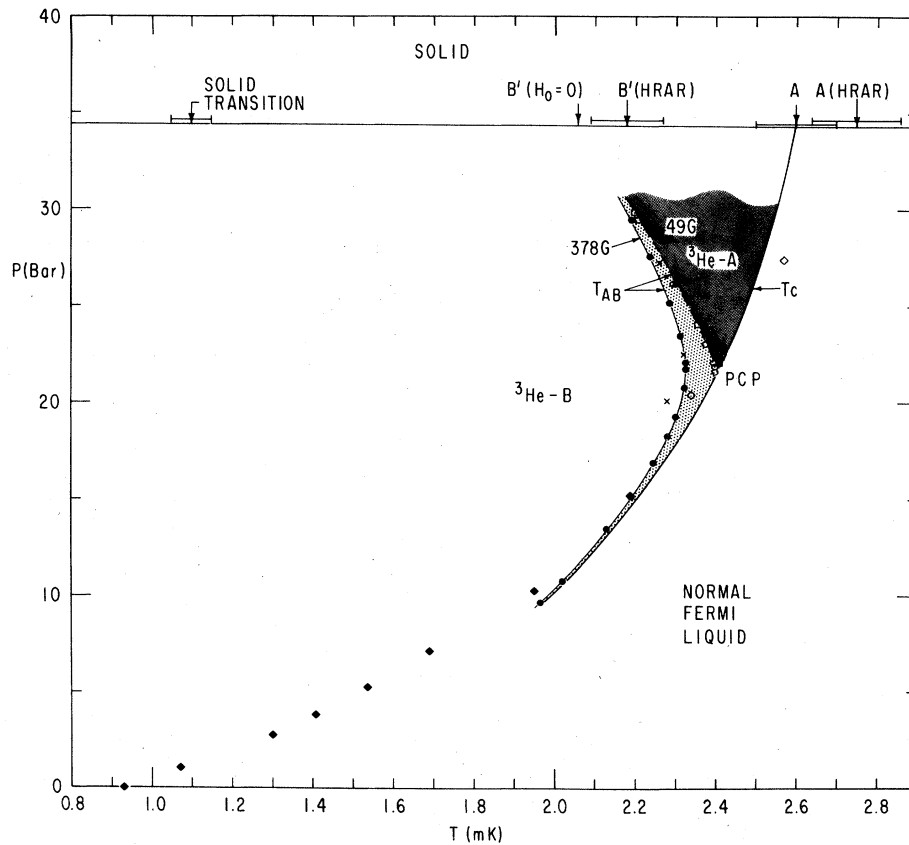
FIG. 1.   Phase diagram of ³He in the low millikelvin temperature region using provisional absolute temperature scales. The line T_c is the second-order transition line as determined at La Jolla (Wheatley, 1973), Appendix A. The points (□) are magnetic $B \rightarrow A$ transitions at 49 G from Paulson, Johnson, and Wheatley (1973b). The points (O) are $B \rightarrow A$ transitions by heat flow in zero field from Greytak, Johnson, Paulson, and Wheatley (1973). The point labeled PCP is the approximate location of the polycritical point. The points ($\bullet$) are magnetic thermodynamic $A \rightarrow B$ transitions in 378 G by Paulson, Kojima, and Wheatley (1974a). The points ($\Diamond$) are second-order transitions observed by Ahonen et al. (1974b) while those labeled ($\blacklozenge$) are the average of T_c and T_{AB}. Points labeled X are observations of T_{AB} in 320 G by Ahonen et al. On the melting curve there are two points labeled A and two labeled B' (H_0 = 0). The point labeled A is the temperature obtained for the A feature on the pressurization curve using noise thermometry by Paulson, Johnson, and Wheatley (see Wheatley, 1973) while that labeled A (HRAR) is the temperature obtained by Halperin, Rasmussen, Archie, and Richardson (1974b) as discussed in Appendix A. Probable errors are shown as horizontal bars. The point labeled B' (H_0 = 0) is the calculated temperature of the B' feature based on T_A = 2.600 mK, the pressure displacement of the B' from the A feature, and the reduced temperature scale of Halperin et al. (1974b). The point labeled B' (H_0 = 0) (HRAR) is the temperature of the B' feature according to Halperin et al. (1974b). The reduced temperature $T_{B'}/T_A$ = 0.792 is the same for both scales. The temperature labeled Solid Transition (HRAR) is the critical temperature according to the measurements of Halperin et al. (1974b) at which the solid entropy drops rapidly, as discovered by Halperin et al. (1974a).

Below the line T_{AB} the liquid is called ³He-B. It shares many of the properties of the A phase in a qualitative sense. However, it differs from the A phase particularly in its magnetic properties. While the A phase magnetism is temperature independent and nearly the same as the normal liquid, both the static magnetism (Paulson, Johnson, and Wheatley, 1973b) and the dynamic susceptibility (Osheroff, Gully, Richardson, and Lee, 1972b; Ahonen, Haikala, Krusius, and Lounasmaa, 1974c) of the B phase decrease substantially with temperature. The perpendicular NMR line may not be shifted grossly but does have strange properties (Osheroff, Gully, Richardson, and Lee, 1972b). More recent measurements (Osheroff and Brinkman, 1974; Webb, Kleinberg, and Wheatley, 1974a; Osheroff, 1974) have shown additional interesting properties, some of which are associated with the effect of boundaries. Also, critical flow velocities are much higher in the B than in the A phase (Greytak, Johnson, Paulson, and Wheatley, 1973).

The above partial listing of properties shows that we are dealing with an extremely interesting physical system which will challenge both experimental and theoretical ingenuity for years to come. From the experimental standpoint just the technical side of the experiments is fascinating. Absolute thermometry, thermal equilibrium, thermal isolation, and refrigeration are all important problems. To provide a proper base for our discussion of experimental properties we will present briefly an example of each of the three types of experimental arrangement used to achieve the necessary low temperature. In all cases the apparatus shown is precooled by means of a dilution refrigerator.

The A and B features on the pressurization curve were first observed by Osheroff, Richardson, and Lee (1972a) in a compressional cooling cell like that shown in Fig. 2. The cooling method was suggested by Pomeranchuk (1950), tested by Anufriyev (1965) to about 20 mK, and then shown to be a powerful cooling method in the low mK
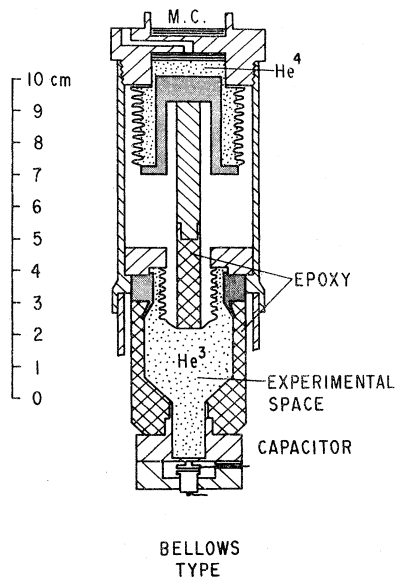
FIG. 2. Compressional cooling cell of the bellows type used by Osheroff, Richardson, and Lee (1972a) to cool ³He into the temperature region of the superfluid phases.
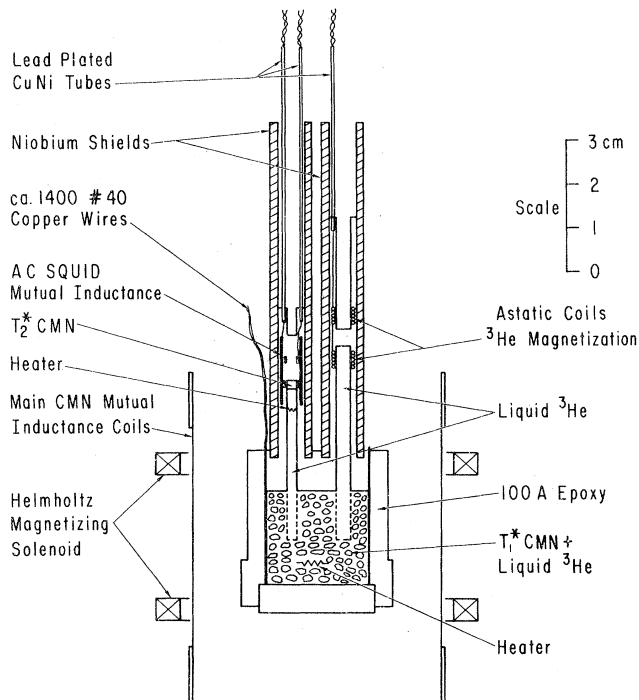

FIG. 3. CMN adiabatic demagnetization cell of the type used by Greytak, Johnson, Paulson, and Wheatley (1973) for heat flow measurements and by Paulson, Johnson, and Wheatley (1973b) for static nuclear magnetization measurements.

region by Johnson, Rosenbaum, Symko, and Wheatley (1969) and by Sites, Osheroff, Richardson, and Lee (1969). The cooling principle is simple: conversion of a low entropy to a high entropy phase of a pure substance produces refrigeration. In the present case the low entropy phase is translationally ordered liquid ³He, and the high entropy phase, spin disordered solid ³He. To convert liquid completely to solid requires about a 5% reduction in molar volume although very low temperatures may be achieved with a relatively smaller reduction. Conversion of liquid to solid takes place in a flexible-walled cell, a Cornell design using metal bellows being shown in Fig. 2. Reduction of frictional heating to a minimum is essential. A standard component of such a cell is a Straty–Adams (1969) capacitor which allows highly precise pressure (and thereby temperature) measurements. This accounts for measurements being plotted in terms of pressure differences from that of the A feature of Osheroff, Richardson, and Lee. A principal advantage of this cooling method for studies of liquid ³He is that the liquid is cooled directly via heat absorption at the solid–liquid interface so that thermal boundary resistance is not in the cooling path. A second advantage is that, since neither solid nor liquid entropy is strongly affected by magnetic fields of a size needed to show significant effects in the liquid, experiments in substantial magnetic fields (several thousand gauss) may be undertaken without impairment of the cooling process. Experiments of high precision in highly homogeneous magnetic fields may be performed under conditions of a stabilized temperature down to nearly 1 mK with secondary temperatures measured readily and well via pressure measurements. Furthermore, many cubic centimeters of liquid can be cooled with most of the liquid in a rather open geometry. An important disadvantage is that both solid and liquid are in the cell together. This led to the original conservative suggestion (Osheroff, Richardson, and Lee, 1972a) that the A and B features were a manifestation of solid effects, to difficulties in extracting information from NMR experiments owing to the much stronger magnetism of solid than liquid ³He, to premature failure of experiments to detect changes in flow

properties by observations of the damping of a vibrating wire, and to uncertainties as to the possible mutual effect of solid on liquid. It is certainly a tribute to the ingenuity of workers using this method that so many important measurements on the liquid have been made in spite of the presence in the cell of solid ³He. A second major disadvantage of this cooling method for liquid ³He measurements is that the pressure is confined to be melting pressure. It is now known that while this allows study of the A phase over the broadest temperature range, it does not permit study of the B phase near T_c, as may be seen on examining Fig. 1.

A second cooling technique is illustrated in Fig. 3, taken from Paulson (1974). In this time-honored method the liquid ³He is mixed with a powder of cerous magnesium nitrate (CMN), which provides cooling via the magnetocaloric effect. The cell is precooled to typically 12–15 mK in a field of ≈1000 G produced by the Helmholtz magnetizing solenoid. Following slow demagnetization, 2–3 cm³ of liquid ³He can be cooled below 2 mK with 15–20 g of CMN. Historically a principal advantage of this method is that no solid ³He need be present; this was important since in early experiments it was not yet certain that the A and B features reflected phenomena in the liquid. It is now known that ability to change the pressure over a wide range has contributed significantly to an understanding of the new phases. Although cooling by CMN does require heat transfer across a solid–liquid interface, it was discovered (Abel, Anderson, Black, and Wheatley, 1965) some time ago that the heat flow was much greater than expected. As we mentioned in a context of Peshkov's (1964) experiments, this was interpreted (Leggett and Vuorio, 1970) to be a

consequence of magnetic coupling between the CMN and ³He spins. This heat transfer property is of paramount importance to both CMN cooling/heating and CMN thermometry since it has provided in part the rapid thermal equilibrium essential to these very low temperature experiments. Ironically the ratio of powdered CMN to liquid ³He used by Webb et al. (1973b) in their experiments under pressure was almost the same as that used by Peshkov (1964) in his early experiments at zero pressure. We now know from the work of Ahonen et al. (1974b) that at zero pressure T_c is at 0.93 mK. The principal disadvantage of CMN is that temperatures which can be readily achieved with it are really not low enough. It has usually been assumed that a disadvantage is that moderately strong magnetic fields cannot be used. However, owing to the high heat conductivity of the ³He this disadvantage can be overcome, as in Fig. 3, by building appendices to the main cooling cell surrounded by superconducting tubes in which substantial fields may be either trapped or excluded. Fine control of the temperature of ³He in the appendices is obtained by adjusting a rather small field, generally less than 50 G, applied by the Helmholtz magnetizing solenoid to the main CMN cell.

A third cooling method is that of nuclear demagnetization. This method as applied to cooling ³He was first employed by Osgood and Goodkind (1967) but has recently been used very successfully by Ahonen, Haikala, Krusius, and Lounasmaa (1974a,b,c). An example of their nuclear demagnetization cell is shown in Fig. 4. Important keys to the success of this method have been the use of high purity copper wires connecting the cell to the source of nuclear refrigeration and their discovery that the thermal contact between sintered copper powder inside the ³He cell and the liquid ³He is very good. The latter probably is another manifestation of the magnetic coupling of energy, in this case between the ³He spins and localized moment impurities in the surface of the metal. This type of energy coupling from metals to ³He was observed by Bishop, Mota, and Wheatley (1974) in the case of impure platinum and then in Pd(Fe) and Au(Gd) by Avenel, Berglund, Gylling, Phillips, Vetleseter, and Vuorio (1973). As interpreted by Mills and Beál-Monod (1974), the temperature dependence of the magnetic thermal boundary resistance to normal liquid ³He can be expected for a magnetic alloy to vary as T above the ordering temperature of the alloy and as T^{-2} at temperatures sufficiently below the ordering temperature. Their theory seems to account for the existing results, where in the temperature region of interest the resistance probably varies as T^{-2}. Although the resistance does not actually decrease with decreasing T as for CMN, the temperature dependence of the thermal time constant with at least normal ³He will be relatively weak. To date there is very little experience with the nuclear cooling method, but if the thermal boundary resistance to samples of copper powder other than those tested is indeed as small as it has been in this early work, its application to ³He work should blossom.

II. SPECIFIC HEAT

Although some of the first measurements off the melting curve of the properties of the new phases of bulk liquid ³He were of specific heat (Webb, Greytak, Johnson, and Wheatley, 1973b), there has been little additional quantita-

MIXING CHAMBER
NO THERMOMETER
TIN HEAT SWITCH
INNER VACUUM JACKET
COPPER SUPPORT FRAME
³He CELL
NMR COILS
SINTERED COPPER POWDER
UPPER COMPENSATING COIL
SADDLE MAGNET
LOWER COMPENSATING COIL
OUTER VACUUM JACKET
LIQUID ⁴He BATH
MAGNET SUPPORT
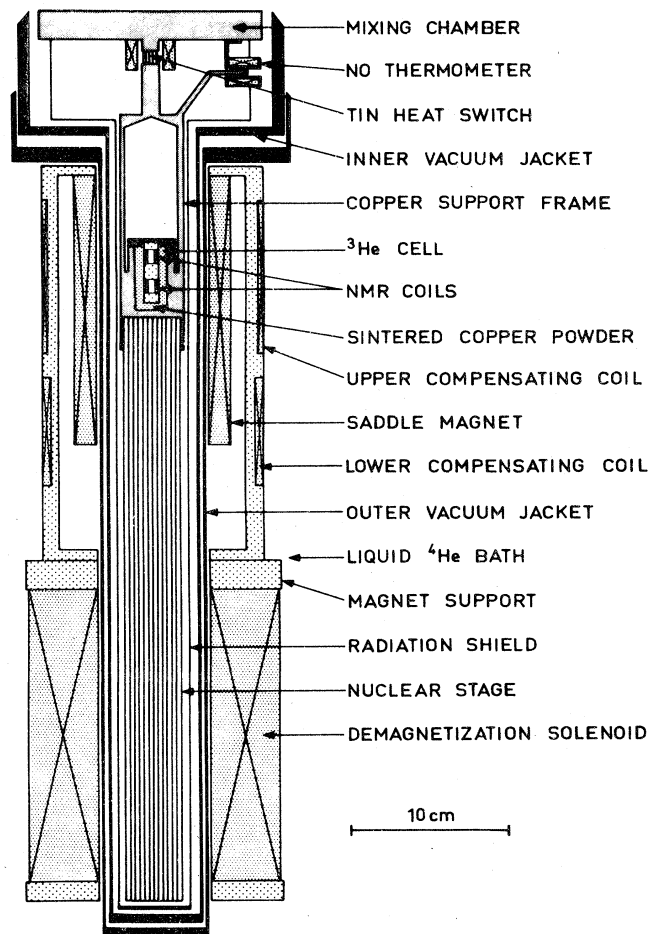RADIATION SHIELD
NUCLEAR STAGE
DEMAGNETIZATION SOLENOID

10 cm

FIG. 4. The nuclear adiabatic demagnetization apparatus of Ahonen, Haikala, Krusius, and Lounasmaa (1974b) used in achieving a ³He temperature of 0.7 mK.

tive work to this date. Two measurements of liquid specific heat have been reported at melting pressure (Anufriyev, Alvesalo, Collan, Opheim, and Wennerström, 1973; Halperin, Buhrman, and Richardson, 1973b). These are based in part on a suggestion by Vvedenskii (1972). The problems with measuring liquid specific heat off the melting curve have been twofold: (1) calorimeter background heat capacity is much larger than the heat capacity of the ³He itself, and (2) to measure heat capacity, small absolute temperature differences must be measured accurately, and the absolute temperature scale is uncertain in the present temperature range. Nevertheless precise observation of the second-order transition T_c as reflected in the discontinuity of liquid ³He heat capacity is now commonplace not only because all measurements should be referred to T_c but also because the (P_c, T_c) curve is now a basis for thermometry in the present temperature range just as ⁴He vapor pressure is at higher temperatures.

In the experiments of Webb et al. (1973b) the calorimeter was rather like Fig. 3, except that there were no appendixes to the cell, which was filled with powdered CMN to 84% of crystalline density. To get around the problem of calorimeter background heat capacity, measurements were made on the CMN magnetic temperature scale of the difference
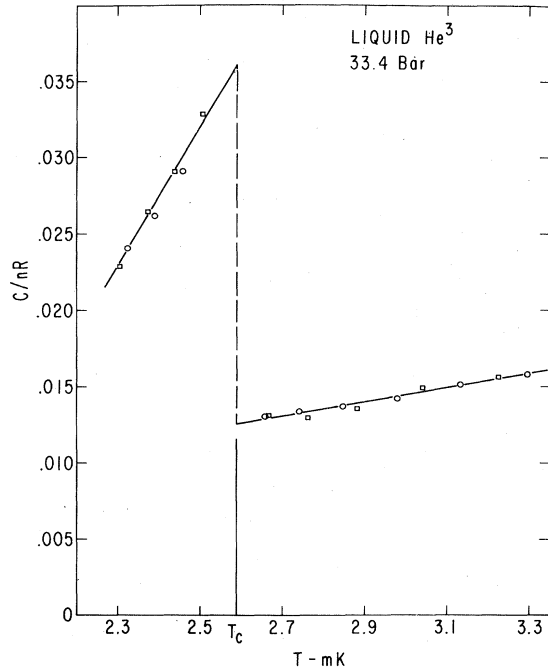
FIG. 5. Molar specific heat relative to the gas constant R for liquid ^{3}He at 33.4 bar near the second-order transition. (After Webb, Greytak, Johnson, and Wheatley, 1973b).

FIG. 6. Ratio $C_</C_>$ of the specific heat of liquid ^{3}He just below to just above the second-order transition as a function of pressure. P_m is melting pressure. (After Webb, Greytak, Johnson, and Wheatley, 1973b).

in the heat capacity between that at pressure P and that at a pressure of 0.13 bar. The *incremental* heat capacity of ^{3}He due to pressure was thus obtained. The total heat capacity could then be found by adding the known heat capacity of low pressure ^{3}He (Abel, Anderson, Black, and Wheatley, 1966) as extrapolated to lower temperatures. The temperature scale was then resolved provisionally (Wheatley, 1973) by taking the absolute temperature of the intersection of the T_c line with the melting curve as 2.600 mK and by assuming that heat capacity in the normal liquid is proportional to absolute temperature. The result for a pressure of 33.4 bar is shown in Fig. 5. The points on this graph are traditional specific heat data obtained from proper fore and after intervals separated by a period in which an accurate amount of heat is introduced. Measurements of this sort cannot be made very close to T_c since the ΔT required for necessary accuracy is too small. Near to T_c the system was allowed to drift under the constant residual heat leak. The time rate of change of temperature is then inversely proportional to the heat capacity. An example of such drift data is shown in Fig. 45. From drift data the ratio $C_</C_>$ of the heat capacity just below to that just above T_c was deduced. This ratio is not dependent on temperature scale. The value of $C_</C_>$ suggests that, although the transition is sharp, C/nR does not continue to rise steeply all the way to T_c but rounds off somewhat before T_c. Values of $C_</C_>$ as a function of pressure deduced by Webb *et al.* (1973b) are given in Fig. 6. As the pressure decreased and T_c decreased the heat capacity of ^{3}He relative to CMN decreased, so the precision of the measurement of $C_</C_>$ was degraded, thus accounting for absence of data at lower pressures.

In recent measurements by Halperin and others at Cornell (R. C. Richardson, private communication) the
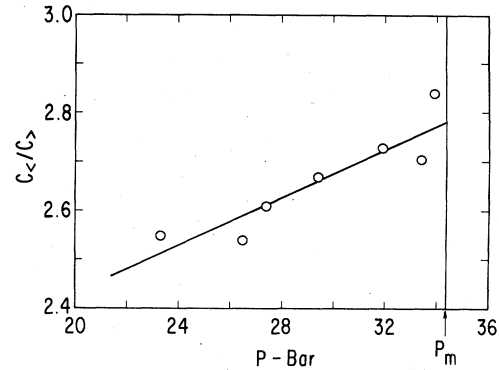
heat capacity of normal Fermi liquid at melting pressure was found to be about 10% lower than the value expected from the 27 atm measurements of Abel *et al.* (1966) above, while the discontinuity in specific heat at T_c was found to be about the same as measured by Webb *et al.* (1973b). This discrepancy emphasizes the already well-known need for specific heat measurements on normal liquid over a wide range of pressure. If indeed the normal liquid heat capacity is somewhat lower than that used to obtain $C_>$, then we can expect the ratio $C_</C_>$ on Fig. 6 to increase.

Several observations regarding the specific heat are in order. First of all, the data shown on Fig. 5 are in good agreement with specific heat data at melting pressure deduced by Halperin *et al.* (1973b), with exceptions as mentioned in the previous paragraph. This is important both because the value of $C_</C_>$ is larger than expected for weak coupling BCS-like theory (Anderson and Morel, 1961) and because measurements of heat capacity were made with the ^{3}He in the interstices of a packed powder of pore size less than 74 μ. In powder of smaller pore size, strange effects have been reported in specific heat (Dundon, Stolfa, and Goodkind, 1973) and magnetic properties (Ahonen, Haikala, and Krusius, 1974a,c), although in the latter case thermal properties seem not to have been grossly affected. However, from the favorable comparison with the melting pressure results one concludes that the thermal properties of the ^{3}He are not strongly affected by confinement in the pores of CMN. In another relevant observation shown in Fig. 46 ultrasonic attenuation *in bulk* as observed by Paulson, Johnson and Wheatley (1973a) is shown to experience nearly a discontinuity at T_c^*, the magnetic temperature equal to the center of the specific heat transition of ^{3}He in powder. Hence confinement of ^{3}He to the pores of the CMN powder shifts the second-order transition by less than a tenth of a percent in temperature. These are important observations with respect to the matter of fourth sound propagation in packed powders (Kojima, Paulson, and Wheatley, 1974; Yanof and Reppy, 1974).

As we indicate above, measurements of specific heat over the full pressure range are badly needed, both in the normal and superfluid states. In our opinion the most favorable approach to these measurements will be to use nuclear refrigeration to cool the ^{3}He. In this way the heat capacity

of the coolant can ultimately be "turned off" by reducing the field on it to a small value. Thermometry will still be a problem, though for the actual specific heat measurements an electronically paramagnetic secondary thermometer with a lower characteristic temperature than that of CMN might be used.

The value of $C_</C_>$ and its trend with pressure are both suggested at least qualitatively by the Brinkman–Anderson (1973) spin fluctuation theory of the fourth-order terms in a Ginzberg–Landau expansion of the free energy, where ^{3}He-A is taken to be the ABM state (Anderson and Brinkman, 1973b) and ^{3}He-B the BW state (Balian and Werthamer, 1963). This work has been extended and corrected by Brinkman, Serene, and Anderson (1974). In this theory $(C_< - C_>)/C_> = 1.43/f(\delta)$, where 1.43 is the BCS value (Bardeen, Cooper, and Schrieffer, 1957), and $f(\delta) = \frac{6}{5}(1 - \delta)$ for the ABM state, δ being a spin fluctuation parameter. [A more detailed discussion of the relevant thermodynamics is given in Sec. IX. We use here a definition of δ to agree with that of Takagi (1974a) which is just half that defined by Brinkman and Anderson (1973)]. The quantity δ was found by Osheroff and Anderson (1974) to be very nearly $\frac{1}{4}$ at melting pressure. Hence at melting pressure the value of $C_</C_>$ consistent with $\delta = \frac{1}{4}$ is 2.59, somewhat lower than the experimentally observed values (Fig. 6).

We note finally that all the specific heat measurements mentioned here for pressures less than melting pressure were obtained with the ^{3}He in the pores of CMN powder with a packing similar to that used in fourth sound measurements.

III. STATIC MAGNETIZATION AND PERPENDICULAR rf MAGNETIC SUSCEPTIBILITY

In this section we will discuss both the measurements of static magnetization, for which there now exist data over a wide range of pressure at temperatures rather close to T_c, and measurements of perpendicular rf magnetic susceptibility obtained in the course of NMR studies of the superfluid phases. We will begin with the static measurements, although discussion of the small static magnetic feature observed at the phase boundary between ^{3}He-A and normal liquid will be deferred to a later section.

The nuclear paramagnetism in liquid ^{3}He is so weak ($\chi_N < 1.1 \times 10^{-7}$) that until recently it has been studied entirely by resonance methods. It is now possible, however, to apply devices based on weak superconductivity to make both static and dynamic nuclear magnetic measurements with excellent sensitivity. A detailed discussion of the experimental methods as applied to the present sort of measurement problem has been given by Giffard, Webb, and Wheatley (1973). As it turns out there is abundant sensitivity, and the trick of the measurements is to suppress or avoid both the ever-present spurious magnetic "background" and effects of pressure on measurement geometry.

Static magnetic measurements in bulk ^{3}He have been reported by Halperin, Buhrman, Richardson, and Lee (1973a) at melting pressure and by Paulson, Johnson, and Wheatley (1973b) and Paulson, Kojima, and Wheatley (1974a) at a variety of lower pressures. In Fig. 3 is shown schematically a cell of the type used at La Jolla which can

be used for measurements of static magnetism. Two towers are built above a main cell containing powdered CMN. In the left tower, temperature measurements can be made with a thermometer consisting of, say, 15 mg of powdered CMN, whose magnetic temperature is sensed by a superconducting device. This tower is shielded by a Nb tube from the effect of field changes on the main CMN produced by the Helmholtz magnetizing solenoid. A field of less than a few tenths of a gauss is trapped in this tube. The right tower contains Nb coils in an astatic arrangement for sensing the flux due to the ^{3}He magnetization using a superconducting device. It too is surrounded by a Nb tube in which the measuring field H_0 is trapped. Temperature inhomogeneity need not be excessive in the superfluid state owing to the hydrodynamic flow of heat in bulk liquid (Greytak, Johnson, Paulson, and Wheatley, 1973). Typical values of H_0 have ranged from 50 to 500 G. In the higher fields the effect of pressure on the flux sensing circuit is extreme [more sensitive than a Straty–Adams (1969) pressure gauge], so care must be taken to keep the pressure constant. In such an apparatus there is also considerable spurious magnetism, apparently electronic in origin, which contributes significantly right down to the lowest temperature but which is suppressed in the strongest fields.

The most difficult measurement problem is calibration. We give a brief discussion of it. The output of the magnetometer is a voltage V which can be rendered insensitive to instrumental drift by dividing it by the voltage change V_{ϕ_o} due to a shift of one flux quantum in the input circuit. In a fixed measuring field the ratio V/V_{ϕ_o} depends on the ^{3}He susceptibility by the formula

$$V/V_{\phi_o} = \lambda[- \mid \chi_d \mid + \chi_p], \tag{3.1}$$

where χ_d is the diamagnetic susceptibility, χ_p is the nuclear paramagnetic susceptibility, and λ is a calibration constant to be determined. For a molar volume v of 37.0 cm^3/mole the Curie constant for ^{3}He is 1.362×10^{-8} K. Then we have $\chi_p = (1.362 \times 10^{-8}$ K$/T^*) (37.0$ cm^3/mole$/v)$, so (3.1) can be written

$$\frac{V}{V_{\phi_o}} \frac{v}{37.0 \text{ cm}^3/\text{mole}} = - \frac{\lambda \mid v\chi_d \mid}{37.0 \text{ cm}^3/\text{mole}}$$

$$+ \lambda \frac{1.362 \times 10^{-8} \text{ K}}{T^*}. \tag{3.2}$$

In this equation $v\chi_d$ is the so-called molar diamagnetic susceptibility and T^* is the magnetic temperature of the ^{3}He. Measurements of T^* by Ramm, Pedroni, Thompson, and Meyer (1970) were used both in calibration and at low temperatures. It is impossible to calibrate by changing the temperature and observing the corresponding change in V since the cell background magnetism is large compared to the ^{3}He magnetism. Rather the cell is partially emptied of liquid ^{3}He, to the bottom of the magnetism tower, for example, and then the temperature held fixed at some T while ^{3}He very slowly is allowed to condense and fill the tower. The background drifts slowly enough that the effect of ^{3}He magnetism can be readily measured. After a single measurement the cell must be heated to remove some ^{3}He and then recooled to measuring temperature for the next measurement. The data are represented by finding from
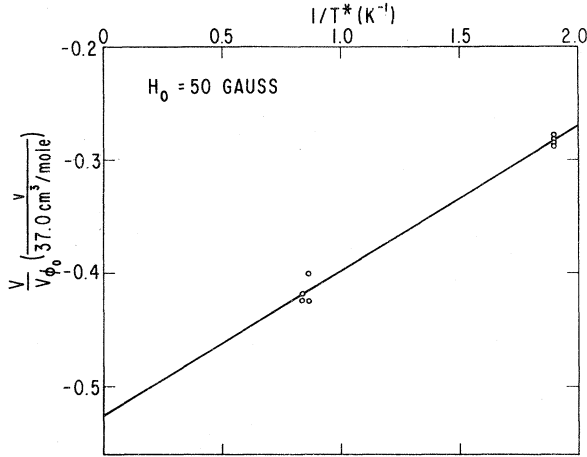
FIG. 7. Calibration in a field of 50 G of SQUID magnetometer output voltage V, relative to the output V_{ϕ_o} for a single flux quantum at the input and relative to a molar volume v of 37.0 cm³/mole, in terms of the reciprocal $(1/T^*)$ of the ³He magnetic temperature. (After Webb, Kleinberg, and Wheatley, 1974, unpublished).

Ramm et al. (1970) the value of T^* at saturated vapor pressure which corresponds to T and then, following (3.2), plotting $(V/V_{\phi_o})(v/37.0 \text{ cm}^3/\text{mole})$ vs $1/T^*$. Data from a calibration of Webb, Kleinberg, and Wheatley (unpublished) are shown in Fig. 7 for a trapped field of 50 G. These data give $v\chi_d = -(2.07 \pm 0.05) \times 10^{-6}$ cm³/mole and $\lambda = (9.40 \pm 0.35) \times 10^6$. Some indication of accuracy of the measurement may be obtained by comparing the molar diamagnetic susceptibility obtained here with the $-(2.02 \pm 0.08) \times 10^{-6}$ cm³/mole measurement of Barter, Meisenheimer, and Stevenson (1960) and the calculation reported by Dorfman (1965) of 1.99×10^{-6} cm³/mole. Since $\lambda \sim 10^7$ for the 50 G trapped field and $\chi_p \sim 10^{-7}$ at low temperature, the voltage output (3.1) of the flux sensing device corresponding to the nuclear paramagnetism is about equivalent to a full flux quantum at the input. This is plenty of signal for precise measurements of static ³He nuclear magnetism and bodes well for the success of experiments on dynamic magnetism which are discussed later. The calibration should be accurate since it is based on $\pm 1\%$ accurate measurements of T^*. However, the precision of the calibration is less. Nevertheless, earlier calibrations than that indicated above by Paulson, Johnson, and Wheatley (1973b) and by Paulson, Kojima, and Wheatley (1974b) on a different cell gave comparable values of $v\chi_d$. Furthermore, measurement of $\Delta\chi_{B\to A}/\chi_N$ [the susceptibility change $\Delta\chi_{B\to A}$ at the $B \to A$ transition relative to the normal susceptibility χ_N as calculated from T^* (for $T \to 0$), v, and the calibration factor λ] by Paulson, Johnson, and Wheatley (1973b) in 49 G and 29.5 bar was 0.470 as compared to 0.476 measured in 50 G in a different apparatus but at the same pressure by Webb, Kleinberg, and Wheatley (1974, unpublished). Although this is much better agreement than expected, it does suggest that the measurements are reasonably reproducible and that major errors, if present, would have to be in the assumptions regarding the measurement process and the calibration.

All measurements of the superfluids are referred to the normal state susceptibility χ_N. This is calculated for each pressure from the limiting low temperature values of T^*

as found by Ramm et al. (1970), and from the known molar volumes (Wheatley, 1966; Grilly, 1971). Experimentally measured voltages V are then compared to $V_N = \lambda\chi_N$.

Some examples of chart recordings collected by Paulson (1974) of what is actually observed are shown in Fig. 8 for a field of 378 G and a pressure of 29.5 bar. The calculated size M_N of the full normal state magnetization is shown at the left. Magnetization increases upward. Before discussing the figure we remark that in these experiments a nearly reversible and rather fine control over the ³He temperature was possible by means of the magnetic field on the CMN produced by the Helmholtz magnetizing solenoid of Fig. 3. Although residual heat leak is constantly acting to warm the apparatus, both the temperature and the sign of the temperature drift can be adjusted using the magnetocaloric effect on the CMN. The needed field adjustments do have a slight effect on the measurements owing to imperfect magnetic shielding of the superconducting circuits, but since there is a small time lag between changing the field and temperature at the main CMN and its thermal effect in the tower there is no real problem in distinguishing field change and magnetization effects. Use of the magnetocaloric effect to change the ³He temperature by either gross or fine amounts in short times is crucial to the success of the measurements since it allows the effect of the magnetic background drift to be removed by extrapolation of adjacent drift data.

Returning to Fig. 8, consider the events in trace (a), which were concerned with measurement of the magnetization discontinuity and the temperature of the AB transition. Starting at the left the ³He is in the B phase and the temperature is slowly rising under residual heat leak. Then the $B \to A$ transition suddenly occurs. Shortly afterward, as indicated by the arrow ↓, the field on the CMN is reduced slightly, the temperature drift is reversed, and in due course the $A \to B$ transition occurs. Following this the CMN field is increased slightly (↑) and another $B \to A$ transition occurs. The subsequent downward field change (↓) was then just enough to start the $A \to B$ transition near the measuring coils but not enough to carry it to completion before heat leak reversed the temperature drift and the transition region backed out of the coils. A subsequent field decrease (↓) then caused the $A \to B$ transition. The above shows that the $A \to B$ transition is reversible, so long as it is not carried to completion, for a configuration in which there is a moderately large field on the tower and only a small field on the CMN. The $B \to A$ transition could not be reversed.

In trace (b) on Fig. 8 is shown how temperature-dependent magnetism in the B phase can be measured. Starting at the left the ³He is in the A phase with some field on the main CMN. This field is rapidly reduced to zero at (↓). Then the $A \to B$ transition occurs and the magnetization continues to decrease until a low temperature is reached. After an equilibrium drift is established the CMN field is rapidly increased (↑) by enough to carry the liquid into the A phase. By extrapolating the drifts into the transition region, taking into account the abrupt changes where the field is changed, one can obtain the magnetization at the low temperature relative to that in the (magnetic) A phase. These measurements are continued as the ³He warms and the low temperature increases. In this way the magnetization in the B phase as a function of temperature can be
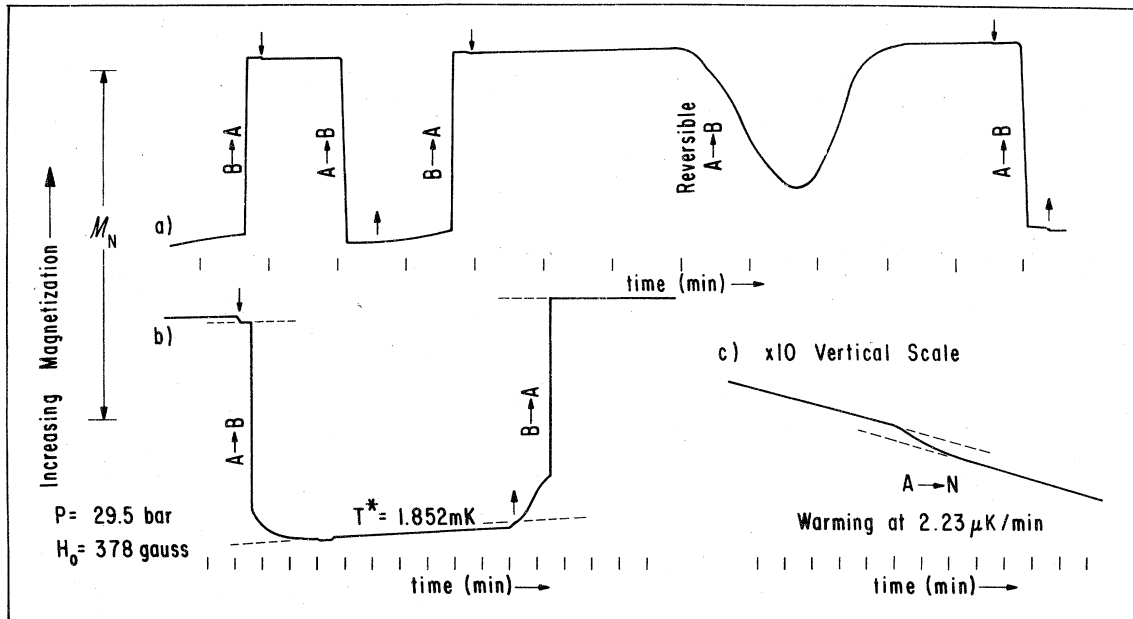
FIG. 8. Examples of magnetometer output as a function of time for a pressure of 29.5 bar and a steady field of 378 G. M_N is the size of the normal liquid paramagnetism. Arrows $\downarrow$ and $\uparrow$ indicate change of Helmholtz magnetizing solenoid current down and up, respectively. (a) Demonstration of $A \rightarrow B$ and $B \rightarrow A$ transitions as induced by very small temperature changes. (b) Magnetic change induced by a large temperature change. The rapidly varying trace immediately after the $A \rightarrow B$ transition and immediately before the $B \rightarrow A$ transition reflect the temperature-dependent magnetism of ³He-B. The total change is that between the final temperature of $T^* = 1.852$ mK and some temperature greater than T_{AB}. (c) Example of the $A \rightarrow N$ magnetic transition. The sloping lines in the fore and after intervals are caused by magnetometer background. (After Paulson, 1974).

mapped out. Similar measurements carried out for temperature changes from deep in the A phase to above T_c led to the conclusion that in the A phase the magnetization is constant to within a few tenths of a percent. Finally, in (c) and on a $10 \times$ expanded vertical scale is shown the magnetic feature that occurs when the liquid warms in 378 G through the $A \rightarrow N$ transition in the region of T_c. The slopes of the fore and after intervals reflect spurious magnetic background. In the immediate vicinity of the second-order specific heat transition in the main cell the magnetization decreases on warming by a few tenths of a percent over a temperature interval of several microdegrees.

The experimental measurements by Paulson, Kojima, and Wheatley (1974b) of the reduced static magnetism χ_B/χ_N of ³He-B as a function of reduced temperature T/T_c are given in Fig. 9. These measurements are all for a steady field of 378 G and for a variety of pressures. Measurements were made on a magnetic temperature scale and provisionally converted to absolute temperatures using a scale based on zero sound attenuation described in Appendix A. On this scale there appears to be little pressure dependence of reduced quantities although χ_B/χ_N at a given T/T_c *may* decrease somewhat with increasing pressure. It is important to note that the highest pressure of 29.5 bar represented on Fig. 9 is still much less than melting pressure of 34.4 bar. It was not possible to obtain data at higher pressures owing to a supercooling effect. The earlier data of Paulson, Johnson, and Wheatley (1973b) obtained at 49 G are in semiquantitative agreement with those presented here. However, the earlier data are much more subject to error owing to the much increased harmful effect of magnetic

background at 49 G. In any event, there does not appear to be a substantial quantitative effect on the results, for measurements in a 3 mm diameter tube, of the size of the measuring field in the range 50–500 G.

Bearing in mind that in a field of 378 G the A phase is interposed between normal liquid and the B phase over the full pressure range, it is remarkable that χ_B/χ_N is a nearly pressure-independent function of T/T_c, where T_c is the second-order transition temperature to the A phase. It appears that within moderate experimental precision χ_B/χ_N extrapolates to 1 at $T/T_c = 1$. The strength of this observation is increased as the pressure decreases. It is the experimental basis for the assumption that T_c is the same for both the A and the B phases.

Also of interest are the susceptibility discontinuities at the AB transition. These are shown as a function of pressure in Fig. 10. Since for $|t| \equiv |(T - T_c)/T_c| \lesssim 0.05$ one has the empirical relation from Fig. 8 that

$$\frac{\chi_N(P) - \chi_B(T, P)}{\chi_N(P)} \simeq 4.7 \, |t|, \qquad (3.3)$$

these susceptibility data at low enough pressure may be used to obtain the reduced temperature difference t_{AB} of the AB transition as a function of pressure for the fields given. The 60-G data plotted on the figure represent the $B \rightarrow A$ transition since it was slower and was more reproducible than the $A \rightarrow B$ transition for this field. However, more recent measurements of Kleinberg, Paulson, Webb, and Wheatley (1974) suggest that the thermodynamic AB transition near the PCP has not yet been observed. In any
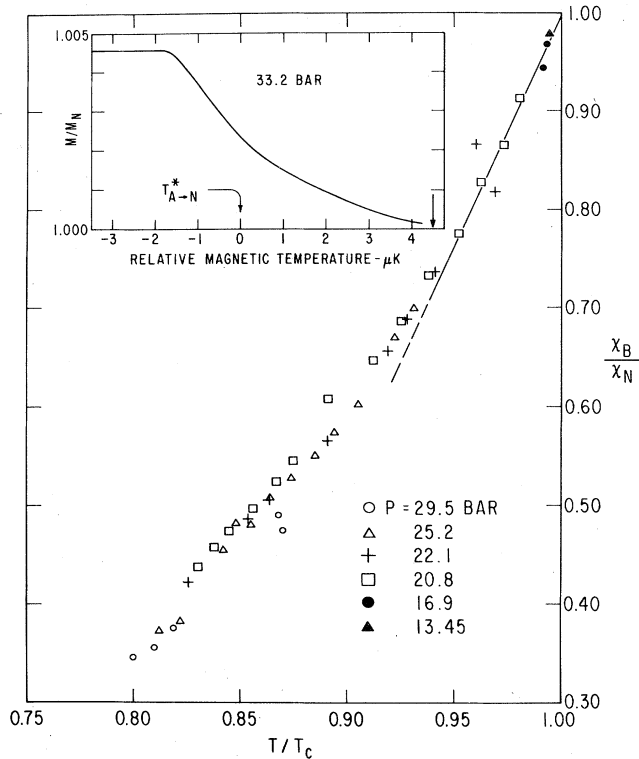
FIG. 9. Nuclear magnetic susceptibility in ³He-B, χ_B, relative to the normal susceptibility χ_N as a function of reduced temperature T/T_c for various pressures as observed in a field of 378 G. The inset shows the magnetization relative to that in normal liquid in the vicinity of T_c for a pressure of 33.2 bar and a field of 378 G. (After Paulson, Kojima, and Wheatley, 1974b).

FIG. 10. Nuclear magnetic susceptibility discontinuity $\chi_N - \chi_B(T_{AB})$ at the AB transition relative to the normal susceptibility χ_N as a function of pressure. The 480 and 378 G points are thermodynamic $A \to B$ transitions while the 60 G points are nonthermodynamic $B \to A$ transitions. The different curves have different calibrations and hence can be shifted slightly with respect to one another. (After Paulson, Kojima, and Wheatley, 1974a).

event the profound effect of such a low field as 60 G on the AB transition near the PCP is clear.

Static magnetic measurements have also been made at melting pressure in a compressional cooling cell by Halperin, Buhrman, Lee, and Richardson (1973a). They observe a discontinuity in static magnetization at the "B" feature on the pressurization (pressure vs time) curve. Interpretation of their result is made difficult both by problems of calibration and by the effect of changes in magnetization due to concomitant solid formation at the transition. They find $\chi_B(T_{AB})/\chi_N = 0.65 \pm 0.15$. A parallel thermodynamic analysis based on a magnetic Clausius–Clapeyron equation for the AB transition at melting pressure gave 0.61 for this quantity, in agreement with their more direct result. Since at melting pressure one expects $T_{AB}/T_c \simeq 0.79$ (see Fig.1), reference to Fig. 9 shows that the static measurement of $\chi_B(T_{AB})/\chi_N$ at melting pressure is quantitatively different from the value obtained for this quantity at the same reduced temperature but at lower pressures.

Let us now turn our attention to the determination of susceptibility by measuring the area under a perpendicular magnetic resonance absorption curve. This should be quite an accurate method to obtain a quantity proportional to the static susceptibility provided all possible resonances have been included. Even if some resonances are excluded the method should give a *lower* limit for the static susceptibility. The method as applied to magnetic properties of
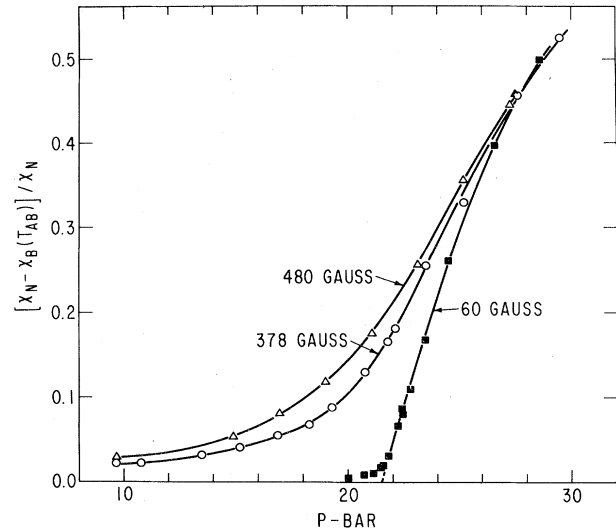
superfluid ³He consists of measuring the "relative susceptibility," *defined* for purposes of this section as the ratio of the area under a resonance curve for $T < T_c$ to the same for $T > T_c$ where the liquid is normal. The results must be treated with some care, as emphasized in the recent measurements at melting pressure by Bozler, Bernier, Gully, Richardson, and Lee (1974), who found in some fields below 70 G that the relative susceptibility in the A phase had decreased to less than half when T had been reduced to $T_{A \to B}$. This result, of great interest in itself, emphasizes the danger of the perpendicular rf magnetic susceptibility method. It is known from static measurements (Paulson, Kojima, and Wheatley, 1974b) that the static magnetization changes by less than a few tenths percent in the A phase, *at least at pressures some distance below melting pressure*. Even the comparison with static measurements is not necessary here since the original perpendicular NMR measurements at higher fields by Osheroff, Gully, Richardson, and Lee (1972b) indicated only small changes with temperature in the relative susceptibility of the A phase at melting pressure.

With the above comments in mind let us turn first to the recent measurements of Osheroff (1974) on the B phase at melting pressure. These are an extension of those reported by Osheroff and Brinkman (1974). The relative susceptivility as defined in the preceding paragraph and measured at each field for a fixed normal liquid linewidth of 400 Hz and a fixed frequency interval of integration of 700 Hz was not constant but rather increased with increasing magnetic field. This is shown on Fig. 11, where $\nu_0/H_0 = 3.24$ MHz/kG. The applied field and the axis of the tube containing ³He were parallel in these measurements. The plot was motivated by a theory of Brinkman, Smith, Osheroff, and Blount (1974) for NMR line shapes using a model of the B phase which assumed it to be in the Balian–Werthamer state. According to this theory, if one finds the
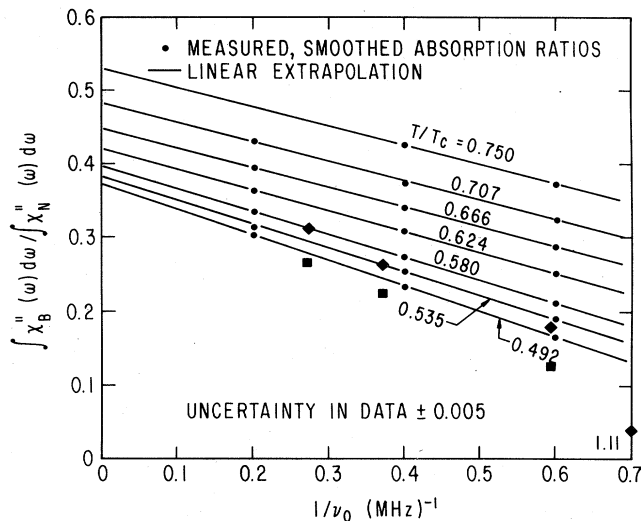
FIG. 11. Ratio of the area for a fixed frequency width of 700 Hz under the perpendicular NMR absorption curve for ³He-B at melting pressure to the corresponding area for normal liquid as a function of the reciprocal of the resonance frequency for various values of reduced temperature. The points ● are experimental observations and the straight lines linear extrapolations. The ♦ and ■ symbols refer to the ratios at T/T_c of 0.58 and 0.49, respectively, of the perpendicular NMR absorption in the B phase to that in normal liquid at the same frequency as the maximum absorption in normal liquid according to data in Osheroff and Brinkman, (1974). The ♦ at right bottom is a point observed at $\nu_0^{-1} = 1.11$ (MHz)⁻¹ or 280 G. The other points correspond to fields of about 520, 840, and 1140G. The axes of the field and of the cylinder of ³He are parallel. After Osheroff (1974).

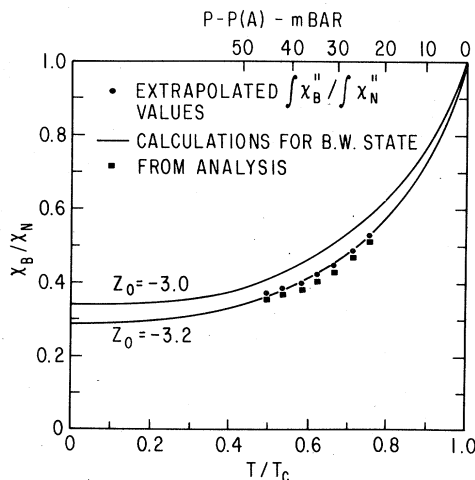

FIG. 12. Relative perpendicular rf susceptibility in the high field limit in ³He-B at melting pressure as a function of reduced temperature. After Osheroff (1974).

relative susceptibility by integrating in frequency only from γH_0 to $\gamma H_0 + \Delta\omega$, where γH_0 is the angular resonant frequency for the normal liquid, then the fraction of the true relative susceptibility observed in a cylinder of radius R (3 mm in the experiment described) at normal liquid resonant field H_0 is given by

$$\left[1 - \frac{H_B R_C}{2H_0 R} \ln\left\{\frac{(\pi\Omega_L/2)^2}{2\Delta\omega\gamma H_0}\right\}\right]^2 \simeq 1 - \frac{H_B R_C}{H_0 R} \ln\left\{\frac{(\pi\Omega_L/2)^2}{2\Delta\omega\gamma H_0}\right\}.$$

(3.4)

In this equation Ω_L is the parallel resonance frequency (to be discussed in a later section) while H_B and R_C are, respectively, a characteristic field and a characteristic length. In the region of temperature in which this equation is applied the logarithm does not change much while the value of $R_C H_B$ increases from 10 to 19 G·cm going from the largest to the smallest value of T/T_c on Fig. 11. The linear extrapolation of the data to $\nu_0^{-1} = 0$ should then give the true relative susceptibility in the B phase at melting pressure for any particular T/T_c. The results both of the linear extrapolation and of a direct fit to the unapproximated Eq. (3.4) are shown on Fig. 12. Osheroff suggests an over-all uncertainty of less than 1% for χ_B/χ_N determined in this way. Recent measurements of χ_B/χ_N by Corruccini and Osheroff (private communication from Osheroff) using pulsed NMR and free induction decays are in quantitative agreement with the above values of χ_B/χ_N as obtained from the analysis of the continuous wave NMR data. Comparison of the the above results with those for static measurements

at lower pressures as on Fig. 9 shows quantitative disagreement.

Also shown on Fig. 11 are some data from Osheroff and Brinkman (1974), ♦ and ■ for $T/T_c = 0.58$ and 0.49, showing how the ratio of the amplitude of the resonance in the B phase to that in normal liquid at the frequency of the maximum in the normal liquid depends on frequency (or steady field). The point on the right border representing data at $\nu_0^{-1} = 1.11$ (MHz)⁻¹ or $H_0 = 280$ G is less than 10% of the extrapolated value: the value that presumably would have been obtained in a static measurement. The amplitude ratios evidently have a similar field dependence to the area ratios, although they tend to drop off somewhat more rapidly with decreasing field.

Recently Ahonen, Haikala, Krusius, and Lounasmaa (1974c) presented measurements of relative susceptibilities also obtained using the perpendicular rf magnetic susceptibility method but at lower pressures and carried to lower temperatures using the nuclear cooling method. Measurements were made in a cylindrical tube 2.25 mm in radius with applied field perpendicular to the tube axis. They found that below $T/T_c = 0.4$ both the amplitude and shape of the NMR absorption signal for constant field were T independent. Some of their results for the field dependence of the signal for $T/T_c < 0.3$ and at 21 bar are given in Fig. 13, which shows both the relative susceptibility χ_B/χ_N and the ratio $\chi_B''(\nu)/\chi_N''$ of the maximum absorption at the low temperature to that for the normal liquid (a slightly different quantity from that measured by Osheroff and Brinkman above). There is no field dependence of the former above the 180 G minimum field [now 100 G (M. Krusius, private communication)] and little of the latter above 300 G. These results can be compared with those at melting pressure of Osheroff, shown on Fig. 11, bearing in mind that although the rigidity of the textures against bending quantitified in Eq. (3.4) would be expected to be even larger at $T/T_c < 0.3$ than it is for $T/T_c = 0.5$ (the lowest T/T_c on Fig. 11), the effect of the confining walls would be different owing to the geometry with H_0 perpendicular to the ³He cylinder axis. In a field of 500 G (or $\nu_0^{-1} \simeq 0.62$
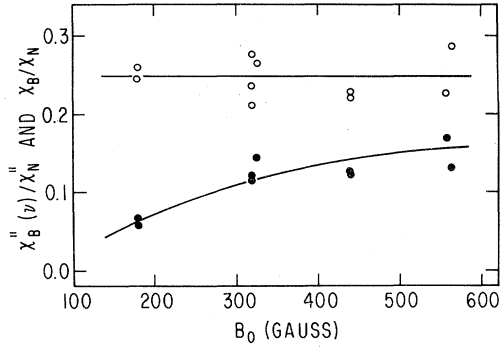
FIG. 13. Ratio $\chi_B''(\nu)/\chi_N$ of the perpendicular NMR absorption amplitude in ^{3}He-B to that in normal liquid and ratio χ_B/χ_N of the corresponding areas under the absorption curves for a reduced temperature T/T_c of 0.3 and a pressure of 21 bar as a function of resonance field. The magnetic field is perpendicular to the axis of the cylinder of ^{3}He. After Ahonen, Haikala, Krusius, and Lounasmaa (1974c).

MHz^{-1}) and at $T/T_c = \frac{1}{2}$ the relative susceptibility in a 3 mm radius tube with axis parallel to the field at melting pressure is less than half its high field limit while that in a 2.25 mm radius tube at 21 bar and at $T/T_c < 0.3$ with axis perpendicular to the field has apparently reached its high field limit already at a fifth of this field. The last statement is somewhat weakened by experimental scatter. Owing to the approximate field independence above 300 G of the ratio $\chi_B''(\nu)/\chi_N''$ in Fig. 13 one can conclude, as suggested by Ahonen *et al.*, that the broadening observed in the B phase at $T/T_c = 0.3$ had already occurred at a higher *temperature*. That is, it would *appear* from the data of Ahonen *et al.* (1974c) at 21 bar that above 300 G the line broadening mechanism is something other than or additional to the strictly field-dependent broadening observed at melting pressure by Osheroff and Brinkman (1974) and Osheroff (1974) and explained in terms of the field bending of textures by Brinkman *et al.* (1974).

If all susceptibility data are accepted at face value then one concludes that while different methods of measurement in a given pressure region agree with one another there is evidence from measurements at melting pressure and at lower pressures, say 21 bar, that ^{3}He-B behaves significantly differently in the two pressure ranges. One would further conclude that the ability of the confining boundaries to disorient the ^{3}He-B in the presence of an orienting magnetic field is much less at a pressure near 21 bar than it is at melting pressure, barring some rather subtle effect of geometry.

We conclude this section with some remarks regarding the possible relationship of the above data with microscopic concepts of the state of the liquid ^{3}He.

The constancy of the magnetization in the A phase at very nearly the normal fluid value is perhaps the strongest evidence that, within a context of BCS-like pairing theories of the superfluid state, ^{3}He-A reflects an equal-spin-pairing for the ordered pairs. For purposes of calculation and the design of experiments ^{3}He-A is usually assumed to be in the $l = 1$ equal-spin-pairing state proposed by Anderson and Brinkman (1973) after the original proposals of Anderson and Morel (1961) and called the ABM state for short. In a series of publications it has been strongly urged

by Anderson and Brinkman (1973), by Brinkman and Anderson (1973), by Osheroff and Brinkman (1974), by Osheroff and Anderson (1974), and by Osheroff (1974) that ^{3}He-B be identified with the $l = 1$ pairing BW (for Balian and Werthamer, 1963) state. This assignment has been on the basis of qualitative and some quantitative features of the phase diagram, on resonance measurements at melting pressure, and on the reduced rf susceptibility data discussed above. A principal problem in any state identification is the known strong coupling in real liquid ^{3}He which must be squared with the weak coupling theory, on the basis of which the BW state was proposed. The spin fluctuation model of Brinkman and Anderson (1973) and of Brinkman, Serene, and Anderson (1974) deals with this problem.

One effect of strong coupling was emphasized some time ago by Leggett (1965) and by Czerwonko (1967). Leggett derived results valid at all temperatures for $l = 0$ pairing, but also valid (Leggett, private communication) near $T = T_c$ for $l > 0$. Czerwonko derived a result applicable to the BW state at $T = 0$. The physical idea involved is as follows. As applied to magnetic measurements one effect of the Fermi *liquid* is to make the effective field polarizing the nuclear moments different from the applied field by a "molecular" field. If there were a homogeneous molecular field over the Fermi surface, which is probably true in the vicinity of T_c, then the effective field $\mathbf{H}_{\text{eff}}$ and the applied field $\mathbf{H}_0$ are related by

$$\mathbf{H}_{\text{eff}} = \mathbf{H}_0 + [(-Z_0)/2\gamma\hbar^2 N(0)]\mathbf{S}, \tag{3.5}$$

where the second term is the molecular field, $\mathbf{S}$ is the spin angular momentum per unit volume, γ is the gyromagnetic ratio (2.04×10^4 radians/G sec for ^{3}He), $N(0)$ is the density of states at the Fermi surface for spins of one sign, and Z_0 is a Landau parameter (see Appendix B for numerical values). The parameter Z_0 is negative for pure ^{3}He, so the molecular field aids the applied field. The enhancement of the applied field is by a factor $(1 + Z_0/4)^{-1}$ in normal Fermi liquid; this factor is nearly 4 over the pressure range of interest here. Now if the condensed pairs are only partially magnetic, as seems to be the case for ^{3}He-B, the molecular field term in (3.5) decreases as $\mathbf{S}$ and T decrease below T_c. The effective polarizing field decreases, so the magnetization decreases relatively more rapidly than it would have if there had been no molecular field in the first place. If the molecular field in (3.5) is accurate then the reduced susceptibility is given by (Leggett, 1965)

$$\frac{\chi(T/T_c)}{\chi_N} = \frac{(1 + Z_0/4)g(T/T_c)}{1 + (Z_0/4)g(T/T_c)}, \tag{3.6}$$

where $g(T/T_c)$ is the expected reduced susceptibility in the absence of molecular field. For the BW state $g(T = 0) = \frac{2}{3}$ (Balian and Werthamer, 1963). In Czerwonko's calculation for the BW state the molecular field becomes anisotropic in the limit $T = 0$, and he finds the result

$$\frac{\chi_{BW}(T = 0)}{\chi_N} = \frac{(1 + \frac{1}{4}Z_0)\frac{2}{3}}{1 + \frac{1}{4}(Z_0 + Z_2/10)\frac{2}{3}}, \tag{3.7}$$

where Z_2 is the as yet unmeasured $l = 2$ spin-type Landau

parameter. Near T_c the derivative of (3.6) is

$$\frac{\chi'(T/T_c)}{\chi_N} = \frac{g'(T/T_c)}{1 + \frac{1}{4}Z_0}, \qquad T \to T_c, \tag{3.8}$$

which should be valid for all l-type pairing and where $(1 + \frac{1}{4}Z_0)^{-1} \simeq 4$.

The molecular field type correction for Fermi liquid effects is only one way in which strong coupling alters the predictions of weak coupling theory. After all, as we saw in Sec. II, the specific heat, which reflects the rate at which the order parameter is developing with decreasing temperature below T_c, is not equal to the weak coupling value. So even with the molecular fields properly accounted for, discrepancies with weak coupling predictions should still be expected. This point has recently been emphasized by Osheroff (1974c) in connection with his susceptibility data, Fig. 12, which tend to fall somewhat below the theoretical curve for a weak coupling BW state adjusted for molecular field using Eq. (3.6) and with $Z_0 = -3.0$ as suggested in Appendix B. Of course in this case T/T_c is small enough that effects of molecular field anisotropy may also have to be accounted for

The static measurements can best be related to weak coupling theory near T_c. For the BW state near T_c, $g(T/T_c) = \frac{2}{3} + \frac{1}{3}[1 - 2(1 - T/T_c)]$ according to weak coupling theory. Further, the specific heat discontinuity at T_c near the PCP is not far from the weak coupling value. Hence, one might expect near T_c that $[\chi_N - \chi_{BW}(T)]/\chi_N \simeq 2.5(1 - T/T_c)$, using a typical value for Z_0 (see Appendix B) near the PCP. The numeric is to be compared with the 4.7 in Eq. (3.3). This quantitative discrepancy has been one impediment to immediate acceptance that ^{3}He-B is a manifestation of the BW state. Indeed the discrepancy was sufficiently large that Paulson $et\ al.$ (1973b) initially suggested that ^{3}He-B might be a manifestation of $l = 2$ pairing. This suggestion has since been abandoned as a result of the phase diagram measurements by Paulson, Kojima, and Wheatley (1974a) which suggested the same l-type pairing for both A and B phases, of the resonance measurements at melting pressure by Osheroff and Brinkman (1974) and Osheroff (1974), and especially of the lower pressure and very low temperature measurements by Ahonen $et\ al.$ (1974c) as shown in Fig. 13. The substantial temperature-independent magnetism found at very low temperatures by Ahonen $et\ al.$ is incompatible with even-l pairing since in that case the condensed pairs would all be nonmagnetic. If at intermediate pressures (e.g., 21 bar) ^{3}He-B did manifest the weak coupling BW state and if all the discrepancy with the limiting $T = 0$ value of $\frac{2}{3}$ for the ratio χ_B/χ_N were to be accounted for by molecular fields as in Eq. (3.7), then it would require $Z_2 > 10$ to obtain agreement with data. Unfortunately, the value of Z_2 is not known from other data.

It is clear that both experimental and theoretical work are needed to make further progress. On the experimental side for static magnetization it would be desirable to do the flux calibration in more than one way, for example, by saturating the perpendicular nuclear resonance in the normal state and then watching the magnetization component along the field recover. Boundary effects will also be very interesting. Experiments should be designed if possible with simple plane parallel geometries with the

possibility of field both parallel and perpendicular to the boundary. This should give very interesting effects in ^{3}He-A where in low enough fields the static magnetization may be quite anisotropic. Also ^{3}He-B will probably continue to offer surprises. Finally, it would be desirable to make static and dynamic magnetism measurements over a range of pressures nearer but not at melting pressure in order to investigate the source of the significant differences between the properties of the B phase on and off the melting curve mentioned in this and other sections. Such measurements are made awkward by the need to heat well above the minimum in the melting curve to change pressure. They are also probably not possible using CMN cooling owing to the substantial "first time" supercooling effect which prevents formation of the B phase unless the temperature can be carried well below the thermodynamic T_{AB}. Such experiments will probably require nuclear cooling.

IV. THERMODYNAMICS OF THE AB TRANSITION

The thermodynamic properties of the AB transition are of considerable interest. The A phase seems to be at least qualitatively understood. But questions of substance have been raised with respect to the B phase, at least for pressures well below melting pressure. So what we can learn thermodynamically about the relationship between the two phases can be of paramount importance. The conclusion of this section will be in part that the thermal differences between the two phases are quite small.

In zero field for pressures above that of the PCP the A phase is stable between T_{AB} and T_c. Below the pressure of the PCP in zero field the B phase is presumed to be stable for T below T_c, at least within the range of present measurements. But application of a magnetic field changes the T_{AB} line dramatically (Paulson, Kojima, and Wheatley, 1974a). In a field the T_{AB} line no longer intersects the T_c line, so the A phase is interposed between normal liquid and the B phase for all pressures. This emphasizes why the presumed critical point has been called provisionally $poly$critical[1]: it represents a limiting condition not only with respect to pressure and temperature but also with respect to magnetic field. We will deal with the question of the phase diagram in the vicinity of the PCP in a separate section, but at this point we comment that neither the shape of the T_{AB} line nor the actual location of the PCP on the T_c line are known precisely at present. This will not alter the substance of our conclusions.

The measurements of static magnetization (Paulson, Kojima, and Wheatley, 1974b) suggest that both A and B phases have the same T_c. The experimental basis for this suggestion is strong for pressures below that of the PCP and then weakens as the pressure increases above the PCP and the temperature separation between T_{AB} and T_c increases. In what follows the consequences of assuming that the A and B phases have the same T_c will be examined. The splitting of the second-order transition by a magnetic field will be neglected. This effect, which is discussed in another section, is small compared to the field effect on T_{AB}.

Between the second-order transition at T_c and the first-order transition at T_{AB} it is assumed that the B phase is

---

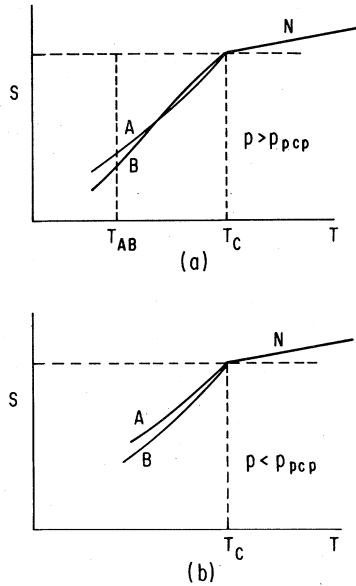[1] We are indebted to Dr. John C. Wheeler for suggesting this name.

FIG. 14. Schematic assumed dependence of entropy on temperature in liquid ³He near the second-order transition at T_c for (a) pressures greater than that of the PCP and temperatures down to below T_{AB}, and for (b) pressures below that of the PCP.
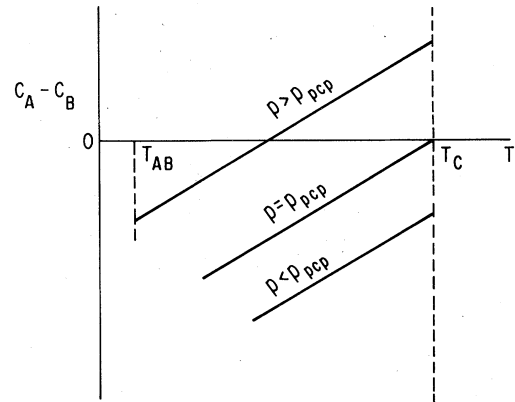

FIG. 15. Simple possible dependence of the difference $C_A - C_B$ of the specific heats of the A and B phases on temperature for pressures above, at, and below that of the PCP.

metastable with respect to the A phase. The concept of metastability is valid over at least part of the temperature range as observed in the phenomena of supercooling and superheating discussed in another section. Thus one assumes $S_A(T_c, H_0, P) = S_B(T_c, H_0, P) = S_N(T_c, H_0, P)$ and $F_A(T_c, H_0, P) = F_B(T_c, H_0, P) = F_N(T_c, H_0, P)$; where S and F are, respectively, entropy and free energy for the three phases: ³He-A, ³He-B, and normal Fermi liquid. Similarly one has $F_A(T_{AB}, H_0, P) = F_B(T_{AB}, H_0, P)$. All volume effects have been neglected since they are small (Wheatley, 1973; Halperin, Buhrman, Richardson, and Lee, 1973a; Bukshpan, Eckstein, and Landau, 1973). First, consider the case $H_0 = 0$, constant $P > P_{PCP}$. Since the free energies of the A and B phases are the same at both T_c and T_{AB} one has

$$\int_{T_{AB}}^{T_c} S_A(T, 0, P)\, dT = \int_{T_{AB}}^{T_c} S_B(T, 0, P)\, dT. \qquad (4.1)$$

The average entropies of the two phases over the temperature interval T_{AB} to T_c are equal. But since the AB transition is first order, one has $S_A(T_{AB}, 0, P) > S_B(T_{AB}, 0, P)$. Thus, the entropies of the states as a function of T might qualitatively appear as in Fig. 14(a). Near T_c the specific heat $C_A(T, P)$ is greater than $C_B(T, P)$, but at some lower temperature they are equal to one another, and at T_{AB} the specific heat of A is less than that of B. As the pressure decreases toward the PCP the point where A and B entropy curves cross approaches T_c. At the PCP the A and B entropy curves have the same limiting slope and intercept at T_c, so that one expects $C_A(T_c, P_{PCP}) = C_B(T_c, P_{PCP})$. For pressures below the PCP the B phase is always stable in zero field. Thus the entropies of the A and B phases might appear as in Fig. 14(b). The specific heat of the A phase will then always be less than that of the B phase. The dependence of the difference of the specific heats of the A and B phases on T for various P might then appear as in Fig. 15. Since only few data are available they have been

fit to the empirical formula for the specific heat difference

$$C_A(T, P) - C_B(T, P) = \Delta C(P) + \alpha t, \qquad (4.2)$$

where $t \equiv (T - T_c)/T_c < 0$, $\Delta C(P)$ is the difference in the specific heats per unit volume at T_c, and α is a constant. This is not the specific heat difference at the AB transition. Rather it is intended to *approximate* the specific heat difference between the A and B phases in the pressure and temperature region of the metastability of the B phase. This specific heat difference will be assumed to be field independent for the small fields of current interest.

To obtain the effect of a magnetic field the empirical results (Paulson, Kojima, and Wheatley, 1974b) can be used for the static magnetization of the two phases:

$$M_A(T, H_0, P) = \chi_N(P) H_0, \qquad (4.3)$$

and

$$M_B(T, H_0, P) = \chi_N(P)[1 + 4.7t] H_0, \qquad (4.4)$$

where the dependence of reduced susceptibility of the B phase on reduced temperature is assumed to have no pressure dependence. Equality of the free energy per unit volume at T_c and T_{AB} then requires

$$\int_{T_{AB}}^{T_c} [S_A(T, P) - S_B(T, P)]\, dT$$

$$= \int_0^{H_0} [M_A(T_{AB}, P, H_0) - M_B(T_{AB}, P, H_0)]\, dH_0. \qquad (4.5)$$

Putting in the assumed forms given in Eqs. (4.2), (4.3), and (4.4) and using the fact that the A and B phases have the same entropy at T_c, one finds to lowest order in the reduced
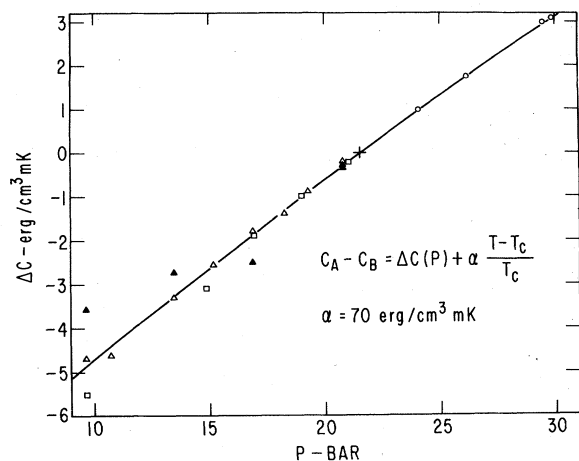
FIG. 16. Difference in specific heat per unit volume of ^{3}He-A and ^{3}He-B at T_c as derived from data for $(1 - T_{AB}/T_c)$: (O) 49 G, thermometric; (▲) 378 G, thermometric; (△) 378 G, susceptibility; (□) 480 G, susceptibility; +, assumed PCP. (After Paulson, Kojima, and Wheatley, 1974a).

temperature difference t_{AB}

$$\Delta C(P) = \frac{[4.7\chi_N(P)H_0^2/T_c] - \alpha t_{AB}^2/3}{t_{AB}}. \qquad (4.6)$$

The constant α is obtained from the value of t_{AB} at the pressure of the PCP where $\Delta C(P)$ is taken to be zero. Then $\Delta C(P)$ is obtained, using the so derived pressure-independent constant α, from empirical values of t_{AB} at various pressures. For this purpose both values of t_{AB} determined thermometrically and values obtained from the equation

$$t_{AB} = -(1/4.7)\{[\chi_N(P) - \chi_B(P, T_{AB})]/\chi_N(P)\} \quad (4.7)$$

[see Eq. (4.4)] were used. The latter values are more precise. The results are shown in Fig. 16. The PCP was taken to have a pressure of 21.5 bar, but small changes in this pressure will have no qualitative effect on the results. The curve of $\Delta C(P)$ could be shifted by small amounts as the PCP is located more precisely. Values of $\Delta C(P)$ determined for $H_0 = 0$ from the T_{AB} line above the PCP reasonably extrapolate from those determined below the PCP from magnetic data. A consistent value of α is 70 erg/cm^3 mK.

The accuracy of the assumption (4.2) is probably not great, particularly as the pressure difference from the PCP increases. But at this point the result has qualitative significance. The total specific heat of the liquid itself near the PCP is about 80 erg/cm^2 mK, so one sees that $C_A - C_B$ is just a few percent at most of the total specific heat in the region between T_c and T_{AB}. The thermal properties of the two phases are very similar indeed. The susceptibility information in Eqs. (4.3) and (4.4) together with thermal assumption (4.2) and its empirical evaluation adequately correlate all the phase diagram data of Fig. 1.

For the form of specific heat difference in Eq. (4.2) and for pressures below the PCP the free energy excess of the A

over the B phase in zero field increases quadratically with the temperature difference from T_c. However, since the A phase is *more magnetic* than the B phase, the magnetism of the B phase decreasing linearly with decreasing temperature, the magnetic free energy of the A phase is less than that of the B phase by an amount which is linearly dependent on the temperature difference from T_c and quadratically dependent on H_0. Hence the magnetic effect always wins out for T very near T_c and the transition in magnetic field from normal liquid is first into ^{3}He-A, as shown in Fig. 1.

Although the above data and analysis have been very important in furthering our qualitative understanding of superfluid ^{3}He, a much better quantitative understanding of the thermal properties of the AB transition can be achieved by measurements of the quantity $(\partial H_0/\partial T_{AB})_P$. Then the entropy difference at the AB transition can be determined using the Clausius–Clapeyron equation:

$$S_A(T_{AB}, P) - S_B(T_{AB}, P) = -[\chi_A(T_{AB}, P)$$
$$- \chi_B(T_{AB}, P)]H_0(\partial H_0/\partial T_{AB})_P. \qquad (4.8)$$

By varying H_0, the temperature dependence of the entropy difference can be determined over a significant temperature region below T_c. Such measurements of the ratio of an incremental field change to an incremental temperature change were not possible in the arrangement of Paulson et al. (1974a) since the measurements were performed with the field H_0 trapped in a Nb tube, and the temperature of this tube had to be increased to about 9 K to change H_0.

Many features of the phase diagram are consistent with the spin fluctuation theory of Brinkman and Anderson (1973) and of Brinkman, Serene, and Anderson (1974). As we have mentioned before this theory accounts for the effects of strong coupling by a spin fluctuation theory described by a single pressure-dependent parameter δ and assumes that ^{3}He-A and ^{3}He-B reflect, respectively, the $l = 1$ pairing ABM and BW states. In particular, Osheroff and Anderson (1974) find agreement between the value of δ needed to explain certain resonance measurements near T_c and that needed to give T_{AB}/T_c at melting pressure correctly. The author is not aware of the extent to which other theories are thereby excluded.

V. FOURTH SOUND

Are the new phases of ^{3}He superfluid? In view of the high probability from the theoretical side that the liquid has anisotropic properties, not unlike those for liquid crystals (DeGennes, 1974), it is preferable to answer the qualitative question regarding superfluidity by an experiment in which the observed effect cannot occur at all unless a superfluid is present. An example of such an experiment is the propagation of sound through a superleak, or fourth sound, as in the experiments by Shapiro and Rudnick (1965) on superfluid ^{4}He.

Propagation of fourth sound in ^{3}He below T_c has been observed by Kojima, Paulson, and Wheatley (1974) over the pressure range from 12.4 to 33.6 bar and more recently by Yanof and Reppy (1974) at pressures from 15.9 to 27
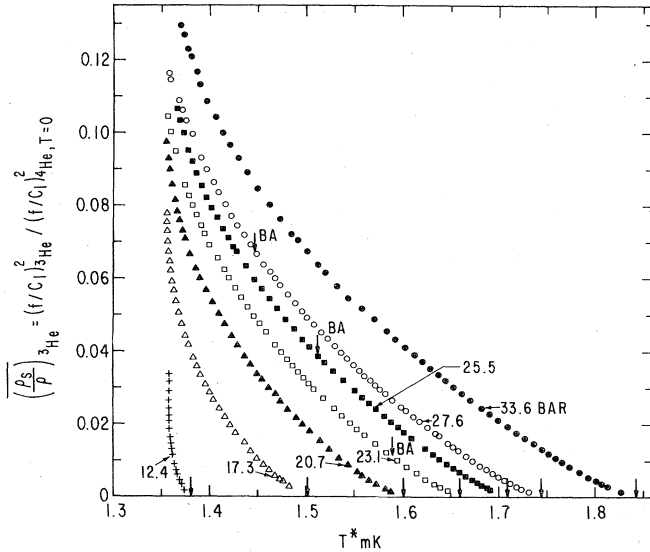
FIG. 17. Experimental values of $\bar{\rho}_s/\rho$ from fourth sound as a function of CMN magnetic temperature for various pressures. The corresponding second-order transition temperatures T_c^* are indicated by arrows on the horizontal axis. The expected locations of T_{AB}^* are shown by arrows on the appropriate curves. The PCP is near 21.2 bar. (After Kojima, Paulson, and Wheatley, 1974.)

bar. A preliminary account of the latter work was given by Yanof, Smith, Lee, Richardson, and Reppy (1974). Since the normal viscosity of ^{3}He near T_c is at least 10^4 times the normal viscosity of liquid ^{4}He near the lambda point physical construction of a superleak is much easier for ^{3}He than it is for ^{4}He in the sense that the pore size can be much larger. The work of Kojima et al. was done with a CMN demagnetization cell similar to Fig. 3, although there were no appendixes and opposite ends of the cell were closed by capacitive pressure transducers to facilitate production and detection of sound. The superleak was the CMN powder itself, which also served as refrigerant and magnetic thermometer. The powder was less than 37 μ in size and was packed to 80% of crystalline density. It is suspected that the actual pore size, if defined in terms of an average distance between CMN grains, is very much less than the 37 μ maximum CMN grain size. Quantitative details of the pore size are unknown in the experiment but may be important in the quantitative interpretation of the measurements. The Yanof–Reppy work was also performed with a powdered CMN superleak, although in their case the CMN grains had an average size of 50 μ, were mixed with 10% by mass of 1 μ aluminum oxide powder, and were packed to 72% of crystalline density. Yanof and Reppy also used a different method of detecting fourth sound based on an ingenious idea of Hall, Kiewiet, and Reppy (1974).

Observation of fourth sound proves the existence of superfluidity. Quantitative measurement of fourth sound velocity yields either a tensor component or an average superfluid density $\bar{\rho}_s$ via the equation

$$\bar{\rho}_s/\rho = n^2(C_4{}^2/C_1{}^2), \tag{5.1}$$

where C_4 is the velocity of fourth sound, C_1 is the velocity

of first or hydrodynamic sound, ρ is the mass density of the fluid, and n is an effective "index of refraction." Thermal corrections to this formula (Shapiro and Rudnick, 1965) are calculated to be negligible. The empirical value of n is large. A substantial correction of the observed velocity (usually in the form of the first longitudinal resonance frequency) for the scattering effect of the CMN powder is required. This correction is obtained by making measurements with ^{4}He at very low T in the cell. The measured $\bar{\rho}_s/\rho$ is difficult to interpret since the geometry is uncertain and the superfluid density likely to be anisotropic, at least for ^{3}He-A (Saslow, 1973; DeGennes, 1973).

The results of measurements by Kojima et al. (1974) of relative superfluid density on a magnetic temperature scale for a number of pressures are shown in Fig. 17. The corresponding critical temperatures T_c as determined via the specific heat discontinuity are shown as arrows on the horizontal axis. Provisional absolute temperatures may be obtained by comparing with the (P_c, T_c) relation (see Appendix A). Saturation of the magnetic susceptibility of the CMN thermometer at low temperatures is clear on the figure.

Several observations regarding Fig. 17 may be made. First, the actual values of $\bar{\rho}_s/\rho$ are quite small. Second, on the T^* plot $\bar{\rho}_s/\rho$ is slightly concave upward while according to theory one expects that $\bar{\rho}_s/\rho \propto (1 - T/T_c)$ near T_c. At the time of these measurements it was thought that this could be an effect of temperature scale, but the later measurements of parallel ringing frequencies Ω (Webb, Kleinberg, and Wheatley, 1974a) on a similar temperature scale showed a linear T^* dependence of Ω^2 near T_c, so it is currently suspected that there is a departure from $(1 - T/T_c)$ dependence in the superfluid density data near T_c. This is a possible effect of pore size (Kriss and Rudnick, 1970) which can only be studied by changing geometry. Furthermore for three of the pressures (27.6, 25.5, and 23.1 bar) the $A \to B$ transition should have occurred during warming at the temperature labeled BA, as determined by the bulk phase diagram. However, no obvious effect on $\bar{\rho}_s/\rho$ occurred at or in the region of these temperatures.

A log–log plot of the relative superfluid density vs reduced temperature difference $(1 - T/T_c)$ as obtained by Kojima et al. using provisional absolute temperatures is shown as dots in Fig. 18 for a pressure of 33.6 bar. The data at other pressures are rather similar with $\bar{\rho}_s/\rho \propto (1 - T/T_c)^\alpha$ and α in the range 1.1–1.3.

Yanof and Reppy (1974) used a different technique in which a cell containing the superleak and the ^{3}He and suspended by a leaf spring was caused to vibrate by a harmonically varying force F_0, both in-phase and quadrature components of the amplitude X being measured. According to to the theory of the measurement, the amplitude is given by

$$X = F_0 \exp(i\omega t) \left[K - (M + m)\omega^2 - i\omega D \right.$$

$$\left. + \frac{m_s\omega^2}{n^2}\left(\frac{\omega}{C_4 k}\right)^2 \left(1 - \frac{2}{kL}\tan\frac{kL}{2}\right) \right]^{-1}, \tag{5.2}$$

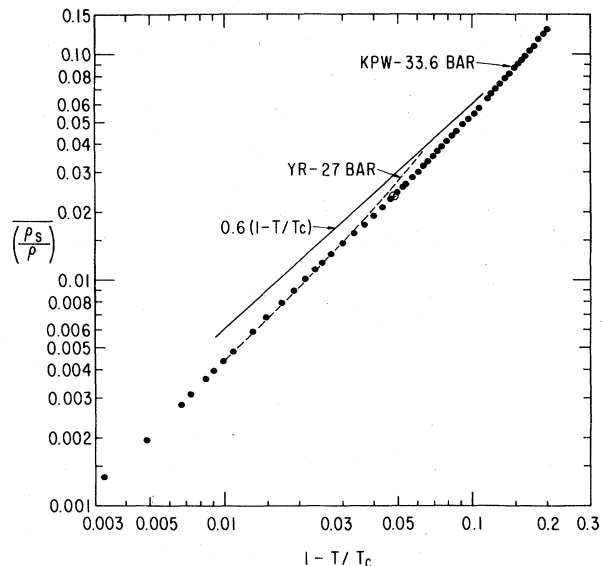where ω is the angular frequency of the drive, K is the spring

FIG. 18. Logarithmic plot of $\bar{\rho}_s/\rho$ against $(1 - T/T_c)$ for ³He-A. The solid line is $\bar{\rho}_s/\rho = 0.60 \cdot (1 - T/T_c)$ obtained from susceptibility measurements as suggested in the text. The dots are experimental data at 33.6 bar from Kojima, Paulson, and Wheatley (1974). The dashed curve gives smoothed data at 27 bar from Yanof and Reppy (1974). The point $\oplus$ is an independent direct measurement by Yanof and Reppy of $m_s/m = \bar{\rho}_s/\rho$.

constant, M is the mass of cell plus superleak, m is the total mass of ³He, D is a cell (mainly suspension) dissipation factor, m_s is the mass of the superfluid, L is the length of the cylindrical cell, and

$$k^2 = (\omega^2/C_4^2)(1 + iQ_4^{-1}). \qquad (5.3)$$

Here the quality factor Q_4 is defined in terms of a loss parameter η by the equation $Q_4 = \omega\rho_s/\eta$. Resonant absorption of energy by superfluid motion in the cell leads to a dip in the amplitude X at constant drive F_0. For a high Q_4 resonance this occurs when $(\omega/C_4)L \simeq kL = \pi, 3\pi, \cdots$. In practice m_s is small while Q_4 is smaller than expected, so the effect of superfluid resonance needs to be amplified by tuning ω for "suspension" resonance in normal Fermi liquid, i.e., $\omega^2 = K/(M + m)$, and then letting the temperature vary until the superfluid ³He is also in resonance. In at least one case Yanof and Reppy fitted entire in-phase and quadrature "resonance curves" where reduced temperature difference $(1 - T/T_c)$ was the variable, in which case they were able to obtain the values of m_s/n^2 and Q_4 for the temperature at which the frequency of the fundamental longitudinal superfluid resonance equalled the suspension resonance. The quantity n^2 was obtained from measurements with only superfluid ⁴He in the cell (as in the procedure used by Kojima et al.). Then $m_s/m = \bar{\rho}_s/\rho$ could be directly determined. This measurement for a pressure of 22.8 bar is shown on Fig. 18 as a $\oplus$. Measurements at other temperatures were obtained by observing other modes pass through the suspension resonance frequency, and the temperature range was extended by using several different suspensions. The results for a pressure of 27 bar are shown on Fig. 18 as a dashed line. They do not differ greatly from those of Kojima et al. in spite of a substantially

different pore structure and index of refraction. The pressure dependence of $\bar{\rho}_s/\rho$ at a given reduced temperature is not great, approximately a 10% increase between 15 and 30 bar.

The direct observation of m_s/m by Yanof and Reppy confirms calculations that thermal contributions to the usual fourth sound formula (Shapiro and Rudnick, 1965) are negligible. Measurements by Yanof and Reppy of Q_4 were considerably smaller than expected on the basis of viscosity calculations.

One of the puzzles of the superfluid density measurements is the failure to observe a change in superfluid density at T_{AB}. No change may be expected for several possible reasons. For one, the A and B phases are thermally very similar to one another, particularly near the PCP. The highest pressure of observations where the BA transition would have occurred in bulk is closer to the PCP than to the melting curve, and thermal differences between the phases at T_{AB} are only a few percent. The following possibility recently discussed by Combescot (1974) is based on weak coupling theory, but the idea may carry over to the actual liquid. It is likely (Ambegaokar, DeGennes, and Rainer, 1974) that in ³He-A the orbital orientation vector l is perpendicular to boundary surfaces, so that the superfluid density is oriented with superflow parallel to its perpendicular component. But for weak coupling near T_c the perpendicular component of the superfluid density tensor for the ABM state (Anderson and Brinkman, 1973), currently the model for ³He-A, is the same as the (scalar) superfluid density for the BW state (Balian and Werthamer, 1963), currently a strong contender as a model for ³He-B. Hence in weak coupling theory and for only the perpendicular component of the $\bar{\rho}_s/\rho$ tensor measured for the ABM state there would be no change in $\bar{\rho}_s/\rho$ expected at the AB transition.

The preceding argument is flawed by the assumption of weak coupling. Leggett (private communication) pointed out to the author that while in weak coupling one has $\langle| \Delta_{ABM}(\hat{K}) |^2\rangle = \frac{5}{6}\langle| \Delta_{BW}(\hat{K}) |^2\rangle$, near the PCP in strong coupling the average square of the modulus of the gap should be the same for the two states assumed to characterize the A and B phases. Hence, if the previous argument on orientation of the A liquid by boundaries is carried through in strong coupling, $\bar{\rho}_s/\rho$ should have increased by a factor 6/5 in the transition from the B to the A phase. But if the A phase were not strongly oriented so that the *average* of the principal values of the ρ_s tensor were measured in the fourth sound experiments, then no change of $\bar{\rho}_s/\rho$ would be expected across the AB transition.

If it is assumed, following what the experiments suggest, that there is no change in measured ρ_s/ρ across the AB transition, then in the absence of molecular field effects ρ_s/ρ should have the same temperature dependence as the nonmagnetic triplet component of the BW state. Since one-third of the condensed pairs for the BW state are non magnetic triplets, one would then expect without molecular fields that $(\chi_N - \chi)/\chi_N = \frac{1}{3}\rho_s/\rho$. Now if both susceptibility and superfluid density are corrected for molecular fields using Fermi liquid factors (Leggett, 1965) one finds near T_c

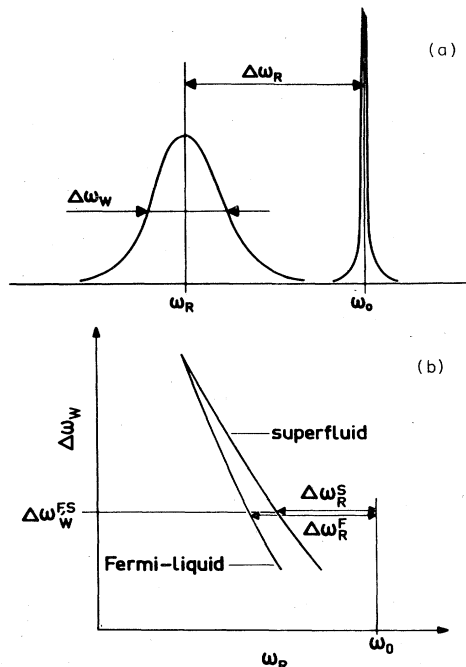$$\frac{\rho_s}{\rho} = 3\,\frac{1 + \frac{1}{4}Z_0}{1 + \frac{1}{3}F_1}\,\frac{\chi_N - \chi}{\chi_N}. \qquad (5.4)$$

FIG. 19. Measured quantities for the resonance of a vibrating wire. The resonance frequency in vacuum is ω_0 and that in ^{3}He is ω_R. The full width at half-maximum is $\Delta\omega_W$. The superscripts F and S refer to measurements in normal Fermi liquid and superfluid, respectively. After Alvesalo, Collan, Loponen, Lounasmaa, and Veuro, (1974b).

Using $(\chi_N - \chi)/\chi_N = 4.7(1 - T/T_c)$ from Eq. (3.3) and values of Z_0 and F_1 from the appendix interpolated for the pressure of 33.6 bar of the data in Fig. 18, one finds that the susceptibility would predict the superfluid density to be $\rho_s/\rho = 0.60(1 - T/T_c)$ near T_c at 33.6 bar. This is shown as a solid line on Fig. 18 and is quite close to the actual measurements. Had the experimental $(\chi_N - \chi)/\chi_N$ been consistent with the prediction of weak coupling theory then Eq. (5.4) would have predicted $\rho_s/\rho = 0.33(1 - T/T_c)$ near T_c at the same pressure, but the agreement would have been more favorable at lower pressure (the numeric would be 0.39 near the PCP). Neither ρ_s/ρ nor $(\chi_N - \chi)/\chi_N$ off the melting curve is predicted at all well by the weak coupling theory using the ABM and BW states as models, but their relationship is predicted quite closely by (5.4). Whether or not this is fortuitous must be settled by further experiments with improved geometry.

It should also be considered that the liquid may be so profoundly affected by its presence in the pores of the CMN that one or the other of the two phases is never formed at all. This seems to be countered by the experiment of Ahonen, Haikala, and Krusius (1974a), who found that neither the T_{AB} line nor the T_c line was strongly affected for ^{3}He in the pores of platinum powder with a pore size comparable to that used in the fourth sound experiment. However, it is conceivable that a substantial magnetic change could occur without much change in ρ_s/ρ.

Since the experimental values of $\bar\rho_s/\rho$ did not follow precisely a $(1 - T/T_c)$ temperature dependence pore size effects may have occurred to some extent. According to simultaneous measurements of T_c and ultrasonic attenuation (see Fig. 46), T_c itself seems not to be shifted meas-

urably by confining ^{3}He in CMN pores, so one would not expect a profound effect on $\bar\rho_s/\rho$. Furthermore, since ϱ_s may be a tensor, one must be quite careful in analyzing data and intercomparing experiments. Nevertheless, the measurements of $\bar\rho_s/\rho$ via fourth sound and those via vibrating wires (Alvesalo, et al., 1974a,b) at melting pressure appear to be different. The latter measurements near T_c, where the present intercomparison is being made, depend very importantly on the quantitative accuracy of knowledge of viscosity. But in the anisotropic fluid, viscosity may be a tensor quantity. The inevitable conclusion is that what is required for a quantitative understanding is additional experiments designed to simplify and quantify flow geometry.

VI. EXPERIMENTS ON THE DAMPING AND RESONANT FREQUENCY OF A VIBRATING WIRE

Measurements of the damping and resonant frequency of a vibrating wire have been used effectively by Black, Hall, and Thompson (1971) and Bertinat, Betts, Brewer, and Butterworth (1974) to measure the viscosity coefficient of normal Fermi liquid ^{3}He. Black et al. also used the method to measure the viscosity of dilute solutions of ^{3}He in superfluid ^{4}He. In experiments of unusual difficulty, a group at the Helsinki University of Technology (Alvesalo et al., 1973, 1974a,b) has applied this technique to the study of viscosity and normal fluid density in both normal and superfluid phases of liquid ^{3}He at melting pressure, using the compressional cooling technique. The experiments are made difficult both by the high viscosity of the fluid (over 0.1 P near T_c) and the consequent large widths of resonance curves and by the possible formation of solid on the wire. Interpretation of the results is made difficult by the possibility that the fluid may be anisotropic with normal and superfluid densities and viscosities which should be represented as tensor quantities.

In the experiments (Alvesalo, Anufriyev, Collan, Lounasmaa, and Wennerström, 1973; Alvesalo, Collan, Loponen, and Veuro, 1974a); Alvesalo, Collan, Loponen, Lounasmaa, and Veuro, 1974b) a straight NbZr wire 2.5 cm long, 0.30 mm diameter, and 7.79 g/cm^3 density is stretched, twisted, and soldered into place and excited with a variable frequency ac current of 0.4 mA rms in a transverse magnetic field which was typically 1490 G (these are valid for Alvesalo et al., 1974a,b). The wire had a resonance frequency in vacuum of about 1900 Hz and a corresponding Q of 5500. In the presence of ^{3}He the resonant frequency ω_R is shifted downward from its value ω_0 in vacuum and the width at half-maximum $\Delta\omega_W$ increases as shown in Fig. 19(a). They found that as the temperature decreased in normal Fermi liquid, the width $\Delta\omega_W$ increased while ω_R decreased until the critical temperature T_c was reached. For temperatures below T_c the width decreased again with decreasing T while the resonant frequency increased. However, for the same width $\Delta\omega_W$ the resonant frequency ω_R was higher for $T < T_c$ than it was for $T > T_c$. This behavior is shown qualitatively in Fig. 19(b). Interpretation of the results was made in terms of the experimental quantities $\Delta\omega_W{}^{F,S}$ and the corresponding $\delta\omega_R \equiv \Delta\omega_R{}^F - \Delta\omega_R{}^S$ defined in Fig. 19(b).

In interpreting the results it was assumed that the force per unit length due to the ^{3}He acting on the wire of radius
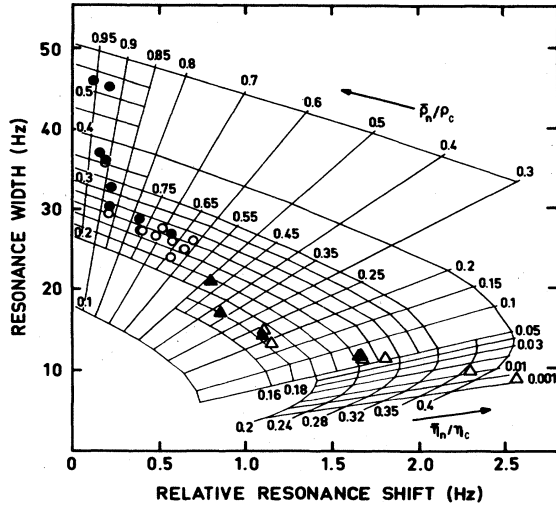
FIG. 20. Plot of resonance width, $\Delta\omega_W^{F,S}$, as a function of relative resonance shift $\Delta\omega_R^F - \Delta\omega_R^S$ valid for this width which can be used to find the reduced effective normal fluid density $\bar{\rho}_n/\rho_c$ and the reduced effective viscosity $\bar{\eta}_n/\eta_c$ of the normal fluid. The grid is computed from theory using a scalar viscosity. Open symbols are data obtained on cooling and closed on warming. Circles are A phase and triangles are B phase. Melting pressure. After Alvesalo, Collan, Loponen, and Veuro (1974a).

FIG. 21. Reduced effective normal fluid density at melting pressure as a function of both temperature and pressure difference from the A feature. Open symbols are data obtained on cooling and closed on warming. Circles are A phase and triangles are B phase. Magnetic field is 1490 G. After Alvesalo, Collan, Loponen, Lounasmaa, and Veuro (1974b).

a vibrating at angular frequency ω with instantaneous velocity $\mathbf{u}$ is

$$\mathbf{F} = -\pi a^2\{[\rho_n k(m) + \rho_s](d\mathbf{u}/dt) + \omega\rho_n k'(m)\mathbf{u}\}, \quad (6.1)$$

where $m = a/2\delta$ and $\delta = (\eta_n/\rho_n\omega)^{1/2}$ is the viscous penetration depth. This is a formula derived by Stokes (1901) and modified for a two-fluid model by Black et al. (1971). A derivation is given in an appendix of Alvesalo et al. (1974b). The functions k and k' are given in terms of Hankel functions (Alvesalo et al., 1974b). Use of the above formula, valid for fluids where ρ_n and η_n are scalars, for ^{3}He may lead to problems in interpretation. In what follows it is assumed that "effective" values $\bar{\eta}_n$ and $\bar{\rho}_n$ replace η_n and ρ_n in Eq. (6.1).

Analysis of the vibrating system based on Eq. (6.1) then leads to

$$\Delta\omega_R = \tfrac{1}{2}\omega_0\{[\bar{\rho}_n k(m) + \bar{\rho}_s]/\rho_V\} \quad (6.2)$$

and

$$\Delta\omega_W = \omega_0[\bar{\rho}_n k'(m)/\rho_V], \quad (6.3)$$

where ρ_V is the density of the wire. By combining these equations for both normal Fermi liquid and superfluid states one then finds the equation

$$\left(\frac{k-1}{k'}\right)^F - \left(\frac{k-1}{k'}\right)^S = \frac{2\delta\Delta\omega_R}{\Delta\omega_W^{F,S}}. \quad (6.4)$$

Referring to Fig. 19(b), $\delta\Delta\omega_R$ is the difference $\Delta\omega_R^F - \Delta\omega_R^S$ in the resonant frequencies in the normal Fermi liquid (F) and superfluid (S) states for the *same* resonance width $\Delta\omega_W^{F,S}$ in the normal Fermi liquid and in the superfluid. ($\Delta\omega_W^F = \Delta\omega_W^S \equiv \Delta\omega_W^{F,S}$). Now Alvesalo et al. (1974a,b)
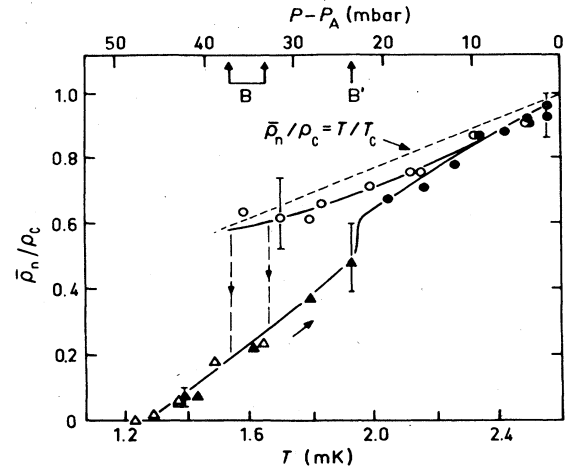
have accurate knowledge of the viscosity and density in the normal Fermi liquid, so m for the Fermi liquid and hence the first term on the left side of (6.4) may be determined. Similarly the right side of (6.4) is obtained from measurement as in Fig. 19(b). It is then possible to find m for the superfluid state from (6.4) and thus $(\bar{\eta}_n/\bar{\rho}_n)^{1/2}$. The quantities $\bar{\eta}_n$ and $\bar{\rho}_n$ may then be separately evaluated using (6.3).

In practice Alvesalo et al. (1974a,b) solved (6.4) to obtain $\Delta\omega_W^{F,S}$ as a function of $\delta\Delta\omega_R$ for $\bar{\eta}_n$ and $\bar{\rho}_n$ as parameters, displaying the results graphically. The experimentally measured coordinates then are plotted on the graph and $\bar{\eta}_n$ and $\bar{\rho}_n$ found by interpolation. This graph and some data, from Alvesalo et al. (1974a), are shown in Fig. 20. Near the critical temperature (A feature) the relative resonance shift $\delta\Delta\omega_R$ is one- or two-tenths of a hertz with a resonance width $\Delta\omega_W$ in the range 30–50 Hz, so one sees that high precision was indeed necessary to obtain meaningful measurements of $\bar{\rho}_n$. What has happened physically is that as T falls below T_c the normal fluid density decreases very slowly while the normal viscosity *decreases* dramatically.

Values of the relative effective normal fluid density $\bar{\rho}_n/\rho$ and the effective viscosity relative to that at T_c are shown in Figs. 21 and 22. Near T_c, $\bar{\rho}_n/\rho$ decreases rather slowly with decreasing temperature, but the decrease nevertheless appears to be substantially more rapid than might be suggested by the superfluid density derived from fourth sound measurements of Kojima, Paulson, and Wheatley (1974). If ^{3}He-A manifests the ABM state (Anderson and Brinkman, 1973) and the vector $\mathbf{l}$ (Fig. 27) is oriented to make the vibrating wire sensitive to the largest component of the superfluid density tensor then in weak coupling theory, as corrected for a "molecular field" effect of the Fermi liquid following Leggett (1966), one expects $d(\rho_n/\rho)/d(T/T_c) = 2/(1 + \tfrac{1}{3}F_1) = 0.32$ using F_1 valid at the melting curve (see Appendix B). This value would probably be increased in the real superfluid, as pointed out by Alvesalo et al. (1974b), since the specific heat measure-
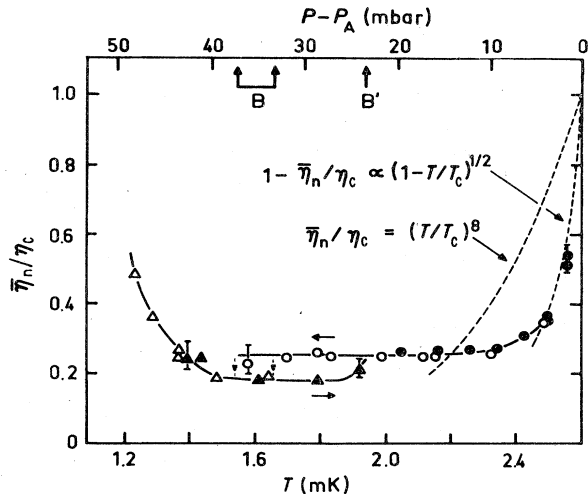
FIG. 22. Reduced effective viscosity at melting pressure as a function of both temperature and pressure difference from the A feature. Open circles are data obtained on cooling and closed on warming. Circles are A phase and triangles are B phase. Magnetic field is 1490 G. After Alvesalo, Collan, Loponen, Lounasmaa, and Veuro (1974b).

ments suggest that the square of the order parameter, to which ρ_s is proportional, increases more rapidly with decreasing temperature than that expected from weak coupling theory. However, it seems unlikely that present theories would be able to produce the rapid decrease near T_c of $\bar{\rho}_n/\rho$ with decreasing T suggested by the authors. As we have seen, the measured dependence of ρ_n/ρ on T/T_c near T_c is determined by observations of very small resonance shifts with relatively very large resonance widths. It is conceivable that where such small differences are important the physical approximation in assuming "effective" values for ρ_n and η_n may lead to quantitative problems, especially in the interpretation of $\bar{\rho}_n$ as *the* normal fluid density. Once the transition is made to ³He-B the normal fluid density decreases rapidly with decreasing temperature and becomes essentially "zero" within the experimental error for $T/T_c <$ 0.45. Again, at this extreme of the measurements, referring to Fig. 20 we see that a very small fractional error in the resonance width can lead to a very large fractional error in $\bar{\rho}_n/\rho$. Hence the very small values of $\bar{\rho}_n/\rho$ should perhaps be viewed with some caution. The relative viscosity measurements vs temperature shown on Fig. 22 show that near T_c changes in the behavior of the wire are determined almost entirely by changes in viscosity. It is interesting that this behavior was anticipated by Greytak, Johnson, Paulson, and Wheatley (1973) from their heat flow measurements at lower pressure in ³He-B. They suggested that η/η_c might vary as $(T/T_c)^n$ with n in the range 6–10. The case $n = 8$ shown on Fig. 22 clearly does not fall as rapidly as the observations, which are more in line with the dependence $(1 - \bar{\eta}_n/\eta_c) = c(1 - T/T_c)^{1/2}$, where c is a parameter, as predicted by Shumeiko (1973) for an isotropic neutral Fermi liquid and Soda and Fujiki (1974) for an anisotropic fluid. However, the more recent heat flow measurements of Johnson, Kleinberg, Webb, and Wheatley (1974) qualitatively support the viscosity measurements of Alvesalo et al. (1974a,b). For a more precise picture of the viscosity near T_c, see Sec. IX.

After the initial rapid drop in $\bar{\eta}_n/\eta_c$ the effective viscosity

becomes essentially temperature independent. This was also predicted as an asymptotic result as $T \to 0$ by Shumeiko (1973). Both ³He-A and ³He-B have a nearly temperature-independent effective viscosity in the intermediate temperature range with $\bar{\eta}_B \simeq 0.7\bar{\eta}_A$, but at lower temperatures $\bar{\eta}_B$ appears to rise again.

It is impossible not to conclude that these are beautiful measurements, but once again the possible intercomparison with other experiments and with theory is strongly affected by the possibility of anisotropy and the consequent effects of orientation and geometry.

VII. HEAT FLOW

Probably some of the most spectacular effects in super-fluid ⁴He are closely related to the hydrodynamic flow of heat, especially in the temperature range from about 1 K to the lambda point. Understanding of the phenomenon itself is rooted in the notion of two interpenetrating fluids. One, the superfluid, carries no entropy and flows with zero curl while the other, the normal fluid, flows like an ordinary fluid and carries the entropy with it. When one attempts to impose a temperature gradient on the two fluids the superfluid accelerates, leading to the helium fountain if the helium is not confined but to a static fountain pressure if the fluid is confined. Under the action of the fountain pressure heat then flows by transport of the normal fluid with a counterflow of superfluid such that there is no net mass transport. Heat thus flows like water flows, or hydrodynamically. The extent of this analogy has been emphasized by Brewer and Edwards (1961). Thus hydrodynamic heat flow is a manifestation of several of the basic concepts of the two-fluid model of superfluidity. Now as we have emphasized earlier ³He is probably different in that the superfluid itself may have several components depending on spin correlations, as would be manifested in experiments involving a magnetic field. But in heat flow the various superfluid components, if any, would presumably flow as a unit. Experiments on heat flow in liquid ³He were therefore undertaken to test whether concepts like interpenetrating superfluid and normal fluid, fountain pressure, curl-free superflow, and normal viscosity had some validity.

Quantitative analysis of heat flow in superfluid ⁴He (London and Zilsel, 1948; Gorter and Mellink, 1949) is made on the basis of a hydrodynamic conductivity κ_h given for a tube of diameter d by

$$\kappa_h = TS^2d^2/32\eta, \tag{7.1}$$

where S is entropy per unit volume and η is normal viscosity. If ³He is an anisotropic fluid both the superfluid and normal fluid densities and the viscosity are probably tensor quantities, so a viscosity derived using Eq. (7.1) would have to be regarded as an effective viscosity and would probably depend on the way the experiment is carried out.

From a qualitative standpoint the question of whether or not heat flows hydrodynamically can be answered with high probability, through not proved, by a very simple experiment. Referring to Fig. 3, the left-hand "appendix" is fitted with a heater and a CMN magnetic thermometer, reading $T_2{}^*$, which are connected by a tube of diameter d to the main cell filled with CMN acting both as thermal
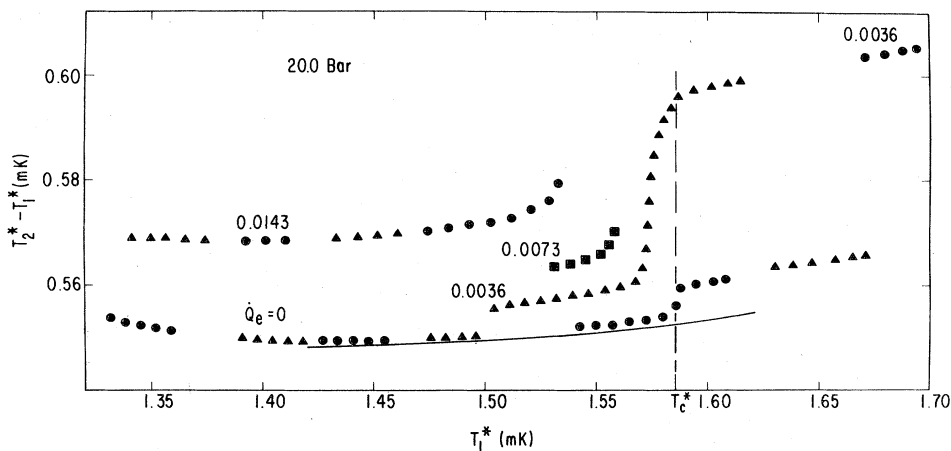
FIG. 23. Difference in the indicated magnetic temperature difference $T_2^* - T_1^*$ across heat flow column as a function of the magnetic temperature T_1^* of the larger (reservoir) thermometer. T_c^* is the temperature of the center of the thermal second-order transition from ³He-B to normal liquid and ³He pressure is 20.0 bar. The different symbols correspond to different runs and the numbers refer to externally applied $\dot{Q}$ in erg/sec. All points at the bottom refer to zero applied $\dot{Q}$. The solid line is the empirically deduced dependence of $T_2^* - T_1^*$ on T_1^* for zero total $\dot{Q}$, the effect of the residual heat flow down the column of 0.73×10^{-3} erg/sec having been accounted for. After Johnson, Kleinberg, Webb, and Wheatley (1974).

reservoir and as a second thermometer, reading T_1^*. If heat flows in ³He by diffusive motions of the quasiparticles only, then for a fixed heat flow rate $\dot{Q}$ the temperature difference between the two thermometers is proportional to the reciprocal κ_d^{-1} of the diffusive conductivity. Now it is known at present from the experiments of Alvesalo et al. (1974a,b) that the effective viscosity for the vibrating wire experiments decreases rapidly below T_c in ³He-A. [Actually it had been suggested earlier by Greytak et al. (1973) on the basis of heat flow measurements that the viscosity would decrease rapidly below T_c.] It is quite reasonable to suppose that all diffusive transport properties would behave similarly, in particular that κ_d would also decrease below T_c. Such behavior has been predicted both by Shumeiko (1973) and by Soda and Fujiki (1974). Thus, for only diffusive conductivity operative, one would expect the temperature difference to *decrease* on warming through the region of T_c. On the other hand, if heat flows hydrodynamically, then in a suitable geometry $\kappa_h + \kappa_d$ will be large enough for temperatures below T_c that the temperature difference will *increase* on warming through the region of T_c. The results of an experiment in ³He-B and normal Fermi liquid by Johnson, Kleinberg, Webb, and Wheatley (1975) are shown in Fig. 23. To show the effect clearly magnetic temperatures T^* are displayed. Even when the two powdered CMN thermometers T_2^* and T_1^* have the same temperature they do not give the same reading owing to differences in shape and packing, but the difference $T_2^* - T_1^*$ does vary slowly with temperature when the two are in thermal equilibrium, giving a slowly varying baseline, The temperature difference $T_2^* - T_1^*$ *increases* very substantially on warming through T_c, thus strongly suggesting that heat flows hydrodynamically.

Figure 23 displays some of the quantitative problems which are experienced in these experiments. First of all the heat flow levels needed to produce large effects are very small. Even when the externally applied $\dot{Q}$ is zero it is observed that $T_2^* - T_1^*$ rises abruptly near T_c. That is because about 0.73×10^{-3} erg/sec of residual heat leak down the column cannot be "turned off." And the difference

ΔT in the absolute temperatures of the two thermometers cannot be simply displayed either since the $T - T^*$ relationship for the two thermometers is not known accurately. (A provisional $T - T^*$ relation is available, see Appendix A, but for ΔT one needs dT/dT^* which is not at all well known.) To display data quantitatively, thermal conductivities (or resistances) are based on the thermal conductivity of low pressure (32 mm Hg) normal Fermi liquid measured in the same temperature range. The change in $T_2^* - T_1^*$, $\Delta(T_2^* - T_1^*)$, produced by a change in heat flow $\dot{Q}$ is measured and a resistance $R^* \equiv \Delta(T_2^* - T_1^*)/\dot{Q}$ defined. Then it is divided by the analogous quantity R_{32}^* measured at low pressure in the same geometry with the same thermometers for the same average temperature in the heat flow column. Now since T is known approximately by (P_c, T_c) thermometry (see Appendix A) the thermal conductivity of the low pressure ³He may be obtained by *extrapolation* to lower temperatures of the data of Abel, Johnson, Wheatley, and Zimmermann (1967) and κ obtained from that at 32 mm Hg pressure, κ_{32}, by

$$\kappa = (R^*/R_{32}^*)^{-1}\kappa_{32}. \tag{7.2}$$

More quantitative information on the heat flow is contained in Fig. 24 for pressures of 20.0 and 29.6 bar from the experiments of Greytak et al. (1973) and Johnson et al. (1975). The question of hydrodynamic heat flow is proved by the data on ³He-B shown in the upper right of Fig. 24. The characteristic feature of the hydrodynamic conductivity is its dependence on geometry as in Eq. (7.1). Since R^*/R_{32}^* should be proportional to d^{-2}, the data of Greytak et al. obtained with a 2 mm diameter tube have been multiplied by a factor of 4/9 to compare them directly with the data of Johnson et al. obtained with a 3 mm tube. The two are not distinguishable within the accuracy of knowledge of the geometry or the general accuracy of the measurements. But in addition to proving the existence of hydrodynamic heat flow this intercomparison shows that the diffusive conductivity κ_d does not play a major role in heat flow below T_c for our measurements. Hence it appears that κ_d drops rapidly below T_c in analogy with the viscosity. This con-
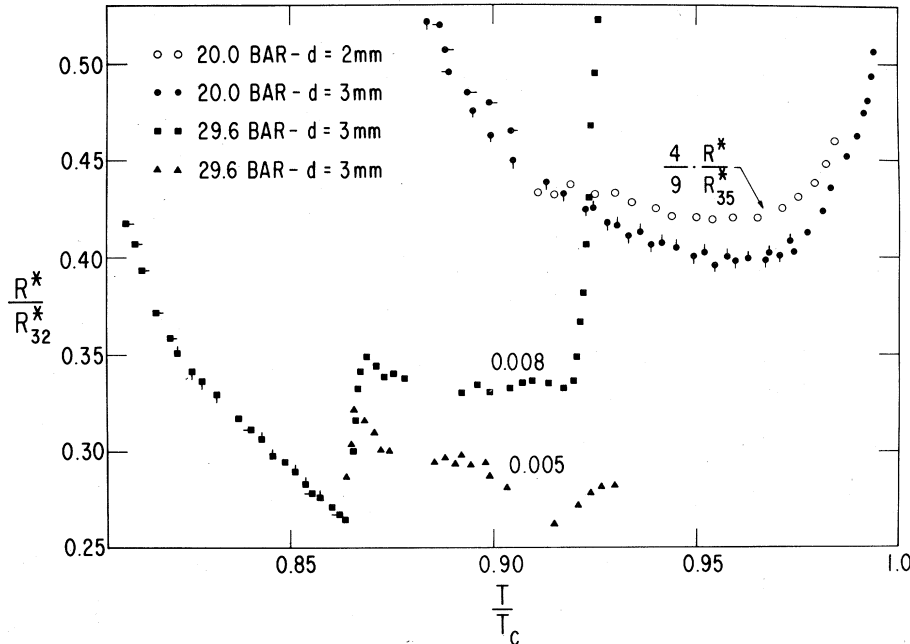
FIG. 24. Ratio $R^* R_{32}^*$ as a function of T/T_c for ^{3}He-B at 20.0 bar [($\bullet$), 3 mm diam tube; ($\bigcirc$), 2 mm diam tube] and at 29.6 bar [($\square$), 3 mm diam tube] and for ^{3}He-A at 29.6 bar in a 3 mm diam tube [($\blacksquare$), $\dot{Q}_e = 0.008$ erg/sec; ($\blacktriangle$), $\dot{Q}_e = 0.005$ erg/sec]. The flags on the points for ^{3}He-B refer to the following $\dot{Q}_e$ in 10^{-3} erg/sec. Solid circles: to right, 28.6; up, 20.0; down, 14.3; to left, 7.1; no flag, 3.6. Solid squares: to right, 19.9; down, 10.0; up, 9.0; no flag, 8.0; left, 3.5. After Johnson, Kleinberg, Webb, and Wheatley (1975).

clusion is surprising, in view of the results of Shumeiko (1973) and Soda and Fujiki (1974) that κ_d should decrease as Δ^2.

Thermal resistance in ^{3}He-B (at 20.0 bar and below $T/T_c \simeq 0.87$ at 29.6 bar) does not depend on $\dot{Q}$ at the levels used, except very near T_c. This is not the case for ^{3}He-A, as can be seen in Fig. 24, where data are displayed for $\dot{Q} = 0.008$ and 0.005 erg/sec. The dependence of R^*/R_{32}^* on $\dot{Q}$ in ^{3}He-A at a fixed temperature is shown in Fig. 25. The data fit a linear law, though the linear extrapolation to $\dot{Q} = 0$ may be questioned. The data may also be displayed using a superfluid–normal fluid relative velocity scale v by using the equation

$$v = \frac{\dot{Q}}{(\rho_s/\rho)(TS)(\frac{1}{4}\pi d^2)}, \qquad (7.3)$$

where S is entropy per unit volume and ρ_s/ρ is the relative superfluid density. Following Kojima et al. (1974) the superfluid density is estimated by $\rho_s/\rho \simeq \frac{1}{2}(1 - T/T_c)$. It is also assumed that $S = S_N(T_c)(T/T_c)^m$ with $S_N(T_c)$ the normal fluid entropy at T_c and $m = C_</C_>$, the ratio of specific heats at T_c. One possible qualitative interpretation of Fig. 25 which is conceivable with anisotropic ^{3}He-A is that the effective viscosity is dependent on flow velocity v, corresponding to gradual change in domain orientation with flow (DeGennes and Rainer, 1974). Careful experiments with different geometries are clearly necessary to check such speculation.

Values of effective viscosity can be deduced from the data via Eq. (7.1). It is found (Johnson et al., 1975) that the effective viscosity $\bar{\eta}$ relative to its value η_c does not depend strongly on pressure and in the B phase has a similar behavior near T_c to that found by Alvesalo et al. (1974a,b) in the A phase. The relative viscosity in the A phase is determined by a linear extrapolation of R^*/R_{32}^* to $\dot{Q} = 0$. Using this approach there is no significant change in $\bar{\eta}/\eta_c$
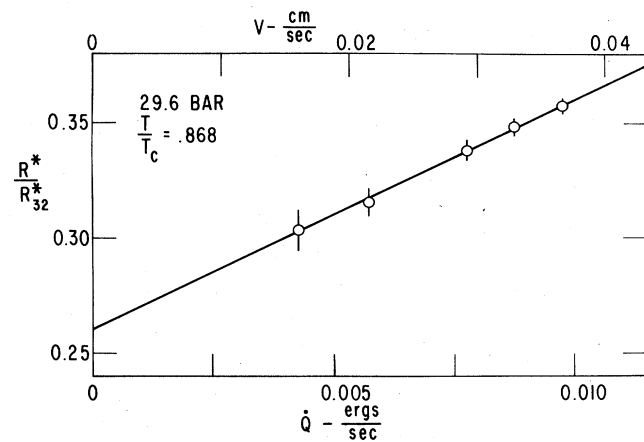

FIG. 25. Dependence of R^*/R_{32}^* in ^{3}He-A on $\dot{Q}$ at fixed $T/T_c = 0.87$ and a pressure of 29.6 bar. The flags on the points show the effect on R^*/R_{32}^* of a 10^{-4} mK change in $\Delta(T_2^* - T_1^*)$. Also shown horizontally is the relative velocity between superfluid and normal fluid as calculated from Eq. (7.3). After Johnson, Kleinberg, Webb, and Wheatley (1975).

across the $B \rightarrow A$ transition. However, Johnson et al. find that in the regions of approximate temperature independence of the relative viscosity that $\bar{\eta}/\eta_c \simeq 0.4$ instead of the 0.25 found by Alvesalo et al. (1974a,b). These results are shown in Fig. 26. In spite of the many uncertain quantities (κ_{32}, η_c, S) entering into the computation of $\bar{\eta}/\eta_c$ from heat flow data it is hard to see how there could be such a large discrepancy, but then of course there is the everpresent uncertainty regarding the interpretation of $\bar{\eta}$.

Near $T/T_c = 1$ we find that the data are fit approximately by the equation

$$1 - \eta/\eta_c \approx 2.9(1 - T/T_c)^{1/2}/(T/T_c)$$

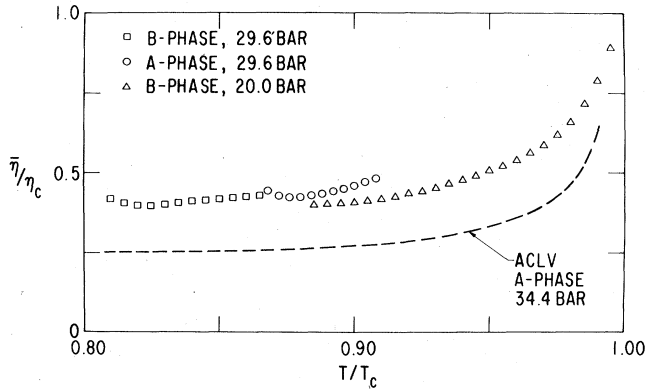$$- 3.5[(1 - T/T_c)^{1/2}/(T/T_c)]^2.$$

FIG. 26. Reduced effective viscosity $\bar{\eta}/\eta_c$ in ^{3}He-A at 29.6 bar and in ^{3}He-B at 29.6 and 20.0 bar as a function of reduced temperatue T/T_c as deduced from heat flow measurements by Johnson, Kleinberg, Webb, and Wheatley (1975). The dashed line marked ACLV is taken from the A phase measurements at melting pressure of Alvesalo, Collan, Loponen, and Veuro (1974a).

The coefficient of the leading term is rather close to that calculated by Soda and Fujiki (1974) for an isotropic superfluid. This result should be regarded with caution, however, since values of η/η_c obtained from heat flow are indirect and subject to error as indicated in the preceding paragraph.

Once again we find a poor quantitative comparison between measurements made at pressures well below melting pressure with those, Sec. VI, made at melting pressure in an adiabatic compression cell. Although improvements in the measurements and their interpretation may resolve possible discrepancies, such as the failure to observe a discontinuity in both η_n and ρ_s/ρ across the AB transition, we should continue to use care in how we interrelate experiments performed under different conditions.

A variety of critical flow or onset phenomena are observed in the heat flow measurements. For ^{3}He-B there is an onset of nonlinear resistance just below T_c which is described by a critical velocity, obtained from Eq. (7.3), of 0.4 to 0.5 cm/sec. For ^{3}He-A there are several different phenomena, the most striking and reproducible being like that shown in Fig. 24 for $\dot{Q} = 0.008$ erg/sec at $T/T_c \simeq 0.92$. Such onset phenomena are characterized by $v \simeq 0.08$ cm/sec for $\dot{Q}$ small (close to T_c) and by $v \simeq 0.045$ cm/sec for larger $\dot{Q}$ (farther from T_c). But there are other more subtle changes that occur with lower velocities. Also, nonreproducibly the thermal resistance can jump to a rather higher value than expected when $\dot{Q}$ is reapplied after a period with $\dot{Q} = 0$. The corresponding critical velocities are as low as 0.02 cm/sec. Unfortunately, the apparatus of Johnson et al. is not suitable for critical velocity studies, particularly since the temperature difference across the column is too large and the temperature cannot readily be held fixed while v is varied.

VIII. DYNAMIC NUCLEAR MAGNETISM

The conception and design of experiments on dynamic nuclear magnetism in superfluid ^{3}He has been more strongly influenced by theoretical models and ideas than any other experimental area. Early suggestions by Leggett (1973a) and Anderson (1973) in particular had a very important effect

on the experimental development subsequent to the discoveries by Osheroff, Gully, Richardson, and Lee (1972b) of a temperature-dependent shift of the perpendicular NMR frequency in the A phase and a reduction of amplitude of NMR in the B phase. Since experiments were devised on the basis of certain theoretical ideas, the experiments themselves can be better understood following a brief discussion of theoretical concepts. Our discussion is based on that given by Leggett (1974a) and Leggett (private communication).

All theoretical discussion of the properties of superfluid ^{3}He has been based on BCS-like pairing theories with the pairs in relative angular momentum states with $l \geqslant 1$ as suggested in early theoretical work by Pitaevskii (1959); Brueckner, Soda, Anderson, and Morel (1960); Emery and Sessler (1960); Thouless (1960); Anderson and Morel (1961); and Balian and Werthamer (1963). For $l = 0$ pairing and superfluid at rest the ordered states are spin singlets with pairing $(+\mathbf{p}\uparrow, -\mathbf{p}\downarrow)$. The "condensed" phase is described by an isotropic order parameter d_0; that is, the order parameter d_0 does not depend on the direction $\hat{\mathbf{n}} \equiv \mathbf{p}/|\mathbf{p}|$. For even l pairing but $l \neq 0$ the order parameter would in principle vary over the Fermi surface so that $d_0 = d_0(\hat{\mathbf{n}})$. For odd l pairing, the order parameter also depends in principle on $\hat{\mathbf{n}}$. Furthermore, the order parameter will depend on spin since for odd l the pairs must be in triplet states. Now it does seem likely from measurements of static magnetism which suggest that ^{3}He-A and ^{3}He-B have the same T_c, from the presently known spin dynamics, and from the phase diagram that both ^{3}He-A and ^{3}He-B have triplet pairing and the same l. For triplet pairing we can have three interpenetrating and weakly interacting superfluids, corresponding to the two magnetic pairings $\uparrow\uparrow$ and $\downarrow\downarrow$ and the nonmagnetic pairing $(1/\sqrt{2})(\uparrow\downarrow + \downarrow\uparrow)$. The superfluids are described by order parameters $d_{\uparrow\uparrow}(\hat{\mathbf{n}})$, $d_{\downarrow\downarrow}(\hat{\mathbf{n}})$, and $d_{\uparrow\downarrow}(\hat{\mathbf{n}})$. An alternative description of the ordering is in terms of a vector $\mathbf{d}$ in spin space with components d_x, d_y, and d_z such that

$$d_{\uparrow\uparrow} = -d_y - id_x, \quad d_{\downarrow\downarrow} = -d_y + id_x \quad \text{and} \quad d_{\uparrow\downarrow} = id_z, \quad (8.1)$$

with the z axis the axis of quantization of the spins and each d component depending on $\hat{\mathbf{n}}$. It is not necessary that all three types of superfluids be present at once. For example, it has been suggested (Ambegaokar and Mermin, 1973) that the splitting of the second-order transition by a magnetic field is to be understood in terms of formation first of a $\uparrow\uparrow$ superfluid and then at a lower temperature of a $\downarrow\downarrow$ superfluid. This idea is explored in detail in Sec. IX. The A phase itself is thought to have only $\uparrow\uparrow$ and $\downarrow\downarrow$ (equal-spin-pairing) components and no $\uparrow\downarrow$ component (Anderson and Brinkman, 1973). This follows immediately from the experimental observation that the static nuclear magnetism in ^{3}He-A is temperature independent; as $H_0 \rightarrow 0$ the $\uparrow\uparrow$ and $\downarrow\downarrow$ pairs are equally magnetic with the excited quasiparticles. The nearly constant NMR absorption in the A phase as observed in the work of Osheroff et al. (1972b) guided early theoretical work in this regard. Similarly, since the static magnetism of ^{3}He-B decreases with decreasing temperature, this phase must have some $\uparrow\downarrow$ component.

These different superfluid components certainly will lead to a richer variety of phenomena than are found in super-
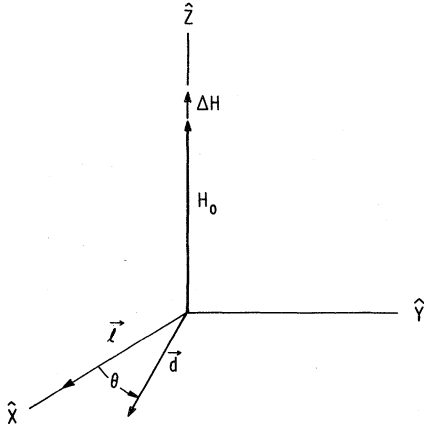
FIG. 27. Diagram illustrating the relative orientations for a parallel incremental field change experiment of the orbital orientation vector l, the order parameter vector **d**, and the magnetic fields H_0 and ΔH.

fluid ⁴He. Both Leggett (1974a) and Maki and Tsuneto (1974) have discussed how the $\uparrow\uparrow$ and $\downarrow\downarrow$ superfluid components of ³He-A can be conceived as two superfluids weakly coupled by a coherent nuclear dipole–dipole interaction leading to Josephson effects.

The new effects in the dynamic magnetism appear to be rooted in a significant average dipolar interaction between spins which results from the correlation of paired spins. The order of magnitude of the dipolar energy per unit volume is estimated by the product of the number of spins per unit volume N, the mutual dipolar energy between two spins $\gamma^2\hbar^2/a^3$, and the joint probability $(\Delta/\epsilon_F)^2$ that each of the spins is one of an ordered pair (Δ is the energy gap). Using $Na^3 \simeq 1$ and $N/\epsilon_F \simeq 2N(0)$ the dipolar energy is then estimated by $[2\gamma\hbar N(0)\Delta]^2$. Near T_c we expect the magnitude of the dipolar energy to increase linearly with the reduced temperature difference $(1 - T/T_c)$ since Δ^2 is proportional to this quantity.

Reflecting the highly anisotropic interaction between a pair of magnetic dipoles, the average dipolar energy per unit volume in the superfluid state depends on the relative orientation of ordered spins and ordered orbital motion. Following Leggett the spin dynamics are described, neglecting relaxation, by the equation

$$dS/dt = \gamma S \times H + R_D,$$ (8.2)

where S is the angular momentum per unit volume, γ is the gyromagnetic ratio, H is applied field (static and dynamic), and R_D is a dipolar torque, zero in equilibrium, which depends in general on the relative orientation of the correlated spins with respect to the correlated orbital motion. The torque R_D depends on the orientation of the $d(\hat{n})$. As long as the angular momentum density S is constant and equal to its equilibrium value $\chi H/\gamma$ there is no torque R_D from the correlated spins tending to change it. However, in the event a nonequilibrium condition is set up then d changes with time and in general a torque R_D may develop to change S. On a sufficiently short time scale the coherent orbital motion is not expected to change but the vector $d(\hat{n})$ executes a simple precession about the vector $H -$

$\gamma S/\chi$:

$$\dot{d} = \gamma d \times (H - \gamma S/\chi),$$ (8.3)

where H is the total magnetic field and χ the susceptibility. Thus the nonequilibrium $d(\hat{n})$ is rotated with respect to the equilibrium $d(\hat{n})$, the torque R_D depending on the axis and angle of rotation.

A general discussion of how R_D can be calculated may be found in Leggett (1974a). But for present purposes it is sufficient to consider two cases. In one d has the same direction for all $\hat{n}$ and has the general form $d(\hat{n}) = \hat{d}f(\hat{n})$ where $\hat{d}$ is a unit vector in the direction of d and f is some function. The corresponding dipolar torque is

$$R_D = \lambda(\hat{d} \times \hat{x})(\hat{d}\cdot\hat{x}),$$ (8.4)

where $\hat{x}$ is the direction of $\hat{d}$ in equilibrium and λ is a temperature-dependent quantity. A torque with these properties describes experiments on ³He-A. In the ABM state (Anderson and Brinkman, 1973), valid for $l = 1$ pairing, a possible angular dependence of d is given by

$$d_{ABM}(\hat{n}) = (\tfrac{3}{2})^{1/2}\hat{d}(n_y + in_z),$$ (8.5)

where n_y and n_z are the y and z components of $\hat{n}$. This is shown pictorially in Fig. 27. This order parameter vector points in the *same* direction $\hat{d}$ for all pairs. The ABM state is an equal-spin-pairing state, so $d_{\uparrow\downarrow} = 0$. From Eq. (8.1) this means that $d_z = 0$ or that in equilibrium d lies in the x–y plane; in particular, in equilibrium d lies along $\hat{x}$ so that $R_D = 0$, Eq. (8.4). Since d is proportional to $(n_y + in_z)$ there are no ordered pairs with only x components of momentum, and pairing is strongest for pair momenta in the plane perpendicular to $\hat{x}$. The form $n_y + in_z$ has an axial quality like a Y_1^1 spherical harmonic referred to the $\hat{x}$ axis. Thus this ordering can be thought of in terms of a correlated orbital motion with axis l parallel to $\hat{x}$. The direction of the axis l is determined (Ambegaokar, De-Gennes, and Rainer, 1974), apart from magnetic torques, by depairing at boundaries, which tends to orient l normal to boundaries, and by flow, which tends to orient l along the flow velocity to minimize the energy of superflow. The corresponding dipolar energy E_D depends on the direction of $\hat{d}$ according to the formula

$$E_D^{ABM} = E_a - \tfrac{1}{2}\lambda \cos^2\theta,$$ (8.6)

where E_a and λ depend on temperature and θ is defined in Fig. 27. In obtaining this equation it is assumed that the orbital ordering described by $n_y + in_z$ remains fixed while the direction of $\hat{d}$, describing the spin ordering, is allowed to change. For the particular symmetry of the ABM state the dipolar energy will be the same for all directions of $\hat{d}$ in a cone of half-angle θ about the axis. According to Eq. (8.6) the dipolar energy is minimized when $\theta = 0$ or π. Further, if θ is different from these values the spin system will experience a torque given by Eq. (8.4).

In the second case of immediate practical interest to ³He a torque R_D develops if d rotates about some axis $\hat{\omega}$, the torque being parallel to $\hat{\omega}$, but no torque results on incremental rotation of d about a perpendicular axis. At the

same time the energy required to change the direction of the axis $\hat{\omega}$ is very small. A torque with these properties describes experiments on ³He-B. The above properties are characteristics of the $l = 1$ pairing BW state (Balian and Werthamer, 1963), for which the order parameter vector is

$$\mathbf{d}(\hat{\mathbf{n}}) = \mathbf{R}(\hat{\omega}, \theta)\hat{\mathbf{n}}, \tag{8.7}$$

where $\mathbf{R}(\hat{\omega}, \theta)$ is a unit rotation matrix describing a rotation by angle θ about axis $\hat{\omega}$. The dependence of dipolar energy on θ is given by

$$E_D^{\mathrm{BW}} = E_b + \Lambda(\cos\theta + 2 \cos^2\theta), \tag{8.8}$$

where E_b and Λ depend on temperature. Brinkman (1974) has derived equations of motion for $\mathbf{S}, \hat{\omega}$, and θ on the basis of the above properties and Leggett's equations [Eqs. (8.2) and (8.3)]. He finds

$$\dot{\mathbf{S}} = \gamma(\mathbf{S} \times \mathbf{H}) + \hat{\omega}\Lambda \sin\theta(1 + 4\cos\theta), \tag{8.9}$$

$$\dot{\theta} = -\hat{\omega}\cdot\mathfrak{IC}, \tag{8.10}$$

and

$$\dot{\hat{\omega}} = \tfrac{1}{2}\hat{\omega} \times \mathfrak{IC} + \frac{1 + \cos\theta}{2 \sin\theta} [\hat{\omega}(\hat{\omega}\cdot\mathfrak{IC}) - \mathfrak{IC}], \tag{8.11}$$

where $\mathfrak{IC} = \gamma(\mathbf{H} - \gamma\mathbf{S}/\chi)$ and Λ is a temperature-dependent parameter. The axis $\hat{\omega}$ is determined in the bulk by the direction of the magnetic field $\mathbf{H}$ and near a surface by the normal to the surface owing to the depairing effect, respectively, of the magnetic field (Leggett, 1974a; Engelsberg, Brinkman, and Anderson, 1974) and boundaries (Brinkman, Smith, Osheroff, and Blount, 1974). If the word "isotropic" is used to describe a system having the above properties, the term in the present context applies to the very weak dependence of system energy on $\hat{\omega}$ at constant θ.

The relationship of the above concepts to experiment can be understood simply in terms of two simple experiments in which the equilibrium of the spin system is suddenly changed. In the first case we imagine that the field is suddenly changed by a small amount parallel to itself, and in the second case we imagine a sudden perpendicular field change. In an ordinary system the response of the spin magnetization to a parallel field change would be a relaxation to the new equilibrium value as heat flows between spins and lattice. The response to an incremental field change perpendicular to a field H_0 would be a precessional ringing of the magnetization at angular frequency γH_0 with eventual relaxational decay. The response of superfluid ³He to parallel and perpendicular incremental field changes is quite different, especially for parallel field changes, which we outline below using for our illustration the axial state torque, Eq. (8.4), which seems to be valid for ³He-A.

In our first example suppose that the ³He is placed in a magnetic field $H_0\hat{\mathbf{z}}$ for a period of time long enough to achieve equilibrium. Then let the magnetic field be changed by an amount $\hat{\mathbf{z}}\Delta H$ *parallel* to the above field as in Fig. 27. In an ordinary system the magnetization would change exponentially with time according to a characteristic spin-lattice relaxation time until a new equilibrium were reached.

However, for superfluid ³He-A, immediately after changing the field by ΔH along $\hat{\mathbf{z}}$ the $\mathbf{d}$ vector starts to precess [Eq. (8.3)] at rate $-\gamma\Delta H$ and, as the magnetization changes, at the rate

$$\dot{\theta} = -\gamma(\Delta H - \gamma\Delta S_z/\chi). \tag{8.12}$$

From Eq. (8.4) the spins experience a torque

$$\mathbf{R}_D = -\lambda \sin\theta \cos\theta\hat{\mathbf{z}} = -\tfrac{1}{2}\lambda \sin 2\theta\hat{\mathbf{z}}, \tag{8.13}$$

which can be approximated by $\mathbf{R}_D \simeq -\lambda\theta\hat{\mathbf{z}}$ for small θ. If we then take the time derivative of Eq. (8.2), noting that $\mathbf{S} \times \mathbf{H} \equiv 0$, and substitute (8.12) and the linear approximation to (8.13) we find

$$d^2\Delta S_z/dt^2 = -\lambda\dot{\theta} = \lambda\gamma(\Delta H - \gamma\Delta S_z/\chi). \tag{8.14}$$

The solution of this equation is

$$\gamma\Delta S_z = \chi\Delta H[1 - \cos\Omega t], \tag{8.15}$$

with

$$\Omega^2 = \gamma^2\lambda/\chi.$$

The incremental magnetization $\gamma\Delta S_z$ rings parallel to itself at the temperature-dependent frequency Ω. Near T_c the dipolar energy parameter λ should be proportional to the square of the energy gap and depend on temperature as $(1 - T/T_c)$. Thus Ω^2 should be proportional to $(1 - T/T_c)$, but have no dependence on H_0. Both the motivation for and the execution of the parallel ringing experiments of Webb, Kleinberg, and Wheatley (1974a) may be understood on the basis of the above analysis. Since a sudden change of field parallel to the steady field H_0 produces a parallel ringing with time at frequency Ω, then a resonance experiment with rf field parallel to the field $\mathbf{H}_0$ should lead to resonance absorption at the same frequency Ω.

In our second example let us examine what happens in the case of an incremental perpendicular field change. The geometry is illustrated in Fig. 28, where the initial field $\mathbf{H}_0$ and initial spin density $\mathbf{S}_i$ have the same direction and lie in the y-z plane as shown. The axis $\mathbf{l}$ is chosen to be along $\hat{\mathbf{x}}$, but any direction perpendicular to $\mathbf{S}$ would have sufficed. After sufficient time has elapsed for equilibrium to be achieved, the field is suddenly changed by the perpendicular increment $\Delta\mathbf{H}$ to $\hat{\mathbf{z}}H_0$ (H_0 is defined as $\mathbf{H}_i\cdot\hat{\mathbf{z}}$). Then for small changes we have

$$\mathbf{H} - \gamma\mathbf{S}/\chi \simeq -\hat{\mathbf{x}}\gamma S_x/\chi - \hat{\mathbf{y}}\gamma S_y/\chi. \tag{8.16}$$

Applying Eqs. (8.2), (8.3), and (8.4) we find

$$\dot{\mathbf{S}} = \hat{\mathbf{x}}(\gamma H_0 S_y) + \hat{\mathbf{y}}(-\gamma H_0 S_x + \lambda\hat{d}_z), \tag{8.17}$$

and

$$\dot{\hat{\mathbf{d}}} = -\hat{\mathbf{z}}[\gamma^2 S_y/\chi], \tag{8.18}$$

where we have set $|\hat{d}_x| = 1$, and neglected terms proportional to $\hat{d}_y$ and $\hat{d}_z$ compared with those proportional to $\hat{d}_x$.
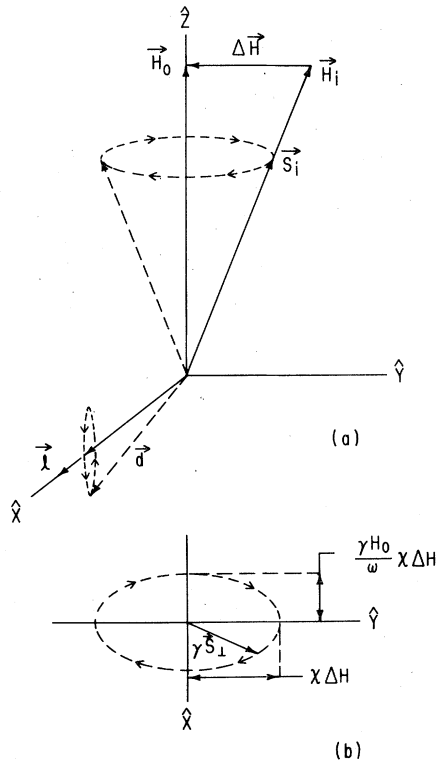
FIG. 28. (a) Diagram illustrating the relative orientation and motion in a perpendicular incremental field change experiment of the spin angular momentum per unit volume vector S (initial value S_i), the magnetic field vector H (H_i initially, H_0 finally, ΔH incremental change), the order parameter vector d, and the orbital axis 1. (b) Top view of the tip of the magnetization vector, $\gamma S_\perp$.

Here $\hat{d}_i$ is the ith component of the unit vector $\hat{d}$. Taking the time derivative of the y component of Eq. (8.17) and substituting from (8.17) for $\dot{S}_x$ and from Eq. (8.18) for $d\hat{d}_x/dt$ we find

$$\ddot{S}_y = -(\gamma H_0)^2 S_y - (\gamma^2 \lambda/\chi) S_y, \tag{8.19}$$

an equation which is solved by

$$\gamma S_y = \chi \Delta H \cos\omega t, \tag{8.20}$$

where

$$\omega^2 = (\gamma H_0)^2 + \Omega^2; \qquad \Omega^2 \equiv \gamma^2 \lambda/\chi. \tag{8.21}$$

Integration of the $\hat{x}$ component of (8.17) then gives

$$\gamma S_x = \chi \Delta H (\gamma H_0/\omega) \sin\omega t. \tag{8.22}$$

Thus on making an incremental perpendicular field change the magnetization undergoes a precessional ringing at frequency $[(\gamma H_0)^2 + \Omega^2]^{1/2}$, the tip of the S vector following an elliptical path as shown in Fig. 28. Note that as $H_0 \to 0$, the frequency $\omega \to \Omega$ and the precessional ringing becomes simply a linear ringing as in the parallel ringing case. It is a particular property of the coherent torque (8.4) that the parallel ringing frequency and the perpendicular ringing shift, defined as $[\omega^2 - (\gamma H_0)^2]^{1/2}$, are equal to one another. Again, since a sudden change of field perpendicular to H_0

leads to a ringing at frequency ω, then a resonance experiment with rf field applied perpendicular to H_0 should lead to resonance absorption at the same frequency ω.

Before any of the above concepts had been developed Osheroff, Gully, Richardson, and Lee (1972b) had performed their remarkable perpendicular NMR experiments on ^{3}He contained in a compressional cooling cell (Fig. 2). These experiments were of crucial importance to the subsequent theoretical development. Some of their results are shown in Fig. 29, which shows the NMR absorption, for the rf field perpendicular to the steady field, as a function of frequency. The pressure change shown is with respect to the A feature on the pressurization curve, so the first profile is for a temperature just above T_c while the last three are at temperatures successively less than T_c. The strange line shape is caused in part by the distribution of ^{3}He and rf field and in part by selective formation of solid ^{3}He in the coil, the solid being much more magnetic than the liquid. The feature to observe is the splitting off, for $T < T_c$ [or $p \equiv (P - P_A) > 0$], of a line at higher frequency with the frequency splitting increasing with decreasing T.

Subsequently experiments have been performed by Osheroff and Brinkman (1974); Bozler, Bernier, Gully, Richardson, and Lee (1974); Webb, Kleinberg, and Wheatley (1974a); and Ahonen, Haikala, Krusius, and Lounasmaa (1974c) on the magnetization dynamics in ^{3}He-A; the former two presenting both parallel resonance and perpendicular resonance shift data at melting pressure and the latter two, respectively, parallel ringing frequencies and perpendicular shifts at lower pressures. The apparatus for the parallel ringing experiments is similar to that shown in Fig. 3 and that for the original perpendicular NMR experiment, less measuring coils, in Fig. 2. A collection of results is given in Fig. 30 although the results of Ahonen et al. appeared too late to be included in the figure. The measurements of Osheroff and Brinkman, and of Bozler et al., were at melting pressure of about 34.4 bar while those shown in the figure of Webb et al. were obtained at a pressure of 33 bar. The reduced temperature-difference scale for the melting pressure data was obtained from pressure measurements using the results of experiments by Halperin, Rasmussen, Archie, and Richardson (1974b). The scale used for the ringing data was the provisional absolute scale based on zero sound attenuation measurements in normal liquid by Paulson, Johnson, and Wheatley (1973a). Examination of the data shows the following: (1) At a given temperature the parallel resonance frequency and the perpendicular resonance shift, $[\omega_{obs}^2 - (\gamma H_0)^2]^{1/2}/2\pi$, are the same within experimental error, at least for the Osheroff and Brinkman data. (2) The parallel ringing frequencies of Webb et al. are in excellent agreement with the Osheroff and Brinkman observations including those for resonance shifts closer to T_c. (3) There is a systematic trend toward higher frequencies at a given $(1 - T/T_c)$ for the Bozler et al. data, although it is now believed that the discrepancy may be traced to a temperature error due to the strain gauge (R. C. Richardson, private communication). The new data on perpendicular resonance shifts by Ahonen et al. (1974c) is also very interesting. First of all, measuring in a field of 320 G, they observed no change of total absorption with temperature in the A phase. Perpendicular shift measurements were performed for pressures of 19.8, 22.4, and 27.2 bar. Near T_c they had the general

FIG. 29. Perpendicular nuclear magnetic resonance absorption in a mixture of solid and liquid ^{3}He at four pressure differences $p \equiv P - P_A$, where P_A is the pressure of the A feature, showing the splitting away for $T < T_A$ of the perpendicular resonance in the liquid from the unshifted resonance in the solid. After Osheroff, Gully, Richardson, and Lee (1972b).
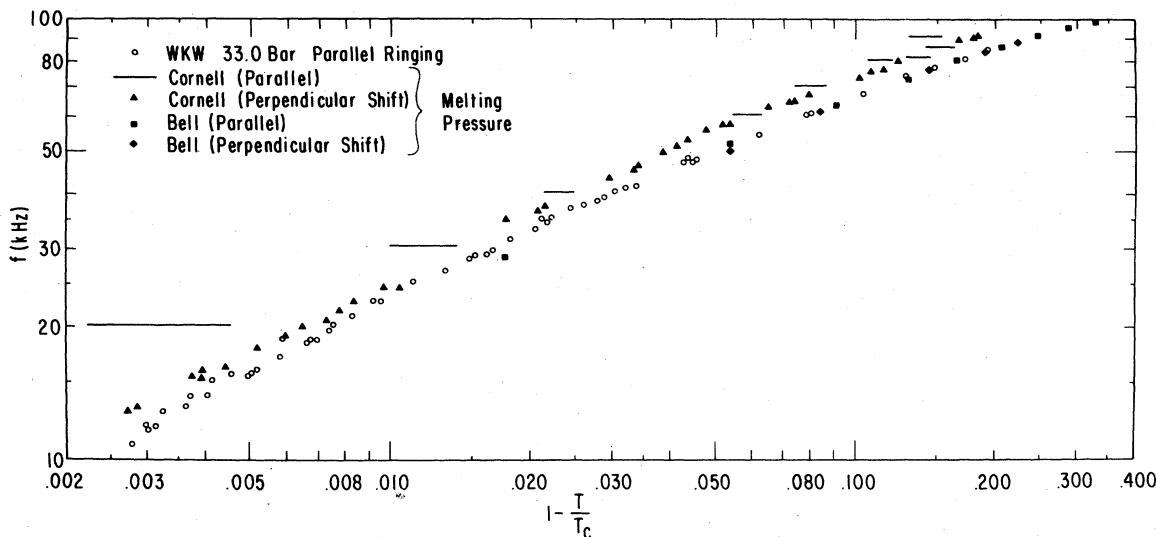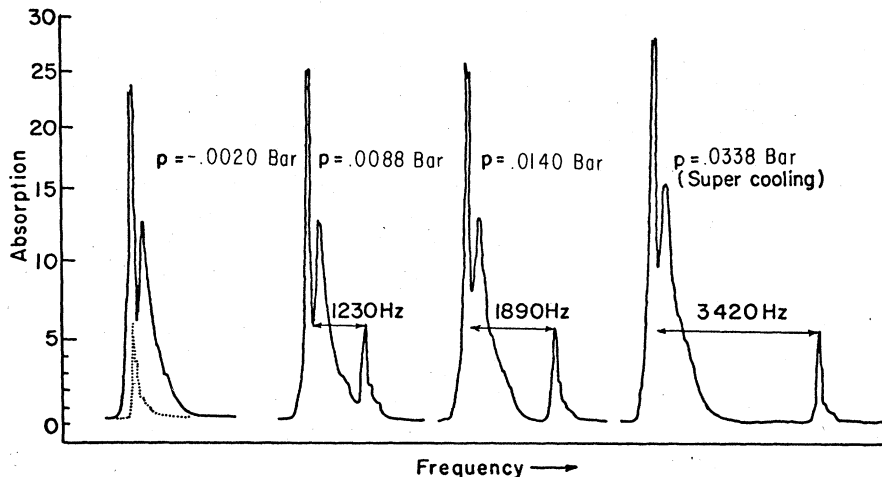

FIG. 30. Comparison of the parallel ringing frequency as measured at 33.0 bar by Webb, Kleinberg, and Wheatley (1974a) with the paralle resonance frequencies and perpendicular resonance shifts at melting pressure measured at Cornell by Bozler, Bernier, Gully, Richardson, and Lee (1974) and at the Bell Laboratories by Osheroff and Brinkman (1974). The reduced temperature difference scale $(1 - T/T_c)$ for the 33.0 bar measurements is obtained by means of the provisional absolute temperature scale of Appendix A.A and for the melting pressure measurements by means of the absolute temperature scale of Appendix A.B.

form $\omega^2 - (\gamma H_0)^2 = f(P)(1 - T/T_c)$. The pressure dependence $f(P)$ is explained by the pressure dependence of Leggett's formula (1972, 1974a) specialized to the ABM state,

$$\Omega^2 = \omega^2 - (\gamma H_0)^2 = \frac{28\pi}{5}\gamma^2(1 + \tfrac{1}{4}Z_0)[2N(0)]$$

$$\times\ a\langle R^2\rangle(k_B T_c)^2 \left(\ln \frac{1.14\epsilon_c}{kT_c}\right)^2 \left(1 - \frac{T}{T_c}\right), \qquad (8.23)$$

where Z_0 is a Landau parameter (see Appendix B), $N(0)$ is the density of states at the Fermi surface for spins of one sign, a is the ratio of the relative specific heat jump to its BCS value (1.43), $\langle R^2\rangle$ is an unknown factor (apparently very close to 1) concerned with strong coupling effects,

and ϵ_c is a cutoff energy taken as $\epsilon_c/k = 0.7$ K (Leggett, 1972). When the measurements for the three pressures are adjusted for pressure dependence to melting pressure then there is rather good agreement with the data of Osheroff and Brinkman and of Webb, Kleinberg, and Wheatley shown on Fig. 30.

Webb, Kleinberg, and Wheatley (1974a) also found exceptional agreement with Eq. (8.23), provided one takes $\langle R^2\rangle = 1$. Using $a = (C_< - C_>)/1.43C_>$ and values of Z_0, $N(0)$, and T_c from the appendixes and with $\epsilon_c/k = 0.7$ K as suggested above, the computed value for $\Omega/2\pi(1 - T/T_c)^{1/2}$ is 246 and 194 kHz at, respectively, 33 and 21 bar, while the experimental values are, respectively, 23_5 and 19_5 kHz. The comparison at intermediate pressures is just as good.

The observation that the parallel resonance frequency and perpendicular resonance shift are the same suggests that the coherent dipolar torque has the form given in Eq. (8.4). The experiments are thus *consistent* with the identification of ^{3}He-A as the ABM state but may not prove it, other odd l values perhaps being possible. Experimentally it is heartening to see several quite different experiments employing differently obtained temperature scales give such close agreement since many important qualitative questions depend on the quantitative correctness of temperature scales.

Webb *et al.* (1974a) found that the squares of the parallel ringing frequencies, when plotted as a function of a magnetic temperature scale, gave a rather good straight line—as expected from the $(1 - T/T_c)$ dependence of the square of the energy gap parameter. However, this line in some cases interesected the temperature axis somewhat above T_c^*, the thermally determined center of the specific heat transition in the main cell. Since significant temperature differences can occur within a cell near T_c owing to the transition from hydrodynamic to diffusive heat flow (Greytak, Johnson, Paulson, and Wheatley, 1973) it is still not known if the above discrepancy is real. In the recent melting pressure measurements of Osheroff and Anderson (1974) very near to T_c no discrepancies were observed to a high precision.

The orbital state of ^{3}He-A is highly anisotropic if it is the ABM state and both boundaries and heat flow are expected to have strong orientational effects (De Gennes, 1973; Ambegaoker, De Gennes, Rainer, 1974; De Gennes and Rainer, 1974) on the orbital order parameter and then, via the dipolar interaction, on the spin ordering. Such effects should be strongly geometry dependent. So far experiments have not been designed to emphasize or measure such effects, so only qualitative observations are available.

In the experiments by Osheroff and Brinkman (1974) at melting pressure the ^{3}He was confined to a 6.4 mm diam cylinder with an axial steady field and with resonance coils with axes both parallel and perpendicular to the cylinder axis. They found that for fields less than 5 G the parallel resonant signal decreased in magnitude, being unobservable in zero field, while in zero field a signal was observable using the perpendicular coil. This was interpreted as an effect of heat flow in the bulk orienting l, Fig. 30, parallel to the axis and hence interchanging the usual effect of the coils parallel and perpendicular to the axis, it being presumed that at higher fields l would orient itself perpendicular to H under the action of dipolar torque. In the parallel ringing experiments of Webb *et al.* (1974a) with H_0 and ΔH parallel to the axis of a 3 mm diam tube containing the ^{3}He, there was no effect of H_0 on the ringing until H_0 fell below 5 G. Then the quality of the ringing signal was impaired near to T_c. When H_0 was reduced to zero the ringing signals were seriously degraded for $(1 - T/T_c) < 0.01$, but for lower temperatures there was no problem. This might be given a similar interpretation as the above effect observed by Osheroff and Brinkman since for a constant heat flow the superfluid velocity will be highest near T_c.

From an experimental standpoint measurements of resonance and ringing frequencies and shifts in the A phase give quite consistent results, both at melting pressure and at lower pressures, and seem to be insensitive to disturbing effects except in very low fields. But for the B phase the
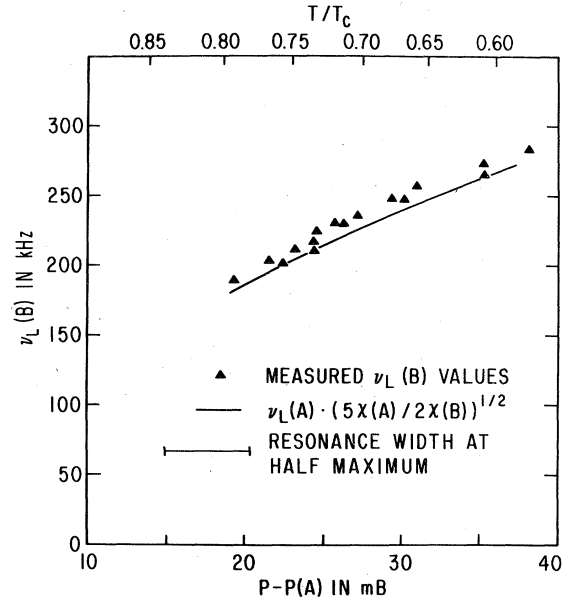

FIG. 31. Parallel resonance frequencies observed in ^{3}He-B at melting pressure as a function of pressure difference from the A feature or the corresponding reduced temperature T/T_c [Appendix A.B]. After Osheroff, 1974.

experimental situation is quite different. From the first report of Osheroff, Gully, Richardson, and Lee (1972b) until the present the dynamic magnetic properties in the B phase have shown curious effects. It is fair to say that many of them can be understood to some extent by a combination of Brinkman's equtions, Eqs. (8.9), (8.10), and (8.11), which are Leggett's equations (8.2) and (8.3) specialized to the BW state, Eq. (8.7); and by estimates (Brinkman, Smith, Osheroff, and Blount, 1974) of the effects of boundaries on the orientation of the axis $\hat{\omega}$, Eq. (8.7) and following. In what follows we shall attempt to outline some of the principal results of B phase measurements.

The most complete report of B phase resonance measurements at melting pressure presently available has been given recently by Osheroff (1974). It follows on the qualitative observation in the B phase of parallel rf power absorption and the observation of a field-dependent perpendicular resonance width by Osheroff and Brinkman (1974) and the observation of parallel ringing in the B phase by Webb, Kleinberg, and Wheatley (1974a). Osheroff observed a very broad ($\approx$ 20 kHz) parallel resonance with center frequencies, shown on Fig. 31, as a function of T/T_c.

To interpret these measurements consider Eqs. (8.9) and (8.11) with $\hat{\omega}$ parallel to the field. A field H_0 does define an axis by breaking $\uparrow \downarrow$ pairs with respect to that axis to the extent $(\mu H_0/\Delta)^2$ (Leggett, 1974; Ambegaokar and Mermin, 1973; Engelsberg, Brinkman, and Anderson, 1974). In equilibrium $S = 0$, so that the equilibrium value of θ is $\theta_0 = \cos^{-1}(-\frac{1}{4})$ from Eq. (8.9). For θ near θ_0, Eq. (8.9) is approximated by

$$\dot{S} = \gamma(S \times H) - \hat{\omega} \cdot (15/4)\Lambda(\theta - \theta_0). \qquad (8.24)$$

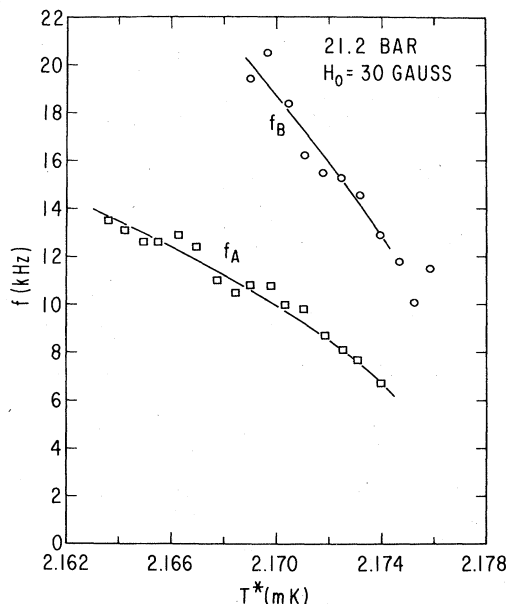Apply the field $H = \hat{z}H_0$ and wait for equilibrium (S and $\hat{\omega}$

FIG. 32. Ringing frequencies f_A and f_B in ^{3}He-A and ^{3}He-B at 21.2 bar in a steady field of 30 G as a function of CMN magnetic temperature near T_c. Observations of the different phases at the same temperature were made possible by the judicious use of supercooling and superheating phenomena. After Webb, Kleinberg, and Wheatley (1974a).

along $\hat{z}$). Then apply a parallel field increment $\hat{z}\Delta H$. From (8.10) we have $\ddot{\theta} = -\gamma[\Delta H - \gamma(\Delta S_z/\chi)]$ so that

$$\ddot{S}_z = -(15/4)(\gamma^2\Lambda/\chi)\Delta S_z + (15/4)\gamma\Lambda\Delta H. \qquad (8.25)$$

Hence a parallel ringing, or a parallel resonance, is expected with frequency $\Omega_B = (15\gamma^2\Lambda/4\chi)^{1/2}$. Note parenthetically that for a perpendicular field change $\hat{\omega}\cdot\Delta\mathfrak{K} = 0$, so $\ddot{\theta} = 0$ and no dipolar torque is developed. There is then a precessional ringing (or a perpendicular resonance) at the Larmor frequency γH_0 only.

Leggett (1974a, 1973a) made a quantitative comparison of the expected parallel frequencies for the ABM state (model for ^{3}He-A) and the BW state (model for ^{3}He-B) and concluded that λ and Λ would be related so that

$$\Omega_B{}^2 = \Omega_A{}^2 \cdot (5/2)[\chi(A)/\chi(B)][\Delta(B)/\Delta(A)]^2 \qquad (8.26)$$

if these state identifications are correct. In this equation Ω_A is the parallel resonance or ringing frequency (or perpendicular shift) for ^{3}He-A and Δ is the average gap. Osheroff applied this equation to find, for the assumption $\Delta(B) = \Delta(A)$, the solid line shown on Fig. 31. He points out that had he used the values of $\chi_B(T/T_c)/\chi_N$ found by measurements of static magnetization (Paulson, Kojima, and Wheatley, 1974b) at lower pressures the good agreement shown on Fig. 31 would have been "totally destroyed." At a variety of pressures near and below the pressure of the PCB, Webb, Kleinberg, and Wheatley (1974a) observed parallel ringing of the magnetization in ^{3}He-B following the turnoff of an incremental field parallel to a steady field, but signals of persistently good quality were observed only for $(1 - T/T_c)$ less than a few tenths of a percent. This small temperature interval in which good quality signals

could be observed did not depend on field over a range of roughly 30–300 G, the ^{3}He being confined to a tube of 3 mm diam. Hence an explanation in terms of a competition between field and wall orientation seems unlikely. Some of their results are shown in Fig. 32, where the ringing frequency in both the B and A phases at a particular pressure and steady field are plotted as functions of magnetic temperature very near T_c. [Measurements are not plotted vs $(1 - T/T_c)$ since the uncertainty in T_c due to thermal inhomogeneities or whatever is too great.] The effects of supercooling and superheating were used here to advantage, the A phase data being obtained after just insufficient cooling to make the $A \rightarrow B$ transition occur and the B phase data being obtained after a deep cooling into the B phase. Similar observations were made over a wide range of field (5–300 G) and pressure (8.5–21.5 bar) consistent with the displacement of the T_{AB} line in a magnetic field and the necessity of making the observations within a few tenths of a percent of T_c. At a given temperature the B phase ringing frequency f_B was (1.9 ± 0.1) times f_A, the ringing frequency for the A phase. If a given field is small enough (say 50 G), as the pressure is lowered the A phase ringing gradually occupies a smaller temperature interval and finally is no longer observable, while the B phase ringing persists, within the temperature limitations given above. We note parenthetically that the quantitative features of the phase diagram of Fig. 1 were supported in detail by the ringing experiments. In fact they give valuable new information near the PCP as we shall indicate elsewhere.

Whereas the melting pressure parallel resonance frequencies measured by Osheroff were essentially predicted by Eq. (8.26), the lower pressure ringing frequencies, including those shown on Fig. 32, are not. Under the conditions of the measurement the pressure is very near that of the PCP where $\Delta^2(B)$ should be the same as $\Delta^2(A)$. Further, near T_c one has $\chi(A) = \chi(B)$ to a very good approximation. Hence, if at the pressure of the PCP and at lower pressures ^{3}He-A is a manifestation of the ABM state and ^{3}He-B a manifestation of the BW state, one would expect $\Omega_B = (5/2)^{1/2}\Omega_A = 1.58\Omega_A$, substantially less than observed. Furthermore, Webb, Kleinberg, and Wheatley (1974a) found in their intermediate pressure work that in fields between 1 and 5 G their parallel ringing phenomenon for a 3 mm diam tube changed qualitatively. But in the melting pressure experiments of Osheroff for a 6 mm diam tube, at a much lower reduced temperature however, the parallel resonance usually disappeared for fields less than 250 G (although in some cases it reappeared for fields less than 30 G). This might reflect [Eq. (8.30)] a spread of orientations of $\hat{\omega}$ already about 30° from H_0 at this field. Webb et al. also observed another type of ringing (to be described later) for fields of 1 G and below across a range of T/T_c down to below $T/T_c = 0.85$, so it would appear that the 1–5 G boundary between "low" and "high" field regions qualitatively holds over the full temperature range available to them. Hence we conclude that both in the relative size of Ω_B and Ω_A and in the size of the field which separates the low and high field regions (which should actually go up for a smaller geometry) there is a substantial difference between results at melting pressure and at lower pressures. According to Brinkman, Smith, Osheroff, and Blount (1974) field size effects are related to the "textures" of $\hat{\omega}$. These in turn are related, for example, to the energy

required to bend $\hat{\omega}$ in space and to the energy which pins $\hat{\omega}$ at surfaces. Both the lower pressure perpendicular resonance experiments by Ahonen, Haikala, Krusius, and Lounasmaa (1974c) already described in Sec. III and the parallel ringing measurements by Webb, Kleinberg, and Wheatley (1974a) suggest that orientation of $\hat{\omega}$ by a magnetic field in competition with wall orientation may be easier in the lower pressure measurements than it is in the melting pressure work. As we remarked in Sec. III, however, the orientation of the resonance field in a plane perpendicular to the cylinder axis, as in the measurements of Ahonen et al., may change the field orientation considerably compared to the case where field and axis are parallel, as in the measurements of Osheroff and of Webb, Kleinberg, and Wheatley.

The rather sudden appearance of good quality ringing signals in ³He-B very near T_c led Webb et al. (1974) to consider a possible effect of flow. It is known (Greytak, Johnson, Paulson, and Wheatley, 1973; Johnson, Kleinberg, Webb, and Wheatley, 1974) that ³He-B has a high critical flow velocity so that flow is inhibited only very near T_c. In the ³He-A there appears to be a spectrum of much lower critical velocities. For ³He-A a chemical potential change $S\Delta T \simeq 2 \times 10^{-23}$ erg/atom across the length of a 3 mm diam tube was sufficient to drive the superfluid critical. For a 2 G field increment the magnetic chemical potential difference from inside to outside the coil (Fig. 3) producing ΔH is greater than this. So it is speculated that counterflowing magnetization supercurrents (Vuorio, 1974; Maki and Tsuneto, 1974b) can flow in ³He-B to stir the magnetization but they cannot in ³He-A. It may be possible to give this suggestion an experimental test either by experiments on spin diffusion (or convection!) or by direct attempts to excite spin waves in a defined geometry.

Let us turn briefly to the matter of the possible influence of "textures" or domain structures in ³He-B. The experimental situation has been reviewed already in Sec. III in a context of the temperature-dependent "static" susceptibility as determined via NMR both at melting pressure by Osheroff and Brinkman (1974) and Osheroff (1974) and at lower pressures by Ahonen et al. (1974c). We have already pointed out the substantial difference between the effect of a magnetic field on Osheroff's measurements and those of Ahonen et al. What is observed in perpendicular resonance, at least in the case of melting pressure, is a shift of a significant amount of absorption toward higher frequencies than the Larmor frequency γH_0. This can be understood in terms of Brinkman's equations (Osheroff and Brinkman, 1974; Brinkman, Smith, Osheroff, and Blount, 1974), Eqs. (8.9) and (8.10) in the case where $\hat{\omega}$ and $\mathbf{H}$ make a fixed angle α with one another. Then, following an incremental field change, if we have a final field $\mathbf{H} = \hat{z}H_0$ and $\hat{\omega} = \hat{z}\cos\alpha + \hat{z}\sin\alpha$ these equations are, writing $\Omega_B{}^2 \equiv (15/4) \times (\gamma^2\Lambda/\chi)$ and $\theta_0 \equiv \cos^{-1}(-\tfrac{1}{4})$,

$$\dot{\mathbf{S}} = \hat{x}[\gamma H_0 S_y - (\chi/\gamma^2)\Omega_B{}^2(\sin\alpha)(\theta - \theta_0)] - \hat{y}\gamma H_0 S_x$$
$$- \hat{z}(\chi/\gamma^2)\Omega_B{}^2(\cos\alpha)(\theta - \theta_0) \qquad (8.27)$$

and

$$\dot{\theta} = [(\gamma^2/\chi)\cos\alpha]\Delta S_z + [(\gamma^2/\chi)\sin\alpha]S_x. \qquad (8.28)$$

Taking the time derivative of (8.27) and substituting (8.28)

one finds that the principal response in strong fields $[\gamma H_0 \gg \Omega_B]$ to a perpendicular field change is a precessional ringing at frequency

$$\Omega_\perp{}^2 = (\gamma H_0)^2 + \Omega_B{}^2 \sin^2\alpha \qquad (8.29)$$

and to a parallel field change is a parallel ringing at frequency

$$\Omega_\parallel{}^2 = \Omega_B{}^2 \cos^2\alpha. \qquad (8.30)$$

In high enough fields these motions are only weakly coupled to one another. They correspond to perpendicular and parallel resonance frequencies. The broadening of the perpendicular NMR line in ³He-B is attributed to a spectrum of values of α. We look forward to quantitative tests of these predictions of Brinkman's equations in well-defined confining geometries.

Next let us consider some observations (Webb, Kleinberg, and Wheatley, 1974a) made in parallel ringing experiments in ³He-B in a tube of 3 mm diameter. Remarkably, as in the case of ³He-A, a field of 5 G was the approximate lower limit of the "high field" results previously shown in Fig. 32. For fields H_0 of 1 G and lower another phenomenon was observed which was most clearly defined for $H_0 = 0$. In fields greater than 5 G the ringing frequency did not depend on ΔH or H_0, except for the "nonlinear effect," which we shall presently discuss. But for $H_0 = 0$ and provided the temperature was not too close to T_c (recall that the usual B phase signals were seen only a few tenths of a percent from T_c) an initial ringing frequency proportional to ΔH ($2\pi f \cong \tfrac{1}{2}\gamma\Delta H$) and roughly independent of pressure and temperature was observed. For $\Delta H = 2$ G there was no evidence of a time-dependent frequency, but for $\Delta H = 10$ G the frequency decayed, as in a "whistler," with a time constant of about 2 msec. Since this frequency does not depend on temperature (except near T_c the ringing is not observable), the ringing frequency does not depend quantitatively on temperature-dependent torques; only on their existence! Since this ringing effect does not occur at all unless H_0 is very small, it is likely that it is to be understood in terms of a wall effect. Maki (private communication to the author) suggested a qualitative explanation of the effect which has been quantified by Maki (1974b), by Maki and Hu (1975), and by Brinkman (1974). It is assumed in their work that when the field remaining after the parallel field ΔH has been removed is sufficiently small (less than a gauss experimentally in the 3 mm diam tube used for the measurements) the axis $\hat{\omega}$, in a context of Brinkman's equations, is perpendicular to $\mathbf{H}_0$ and $\mathbf{S}$, which are coaxial. Then from Eq. (8.10) we see that initially $\theta = 0$, so no dipolar torque is developed initially; θ remains at $\theta_0 = \cos^{-1}(-\tfrac{1}{4})$. However, from Eq. (8.11) it is clear that $\hat{\omega}$ itself starts to move immediately after the field is turned off. For $H_0 = 0$ we have $\mathfrak{K} = -\gamma^2\mathbf{S}/\chi$. This possibility of motion of the axis $\hat{\omega}$ without developing a dipolar torque seems to be one of the principal properties of the B phase. But as time goes on there is a tendency for θ to change from θ_0 and there is then a rather complex time development (Maki and Hu, 1975). Brinkman (1974) suggested a very simple solution to his equations valid for $\gamma\Delta H \ll \Omega_B$ which presumes that the initial transient does not have a substantial effect. He assumed $\hat{\omega} \cdot \mathbf{S} = 0$, not only initially
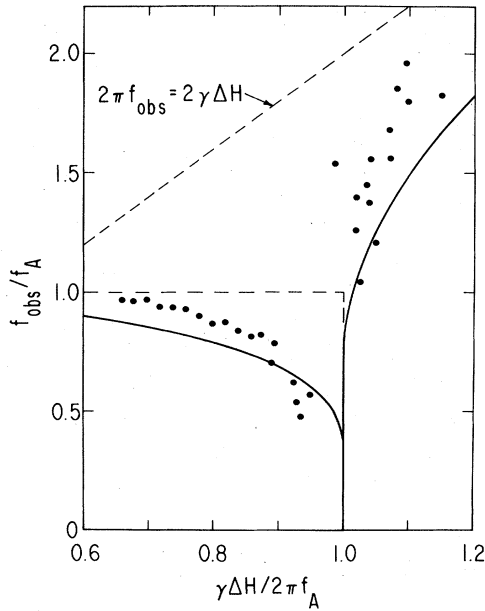
FIG. 33. Nonlinear ringing phenomena in ³He-A. f_{obs}/f_A is the ratio of the observed frequency f_{obs} to that f_A observed in the linear regime with small ΔH as a function of $\gamma\Delta H/2\pi f_A$, the maximum precessional frequency of the **d** vector, divided by f_A. The solid line is calculated from the theory by Maki and Tsuneto. (After Webb, Kleinberg, and Wheatley, 1974b).

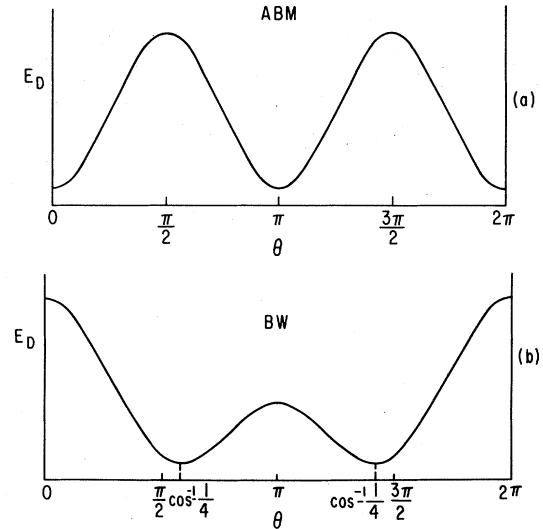FIG. 34. Dependence of coherent dipolar energy on the angle θ of the **d** vector for (a) the ABM state and (b) the BW state. In equilibrium, Θ is 0 or π for the ABM state and $\cos^{-1}$ $(-1/4)$ for the BW state.

where $\theta = \theta_0$ but, as well, in the final state where $\theta \neq \theta_0$. The resultant motion may be found from Eqs. (8.9) and (8.11) on using $d(\hat{\omega}\cdot\mathbf{S})/dt = 0$ as well as $\hat{\omega}\cdot\mathbf{S} = 0$. In this motion $\dot{\mathbf{S}}$ is coaxial with $\hat{\omega}$, which is perpendicular to $\mathbf{S}$, so the magnitude of $\mathbf{S}$ does not change. When the field is turned off $\hat{\omega}$ is kicked out of its weakly "bound" orientation perpendicular to a wall and starts to precess with components of $d\hat{\omega}/dt$ along both $\mathbf{S}$ and $\hat{\omega} \times \mathbf{S}$. For small field changes H_0, once initial transients have passed, $\hat{\omega}$ and $\mathbf{S}$ have a precessional angular velocity whose magnitude is constant at $\gamma H_0(2/5)^{1/2} = 0.63\gamma H_0$. The motion is actually quite complicated, especially for larger amplitudes (Maki and Hu, 1975). It also depends importantly on the relative magnitudes of the field turned off and the remaining field (Maki, private communication). The entire phenomenon would appear to be basically a nonlinear effect.

Let us now return to the subject of parallel ringing in ³He-A where some interesting nonlinear effects may be observed (Webb, Kleinberg, and Wheatley, 1974b). Consider the full dependence of $\mathbf{R}_D$ on θ as in Eq. (8.13). If ΔH is small enough the sequence of events is as follows, following Eqs. (8.2) and (8.12). After the rapid *turnoff* ΔH the d vector starts to precess at $\dot{\theta} = \gamma\Delta H$. As θ develops a torque develops to decrease S_z. As S_z changes, $\dot{\theta}$ decreases, finally reaching $\dot{\theta} = 0$ when $\gamma\Delta S_z = \chi\Delta H$. However, at this point θ itself is not zero; rather θ still has the sign to decrease S_z. So although θ now decreases the torque is still such as to decrease S_z. Thus S_z continues to decrease, reaching a minimum when $\theta = 0$ again. The next half-cycle then ensues with θ on the opposite side of equilibrium. The dipolar torque is however not unlimited. If ΔH is too large, then the angle θ will be carried beyond the region where the torque is linear in θ. The system will appear less "stiff," and the ringing frequency will drop. If ΔH is made large

enough then the ringing is extinguished altogether. If ΔH is made very large then ΔS_z never has a chance to respond fully to the rapidly rotating **d** vector. Rather, Eqs. (8.12) and (8.13) show that the spins are subject to a doubly periodic torque at frequency $2(\gamma\Delta H)$. The magnetization then oscillates at a "driven" frequency $2\gamma\Delta H$. The detailed theory of this has been worked out by Maki and Tsuneto (1974) from a different foundation, but the equations are identical to those which follow from the above.

An example of results for this nonlinear effect is given in Fig. 33 along with a solid theoretical curve. It is possible that the extinction point of the "theoretical" curve should be farther to the left with respect to the experimental points since both ΔH and f_A, the frequencies under linear conditions, are subject to error. From examination of Fig. 33 we conclude that the observed frequency f_{obs} for ΔH incremental field change stays closer to the "linear" value f_A than expected by the theory—as if the linear region were larger than anticipated. The ringing signals for $\gamma\Delta H/2\pi f_A > 1$ are of poorer quality and rather rapidly disappear in noise as the higher frequency branch develops.

Unless damping and texture effects have a major influence, the preceding type of experiment should be valuable in studying the dependence of dipolar energy on the angle of rotation of the **d** vector. For sudden changes ΔH in a parallel field Eqs. (8.2), (8.3) [and (8.9) and (8.10)] have a first integral, or an energy integral, which can be expressed as

$$\tfrac{1}{2}(\chi/\gamma^2)[\dot{\theta}^2 - (\gamma\Delta H)^2] = -[E_D(\theta) - E_D(\theta_0)], \quad (8.31)$$

where the right side is the negative of the change of coherent dipolar potential energy from its equilibrium value at $\theta = \theta_0$. Here θ is the angle of twist of the order parameter vector **d** about the field change $\Delta\mathbf{H}$. (We assume that $\mathbf{H}_0$, $\hat{\omega}$, and $\Delta\mathbf{H}$ are all parallel to one another.) The dependence of $E_D(\theta)$ on θ is shown, respectively, for the ABM state [Eq. (8.6)] and the BW state [Eq. (8.8)] in Figs. 34(a) and
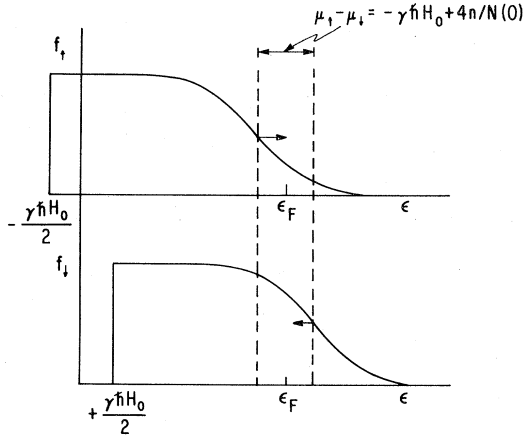
FIG. 35. Diagram illustrating the distribution functions $f \uparrow$ and $f \downarrow$ and the relative chemical potentials $\mu_\uparrow$ and $\mu_\downarrow$ for $\uparrow$ and $\downarrow$ spins as a function of quasiparticle energy when a field H_0 is suddenly applied to ³He-A.

34(b). In the case of the ABM state, Eq. (8.31) can be made to look exactly like that of a pendulum of mass m and length l with acceleration of gravity g which has been given an initial impulsive angular velocity $\dot\phi_i$, where ϕ is the angle the pendulum makes with the vertical. For the pendulum the equation analogous to (8.31) is

$$\tfrac{1}{2}ml^2(\dot\phi^2 - \dot\phi_i{}^2) = -mgl(1 - \cos\phi). \qquad (8.32)$$

The ABM state gives the same equation provided we make the identifications $\phi = 2\theta$, $ml^2 = \chi/\gamma^2$, $mgl = \lambda$ [Eq. (8.6)], and $\dot\phi_i = 2\gamma\Delta H$. If the pendulum is struck a slight blow ($\tfrac{1}{2}ml^2\dot\phi_i{}^2 \ll 2mgl$) then it will oscillate at frequency $\omega = (g/l)^{1/2}[= (\gamma^2\lambda/\chi)^{1/2} = \Omega_A]$. As it is struck harder the period will increase. If it is struck just so that $\tfrac{1}{2}ml^2\dot\phi_i{}^2 = 2mgl$, then the bob ends up in a position of unstable equilibrium at $\phi = \pi$. The value of $\dot\phi_i$ that it takes to do this is $2(g/l)^{1/2}$. This corresponds to $2\gamma\Delta H = 2\Omega_A$ for the ABM state in ³He. But if the bob is struck with great force, so that $\tfrac{1}{2}ml^2\dot\phi_i{}^2 \gg 2mgl$, it will rotate at $\dot\phi_i$ with very little influence of gravity. The corresponding angular frequency for the ABM state is $2\gamma\Delta H$. The experiments of Webb, Kleinberg, and Wheatley (1974b) support the above picture qualitatively; but not in quantitative detail, especially for $\gamma\Delta H < \Omega_A$ when the ringing frequencies are higher than expected as mentioned above.

Assuming that the B phase is a manifestation of the BW state then from Fig. 34(b) there should be two impulses ΔH at which the ringing frequency goes to zero (Maki, 1974c; Maki and Hu, 1975). From Eq. (8.31) these are found by setting $\chi(\Delta H)^2/2$ equal to $E_D(\pi) - E_D(\theta_0)$ and to $E_D(0) - E_D(\theta_0)$. The results, expressed in terms of the frequency Ω_B observed when $\theta - \theta_0$ is small, are, respectively, $\gamma\Delta H = (3/5)^{1/2}\Omega_B$ and $(5/3)^{1/2}\Omega_B$. We would imagine that not only these "extinction" values but also the full dependence of Ω on $\gamma\Delta H$, testing the form of $E_D(\theta)$, should come from such measurements. However, great care will have to be exerted, especially with geometry, to achieve ideal conditions. Preliminary measurements by Webb, Kleinberg, and Wheatley (1974b) suggested larger values for the B phase extinctions, but this might be explained in terms of non-parallelism of $\hat\omega$ and $\Delta\mathbf{H}$.

The preceding experiments are illuminated further by an idea introduced by Leggett (1974a) and further developed by Maki and Tsuneto (1974). The two equal spin pairing states in ³He-A are conceived as two interpenetrating superfluids with order parameters $d_{\uparrow\uparrow}$ and $d_{\downarrow\downarrow}$. Following Eq. (8.1) and Fig. 27 for $\mathbf{d}$ making angle θ, these order parameters are $d_{\uparrow\uparrow} = d_{\downarrow\downarrow}{}^* = -id(\hat{\mathbf{n}})e^{-i\theta}$. The phase difference between the $\uparrow\uparrow$ and $\downarrow\downarrow$ states is just $\pi - 2\theta = \pi + \phi$, so the energy E_D in (8.6) may be written

$$E_D = E_a - \tfrac{1}{4}\lambda - \tfrac{1}{4}\lambda\cos\phi, \qquad \phi = -2\theta. \qquad (8.33)$$

One may then think of the two nearly independent superfluids as being weakly coupled together by an energy dependent on the cosine of their phase difference as in the Josephson effect. Let us explore this idea further, following Maki and Tsuneto but ignoring the effective spin interactions among the particles. Apart from constant terms the energy may be written

$$\mathcal{H} = \sum (\mu_\uparrow \delta n_\uparrow + \mu_\downarrow \delta n_\downarrow) - \tfrac{1}{4}\lambda\cos\phi, \qquad (8.34)$$

where $\mu_\uparrow$ and $\mu_\downarrow$ are the chemical potentials for the $\uparrow$ and $\downarrow$ spins, $\delta n_\uparrow$ and $\delta n_\downarrow$ refer to changes in the distribution of $\uparrow$ and $\downarrow$ spins, and the phase term comes from (8.33). When δn pairs of correlated particles are transferred between the $\uparrow\uparrow$ distribution and the $\downarrow\downarrow$ distribution the corresponding increase in the number of $\uparrow$ with respect to $\downarrow$ spins is related to δn by

$$\delta n = \tfrac{1}{4}(\delta n_\uparrow - \delta n_\downarrow). \qquad (8.35)$$

In terms of n the equations of motion are

$$\dot n = (1/\hbar)(\partial\mathcal{H}/\partial\phi), \qquad (8.36)$$

and

$$\hbar\dot\phi = -\partial\mathcal{H}/\partial n. \qquad (8.37)$$

Application of the first equation to (8.34) gives

$$\dot n = (\lambda/4\hbar)\sin\phi. \qquad (8.38)$$

If now we imagine a change in which δn pairs are transferred from the $\downarrow\downarrow$ to the $\uparrow\uparrow$ superfluid at constant ϕ we have

$$\delta\mathcal{H} = \mu_\uparrow \delta n_\uparrow + \mu_\downarrow \delta n_\downarrow = 2(\mu_\uparrow - \mu_\downarrow)\delta n, \qquad (8.39)$$

where we have used Eq. (8.35) together with $\delta n_\uparrow + \delta n_\downarrow = 0$. Thus, from Eq. (8.37) we find

$$\hbar\dot\phi = -2(\mu_\uparrow - \mu_\downarrow). \qquad (8.40)$$

Before proceeding further consider Fig. 35 in which we show the distribution functions $f_\uparrow$ and $f_\downarrow$ for the $\uparrow$ and $\downarrow$ spins plotted as a function of $\epsilon = p^2/2m \pm \tfrac{1}{2}\gamma\hbar H_0$, where the $\uparrow$ spins have the $(-)$ sign and the $\downarrow$ spins the $(+)$ sign. The distributions shown are valid for the instant after the field H_0 has been applied when $\mu_\uparrow - \mu_\downarrow = -\gamma\hbar H_0$. From Eq. (8.40) ϕ will start to increase at rate $2\gamma H_0$ while n will then start to increase at rate $\lambda\phi/4\hbar$. But as $\downarrow\downarrow$ pairs are

changed to ↑ ↑ pairs the difference in chemical potential increases, and by an amount $4/N(0)$ for each pair transferred. Thus the chemical potential difference after n pairs are transferred is

$$\mu_\uparrow - \mu_\uparrow = -\gamma\hbar H_0 + 4n/N(0). \tag{8.41}$$

Equation (8.40) can then be written

$$\hbar\dot{\phi} = 2\gamma\hbar H_0 - 8n/N(0). \tag{8.42}$$

In the equilibrium case we have $\dot{\phi} = 0$ so that $n_{\text{equil}} = \frac{1}{4}\gamma\hbar N(0)H_0$. The resultant magnetic moment per unit volume is

$$M_{\text{equil}} = 4(\tfrac{1}{2}\gamma\hbar)n_{\text{equil}} = \tfrac{1}{2}\gamma^2\hbar^2 N(0)H_0, \tag{8.43}$$

or

$$\chi = \tfrac{1}{2}\gamma^2\hbar^2 N(0), \tag{8.44}$$

the susceptibility expected for the noninteracting gas which we have assumed. Equation (8.42) can then be written

$$\tfrac{1}{2}\dot{\phi} = \gamma[H_0 - 4n/\hbar\gamma N(0)]. \tag{8.45}$$

Now if we use $n = S/2\hbar$ and $N(0) = 2\chi/\gamma^2\hbar^2$ [from (8.44)] in (8.45) we find

$$\dot{\theta} = -\tfrac{1}{2}\dot{\phi} = -\gamma(H_0 - \gamma S/\chi), \tag{8.46}$$

in agreement with Eq. (8.12), apart from the use of incremental field and spin changes. So far as that is concerned all the preceding equations hold for incremental changes of H_0 and n, so the results will not depend essentially on the actual value of a steady field H_0.

Let us next make the assumption that the field change H_0 is small enough that ϕ always remain small and $\sin\phi \simeq \phi$. Then taking the time derivative of Eq. (8.38) and substituting (8.42) we get

$$\ddot{n} = (\lambda/4\hbar)[2\gamma H_0 - 8n/\hbar N(0)]. \tag{8.47}$$

Rewriting this equation using Eq. (8.44) to eliminate $N(0)$ we then find

$$\ddot{n} + (\gamma^2\lambda/\chi)n = (\lambda\gamma/2\hbar)H_0. \tag{8.48}$$

This is the same equation, effectively, as (8.14). Thus this approach gives the same results as our earlier one, but it does put these results in a new and interesting perspective. We have an effect which can be interpreted as analogous to the Josephson effect in superconductors. Actual experimental observation then suggests that the concept may be good that ³He-A is a two-component superfluid in which the two components interact weakly with one another. This view may in fact be more fundamental than the more mechanical approach typically used. However, mechanical pictures are frequently more helpful in designing experiments.

We conclude this section with a few remarks on damping or linewidth of dynamic magnetism. The most detailed

measurements are those of Bozler et al. (1974) on the width of the perpendicular resonance in ³He-A at melting pressure. They found that, except near T_c, their data for the linewidth ΔH_0, defined as the full width at half-maximum, could be represented approximately by the expression $\Delta H_0 \simeq 1.1(\Omega_A/\gamma H_0)^2$ G, where Ω_A is the parallel resonance frequency or the perpendicular resonance shift. Similar results were found by Osheroff and Brinkman (1974). Combescot and Ebisawa (1974) developed a theory of linewidths in which the frequency width $\Delta\omega_\perp$ of the perpendicular resonance obeys the formula

$$\Delta\omega_\perp = \frac{\Omega_A^4(T)\tau(T)}{(\gamma H_0)^2 + \Omega_A^2(T)}\frac{f(T)}{1 + \tfrac{1}{4}Z_0}, \tag{8.49}$$

where $\tau(T)$ is the quasiparticle collision time and $f(T)$ is a function which is 1 at T_c and which decreases toward zero at $T = 0$. This formula can be reconciled with the empirical formula above, except near T_c, where no simple experimental result holds. Combescot and Ebisawa were rather successful in fitting Eq. (8.49) to the data of Bozler et al. except possibly at the lowest frequency and near T_c. Owing to large widths and corresponding weak resonances the parallel resonance widths in ³He-A are not known in such detail as those for the perpendicular resonances. The Bozler et al. data for the A phase at melting pressure are given as temperature widths as on Fig. 30, while Osheroff and Brinkman quote $\Delta\nu_{||}$ of 2.5 kHz at 50 kHz and 4 kHz at 90 kHz. These are in only qualitative agreement with Combescot and Ebisawa's result:

$$\Delta\omega_{||} = \Omega_A^2(T)\tau(T)\frac{f(T)}{1 + \tfrac{1}{4}Z_0}. \tag{8.50}$$

In the experiments of Webb, Kleinberg, and Wheatley (1974a) on parallel ringing in ³He-A the decays were characterized by a "beat" phenomenon rather than by exponential decays, so no conclusions on intrinsic damping have been made. Osheroff (1974) found in his measurements at melting pressure a parallel resonance linewidth in the B phase of 20 kHz which is said to be in good agreement with the Combescot–Ebisawa theory for parallel linewidth in the BW phase.

Maki and Ebisawa (1975) have also developed a theory of linewidths for the A phase. In this theory the temperature and field dependence of the perpendicular resonance are determined by a factor $\Omega_A^2/[(\gamma H_0)^2 + \Omega_A^2]$ while the width of the parallel resonance is expected to be temperature and field independent. The latter result agrees qualitatively with the data of Bozler et al., who found a parallel linewidth of (4.5 ± 1) kHz, roughly independent of temperature.

IX. EFFECT OF A MAGNETIC FIELD ON THE SECOND-ORDER TRANSITION, RELATED TOPICS

When ³He in a compressional cooling cell is in a magnetic field, the A feature on the pressurization curve is split into two similar features, called A_1 and A_2, with a pressure separation proportional to field. A summary of these measurements is given by Gully, Osheroff, Lawson, Richardson, and Lee (1973). Both the A_1 and A_2 features are a discontinuity in slope but not a hesitation in pressure on a pressure–time curve, so with current understanding they
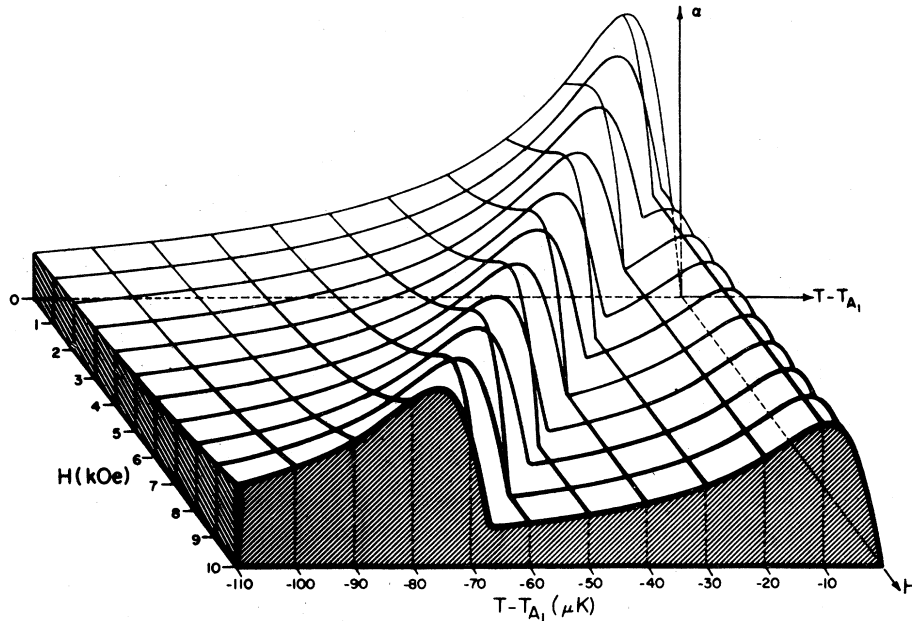
FIG. 36. Surface of ultrasonic attenuation α for a frequency of 10 MHz and for melting pressure as a function of magnetic field H and temperature displacement $T - T_{A1}$ from the higher of the two second-order transitions. After Lawson, Gully, Goldstein, Richardson, and Lee (1974).

reflect two second-order transitions with a pressure (temperature) splitting proportional to H. There is no evidence for a first-order transition in a magnetic field at T_c. Since the A feature is thought to manifest the termination of the T_c line at melting pressure we conclude that in a magnetic field the second-order transition is split into two second-order transitions with a separation

$$T_{c_1} - T_{c_2} = \alpha H. \tag{9.1}$$

The actual value of α is presently somewhat uncertain. It has been measured only at melting pressure. What is actually measured is a pressure difference, rather than a temperature difference, and then the temperature difference is deduced from the slope of the melting curve. Gully et al. (1973) observe a pressure difference (0.20 mbar/kG) H. For the work of Alvesalo, Collan, Loponen, Lounasmaa, and Veuro (1974b) the numeric is 0.22. According to the thermometric data of Halperin, Rasmussen, Archie, and Richardson (1974b), as quoted in Bozler et al. (1974), near the A transition $dP_m/dT = -(100/T_A)$ mbar. Thus using the data of Gully et al. one finds $\alpha = 2 \times 10^{-3}T_A/\text{kG}$. For $T_A = 2.60$ mK then one finds $\alpha = 5.2$ μK/kG and about 10% higher for the data of Alvesalo et al. Osheroff and Anderson (1974) quote $\alpha = 6.4$ μK/kG based on a new measurement of 0.23 mbar/kG and a melting curve slope of -35.6 mbar/mK. They also find some field dependence of α.

There is no doubt that studies of ^{3}He in the small temperature region between T_{c_1} and T_{c_2} are extremely interesting since in this region, according to current thought, there is only one superfluid component.

The splitting of the second-order transition in a magnetic field also affects profoundly the attenuation of collisionless sound. An interesting illustration of the effect taken from the work at melting pressure by Lawson, Gully, Goldstein,

Richardson, and Lee (1974) is shown in Fig. 36, where the frequency is 10 MHz. In zero field the attenuation of collisionless sound suddenly increases as the temperature cools through T_c and peaks at a frequency-dependent temperature below T_c. In a magnetic field the attenuation peak is broadened and split as shown. The onset of attenuation increase correlates well with the pressure features corresponding to the thermal transitions T_{c_1} and T_{c_2}.

Another interesting effect of the splitting of the second-order transition was discovered by Alvesalo, Collan, Loponen, Lounasmaa, and Veuro (1974b) in their experiments on the motion of a vibrating wire. Near T_c the normal fluid density has not changed very much, but the damping of a vibrating wire decreases rapidly, reflecting a rapid decrease in effective viscosity. In a magnetic field there are two distinct discontinuities in the temperature derivative of the normal viscosity, as shown in Fig. 37. In the interval between T_{c_1} and T_{c_2} the temperature dependence of the viscosity is nearly $(1 - T/T_c)^{1/2}$, which is the same temperature dependence as that of the energy gap, as predicted by Shumeiko (1973) for an isotropic neutral Fermi superfluid and by Soda and Fujiki (1974) for an anisotropic fluid. It is clear from the figure that if a field of order 10^4 G can be applied to the ^{3}He then a very significant temperature range is available for experiments on what may be a one-component magnetic superfluid.

The above effects have not yet been studied at pressures below melting pressure, primarily because it is more complicated to apply a large field using electronic paramagnetic cooling. However, Paulson, Kojima, and Wheatley (1974b) did find a static magnetic effect in a moderate magnetic field at the second-order transition, as shown in the inset to Fig. 9. As the temperature warms through T_c the magnetization of the ^{3}He decreases by a few tenths of a percent over a temperature interval of a few microdegrees. The shape of this magnetic transition is a rather rapid drop at
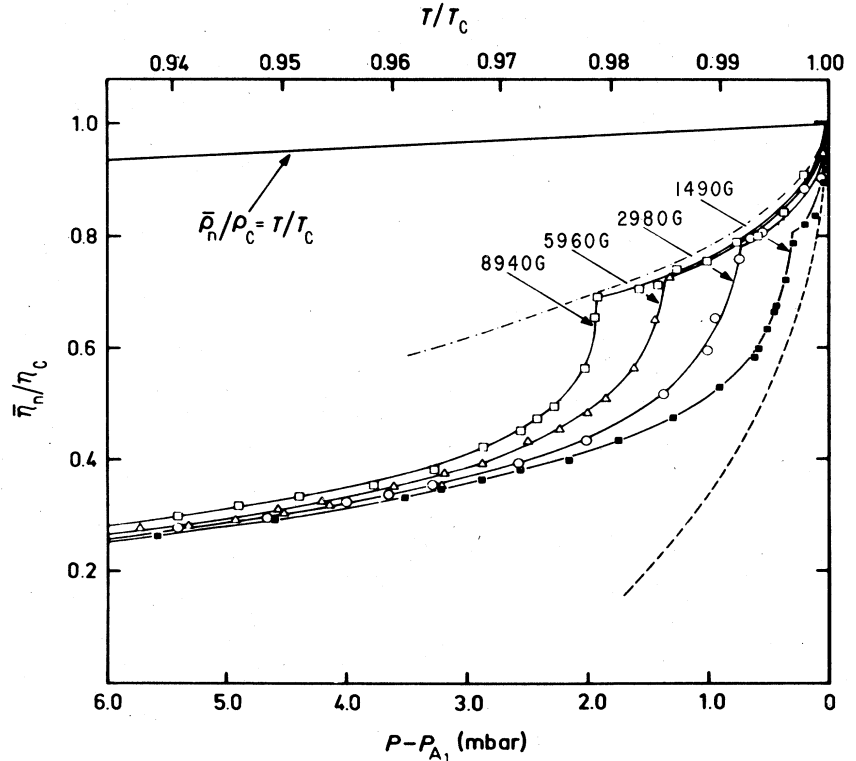
FIG. 37. Reduced effective viscosity $\bar{\eta}_n/\eta_c$ at melting pressure near the second-order transition and for several magnetic fields as a function of both T/T_c and the pressure displacement $P - P_A$, from the higher of the two second-order transitions. These data were obtained by Alvesalo, Collan, Loponen, Lounasmaa, and Veuro (1974b) from peak amplitude data on the resonance of a vibrating wire assuming $\bar{\rho}_n/\rho_c = T/T_c$ as shown. The dashed and dash–dot lines are proportional to $(1 - T/T_c)^{1/2}$.

the low temperature end followed by a more slowly varying tail at higher temperatures. Experimental observation, already near the limit of precision, is made more difficult by what appears to be a discontinuity in the rate of change of magnetometer background with time at T_c. The temperature width of the rapidly changing part correlates well with Eq. (9.1). The tail has been interpreted by Patton (1974) as an effect of fluctuations. Measurements of the tail can be interpreted in terms of the effective coherence length ξ_0 which can be interpreted in terms of a theoretical coherence length ξ_0 with

$$\xi_0{}^2 = 7\zeta(3)\hbar^2 v_F{}^2/48\pi^2 k^2 T_c{}^2, \qquad (9.2)$$

where v_F is the Fermi velocity and T_c is the critical temperature. For the conditions of the measurements of the inset to Fig. 9 one calculates $\xi_0 \simeq 120$ Å while a fit to the measurements suggests $\xi_0 = 50$ Å. More precise measurements are desirable but difficult owing to the smallness of the effect and to the interfering effect of the response of magnetic background near T_c.

The nonfluctuation part of the effect of field on the second-order transition from normal liquid to equal-spin-pairing ^{3}He-A has been discussed in terms of a Ginzburg–Landau theory by Ambegaokar and Mermin (1973), by Brinkman and Anderson (1973), who introduced the effect of spin fluctuations, and by Takagi (1974a), who started with the Brinkman and Anderson free energy and calculated additional properties. In what follows we use Takagi's definition of the parameter δ, which is just half that defined by Brinkman and Anderson. The free energy difference between

superfluid and normal states is taken to be

$$F_S - F_N = \tfrac{1}{2}N(0)\{(t - \eta h)\Delta_\uparrow{}^2 + (t + \eta h)\Delta_\downarrow{}^2$$
$$+ [\beta/2(kT_c)^2](\Delta_\uparrow{}^4 + \Delta_\downarrow{}^4) - [\beta\delta/(kT_c)^2]\Delta_\uparrow{}^2\Delta_\downarrow{}^2\},$$

$$(9.3)$$

where $\Delta_\uparrow$ and $\Delta_\downarrow$ are the energy gap parameters for $\uparrow$ $\uparrow$ and $\downarrow$ $\downarrow$ pairing, respectively; $t \equiv (T - T_c)/T_c$ is reduced temperature difference; $h \equiv \gamma\hbar H/2kT_c$ is the ratio of magnetic energy for one spin to thermal energy at T_c; $N(0)$ is the density of states at the Fermi energy for spins of one sign; η is a parameter which in weak coupling would be proportional to the derivative of $N(0)$ with respect to energy and which is to be determined experimentally; and β and δ are two parameters to be determined experimentally but with the restrictions $\beta > 0$ and $\delta < 1$. Study of this equation shows that for $\eta h > t > -\eta h(1 - \delta)/(1 + \delta)$ the free energy is minimized for $|\Delta_\uparrow|^2 \neq 0$ and $|\Delta_\downarrow|^2 = 0$, giving a one-component superfluid. But for lower t both $|\Delta_\uparrow|^2 \neq 0$ and $|\Delta_\downarrow|^2 \neq 0$ are required to minimize the free energy (see below). The corresponding entropy and magnetization differences from those for the normal state are shown in Figs. 38(a) and 38(b). Examination of these figures shows the following (Takagi, 1974a):

$$t_1 - t_2 = (T_{c1} - T_{c2})/T_c = 2\eta h/(1 + \delta), \qquad (9.4)$$

$$C_2 - C_N = N(0)k^2 T_c/\beta(1 - \delta) \equiv \Delta C, \qquad (9.5)$$

and

$$\chi_2 - \chi_N = N(0)(\tfrac{1}{2}\gamma\hbar)^2\eta^2/\beta(1 + \delta) \equiv \Delta\chi, \qquad (9.6)$$
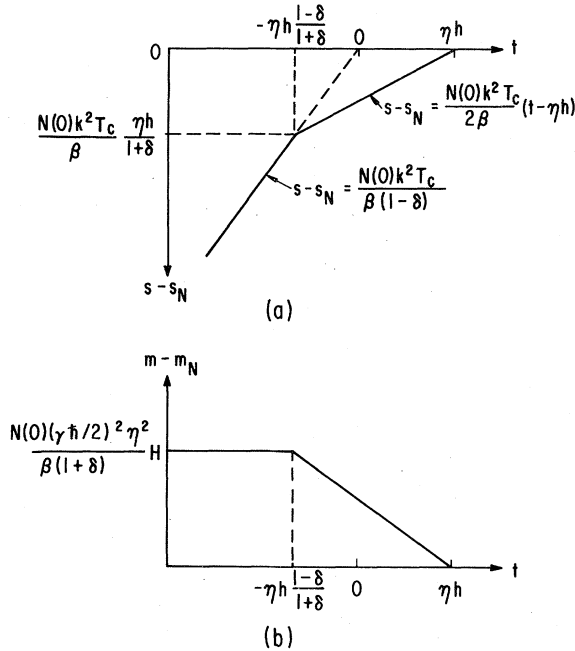
FIG. 38. Dependence according to mean-field theory of (a) entropy difference $s - s_N$ and (b) magnetization difference $m - m_N$ with respect to the normal state on reduced temperature difference $t \equiv (T - T_c)/T_c$ near the second-order transitions in a magnetic field. See text for definitions of quantities.

where $t_1 = (T_{c1} - T_c)/T_c$, $t_2 = (T_{c2} - T_c)/T_c$, and C_2 and χ_2 are the specific heat and susceptibility for $t < t_2$. Thus, measurements of ΔC, $\Delta \chi$, and $T_{c1} - T_{c2}$ should be sufficient to determine the parameters β, δ, and η. Note that $C_1 - C_N = \frac{1}{2}N(0)k^2 T_c/\beta$ does not depend on the parameter δ. Hence the ratio $(C_1 - C_N)/(C_2 - C_N) = (1 - \delta)/2$ can be used to give an independent value of δ. If Eqs. (9.4)–(9.6) are combined one finds

$$\Delta \chi = \frac{1}{4}(\Delta T/H)^2(\Delta C/T_c)(1 - \delta^2), \qquad (9.7)$$

where $\Delta T \equiv T_{c1} - T_{c2}$. This is a special case of an inequality

$$\Delta \chi \leqslant \frac{1}{4}(\Delta C/T)(\partial \Delta T/\partial H)^2 \qquad (9.8)$$

derived by Leggett (private communication). Application of these results to ³He properties near the second-order transition in a magnetic field has been obscured by the effect of fluctuations on the magnetization making a mean-field theory inaccurate. However, the existing data do satisfy Leggett's inequality.

The values of $\Delta_\uparrow$ and $\Delta_\downarrow$ which minimize the free energy (9.3) are as follows (assuming $\eta > 0$):

For $t > t_1$,

$$\Delta_\uparrow = \Delta_\downarrow = 0; \qquad (9.9)$$

for $t_1 > t > t_2$,

$$\Delta_\downarrow = 0; \quad \Delta_\uparrow^2 = A\,\frac{t_1 - t}{t_1 - t_2}\,; \qquad (9.10)$$

and for $t_2 > t$,

$$\Delta_\uparrow^2 = A + B\,\frac{t_2 - t}{t_1 - t_2}\,; \quad \Delta_\downarrow^2 = B\,\frac{t_2 - t}{t_1 - t_2}\,; \qquad (9.11)$$

where

$$A = [(t_1 - t_2)/\beta](kT_c)^2; \quad B = A/(1 - \delta). \qquad (9.12)$$

In some very nicely conceived and executed experiments Osheroff and Anderson (1974) have been able to test the form of the above equations by measuring parallel resonance frequencies $\Omega_{||}$ and perpendicular resonance shifts $\Omega_\perp$ in the vicinity of the T_{c1} and T_{c2} transitions. They and Takagi (1974b) have shown that

$$\Omega_{||}^2 = C\Delta_\uparrow\Delta_\downarrow \qquad (9.13)$$

and

$$\Omega_\perp^2 = C[\tfrac{1}{2}(\Delta_\uparrow + \Delta_\downarrow)]^2, \qquad (9.14)$$

where C is a constant. Well below T_{c2} where $\Delta_\uparrow \simeq \Delta_\downarrow \simeq \Delta$ then both $\Omega_{||}^2$ and $\Omega_\perp^2$ are equal to $C\Delta^2$. However, in the A_1 phase, where $\Delta_\downarrow = 0$, there is no parallel resonance. This might have been expected quite generally on the basis of the interpretation of parallel ringing in the A phase as a Josephson effect in which the relative numbers of $\uparrow\,\uparrow$ and $\downarrow\,\downarrow$ pairs oscillate, since in the A_1 phase there are $\uparrow\,\uparrow$ pairs only. Indeed Osheroff and Anderson find no parallel resonance in the A_1 phase. There is however a perpendicular resonance shift in the A_1 phase given by, from Eqs. (9.10, (9.11), and (9.14),

$$\Omega_\perp^2 = \frac{C}{4}A\,\frac{t_1 - t}{t_1 - t_2}, \qquad t_1 > t > t_2 \qquad (9.15)$$

and

$$\Omega_\perp^2 = \frac{C}{4}\left[A + 2B\,\frac{t_2 - t}{t_1 - t_2}\right.$$
$$\left. + 2\left(A + B\,\frac{t_2 - t}{t_1 - t_2}\right)^{1/2}\left(B\,\frac{t_2 - t}{t_1 - t_2}\right)^{1/2}\right], \quad t_2 > t. \qquad (9.16)$$

For $(t_2 - t)/(t_1 - t_2) \gg 1$, Eq. (9.16) is approximately

$$\Omega_\perp^2 \simeq \frac{C}{4}\left[A + 4B\,\frac{t_2 - t}{t_1 - t_2}\right]; \qquad t_2 - t \gg t_1 - t_2. \qquad (9.17)$$

Thus the temperature derivative of $\Omega_\perp^2$ in the A_1 region and that well below the A_1 region are in the ratio $(A/4B) = (1 - \delta)/4$ from (9.12). Osheroff and Anderson performed their experiment at 16 and 24 MHz (4950 and 7400 G), obtaining results which were quite internally consistent. They find $4B/A = 5.33 \pm 0.10$ corresponding to $\delta = 0.25$. Furthermore Osheroff and Anderson find that Eq. (9.16) precisely characterizes the experimental results over the entire temperature range explored, as shown in Fig. 39 which is taken from their paper. Also, for $\delta = \frac{1}{4}$, one would expect $t_1 = \frac{5}{8}(t_1 - t_2)$ and $t_2 = -\frac{3}{8}(t_1 - t_2)$. In terms of pressures this is equivalent to $P(T_c) = \frac{5}{8}P(A_2) + \frac{3}{8}P(A_1)$. Values of $P(T_c)$ obtained in this way fell on a straight line, when plotted vs H_0^2, passing through $P(T_c)$ in $H_0 = 0$. This would correspond to T_c being a fixed temperature.

$$\frac{t_2 - t}{t_1 - t_2}$$

$$-1 \quad 0 \quad 1 \quad 2$$

$$\frac{\gamma H_0}{2\pi} = 16.0 \text{ MHz}$$

• DATA FROM FOUR RUNS
— THEORY

$(\Omega_\perp / 2\pi)^2$ IN 10^8 (Hz)^2

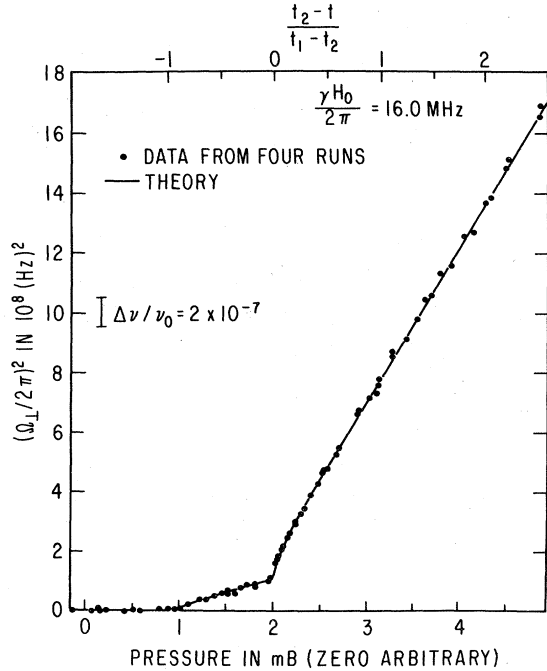$\Delta \nu / \nu_0 = 2 \times 10^{-7}$

PRESSURE IN mB (ZERO ARBITRARY)

FIG. 39. Perpendicular resonance shifts $(\Omega_\perp/2\pi)^2 = [(\omega/2\pi)^2 - (\gamma H_0/2\pi)^2]$ as a function of melting pressure (lower abscissa) and of a reduced temperature difference (upper abscissa) for $\gamma H_0/2\pi = 16$ MHz. The solid curve is a fit of Eqs. (9.15) and (9.16) to the data. After Osheroff and Anderson (1974).

Finally, using $\alpha \simeq 6 \times 10^{-9}$ K/G [Eq. (9.1)], we find using $\delta = \frac{1}{4}$ at melting pressure that $\eta = 5 \times 10^{-2}$. Also, using $\beta = [3/2\pi^2(1 - \delta)][C_N/(C_2 - C_N)]$ we find at melting pressure that $\beta = 0.11$. The BCS value of β is 0.128 for the ABM state. In the theory of Brinkman, Serene, and Anderson (1974) the quantity β in Eq. (9.3) should be the BCS value, all effects of strong coupling reposing in the quantity δ.

In the above we have taken ↑ to be the direction of the ^{3}He nuclear magnetic moment. Also we have taken $\eta > 0$, but this may not be the case according to Engelsberg et al. (1974) and K. Levin (private communication). If $\eta < 0$ then ↓ ↓ pairs will form first (at T_{c_1}). Whether the pairs in the A_1 phase are ↑ ↑ or ↓ ↓ can be determined by the *sign* of the probable magnetomechanical effect. This matter is important since it relates to the mechanism for the formation of the superfluid state, as has been emphasized by Levin.

X. PROPAGATION OF ULTRASOUND

Experimental work on the propagation of longitudinal collisionless sound in liquid ^{3}He has been performed by Lawson, Goldstein, Gully, Richardson, and Lee (1973, 1974) at melting pressure and 10 MHz and by Paulson, Johnson, and Wheatley (1973a) at 5, 15, and 25 MHz at lower pressures. The former experiments were very effective in studying the effect of a magnetic field on the second-order transition as discussed elsewhere but experienced quantitative difficulties owing to the presence of solid. In this section we shall present briefly the results of Paulson et al. on both the velocity and attenuation of collisionless sound and of

Lawson et al. on fluctuations in the attenuation in a magnetic field.

Measurements were made extensively at only two pressures, 33.16 and 19.61 bar, and before the phase diagram of Fig. 1 was discovered. It is likely that the measurements at 33.16 bar supercooled through the T_{AB} transition so that at this pressure there is purely ^{3}He-A behavior. On the other hand, 19.61 bar is below the PCP, so at this pressure there is behavior for ^{3}He-B only. Since a velocity decrease of about 1% for the $A \to B$ transition was reported by Lawson et al., it would be very interesting to look into this in an extension to intermediate pressure of the above work.

The results of the experiments are shown in Figs. 40(a), 40(b) and 41(a), 41(b). The relative attenuation and reduced velocity differences from first sound are shown on a reduced absolute temperature scale (see Appendix A), where T_c at a given pressure may be found from Fig. 1 or Appendix A. Relative attenuation means here that the measured attenuation has been divided by the attenuation of normal Fermi liquid ^{3}He zero sound ($\alpha_0 \propto T^2$) which would have been observed had the transition at T_c not taken place. It was possible to know the latter on the magnetic temperature scale used through zero-sound attenuation measurements at 9.7 bar, where T_c occurred very near the lowest temperature obtainable. The ultrasonic phonon energy quantum in these experiments is not small. The value $h\nu/k$ is 0.24, 0.72, and 1.20 mK at 5, 15, and 25 MHz, respectively. These are to be compared with T_c, which is of order 2.5 mK.

The results show certain similarities and differences. We first comment on similarities: (1) In all cases a thermal transition T_c^* can be determined precisely. (2) Just above T_c^* the attenuation is somewhat larger than that for ordinary zero sound, as if the transition were being anticipated. (3) Just at T_c^* and on cooling the attenuation coefficient rises rapidly, essentially discontinuously at 5 MHz. The attenuation has a peak on the low side of T_c^* and then decreases at the lowest temperatures to a value which is nearly frequency independent. (4) The velocity difference from first sound drops rapidly near T_c^* and becomes frequency independent at the lowest temperatures, possibly approaching zero. (5) A small frequency dependence of zero-sound attenuation above T_c^* is thought to be an experimental effect. The frequency effect on relative velocity above T_c may reflect incomplete development of zero sound at 5 MHz.

Both attenuation and relative velocity are very different just below T_c^* for ^{3}He-A and ^{3}He-B. (1) At 5 MHz the attenuation in both phases rises so rapidly just below T_c that measurements on the edge are not available. The fractional increase of attenuation is greater in the B than in the A phase. (Here and in what follows we *assume* that the pressure difference would have only a quantitative effect while the change from B to A phase is responsible for the qualitative differences. This assumption is currently unproved.) (2) Refer to Fig. 42, where the excess attenuation of 15 MHz over 5 MHz is plotted vs T/T_c. As T decreases below T_c the attenuation rises more rapidly and reaches a smaller maximum closer to T_c in the A than in the B phase: the temperature displacement of the peak is $1 - T/T_c \simeq 0.003$ for A phase and 0.004_5 for B phase.
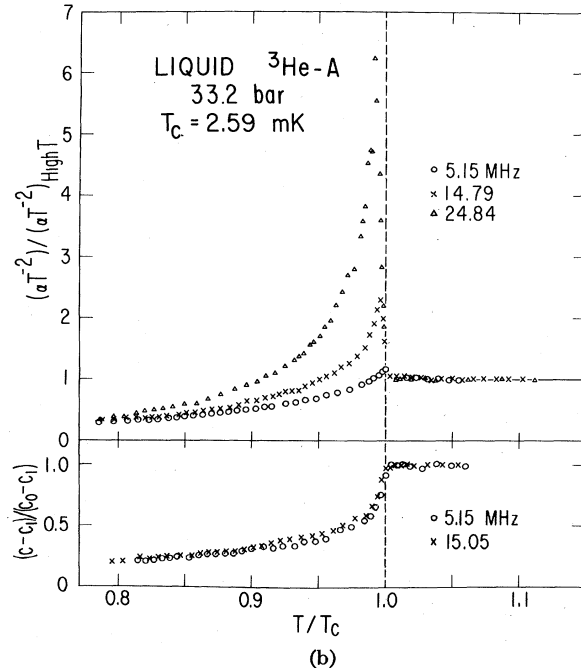
FIG. 40. (a) The logarithm of the amplitude attenuation coefficient α and the fractional velocity change relative to the first sound velocity c_1 for liquid ^{3}He-B and normal Fermi liquid at 19.6 bar for 15.15 MHz ($\times$) and 5.15 MHz ($\bigcirc$) as a function of the magnetic temperature of a powdered CMN thermometer. $c_1 = 354$ m/sec. (b) The reduced amplitude attenuation coefficient $(\alpha T^{-2})/(\alpha T^{-2})_{\text{high }T}$ and reduced velocity difference $(c - c_1)/(c_0 - c_1)$ as a function of reduced temperature T/T_c for ^{3}He-B at 19.6 bar, for which $T_c = 2.36$ mK; ($\bigcirc$): 5.15 MHz; ($\times$): 15.15 MHz. After Paulson, Johnson, and Wheatley (1973a).
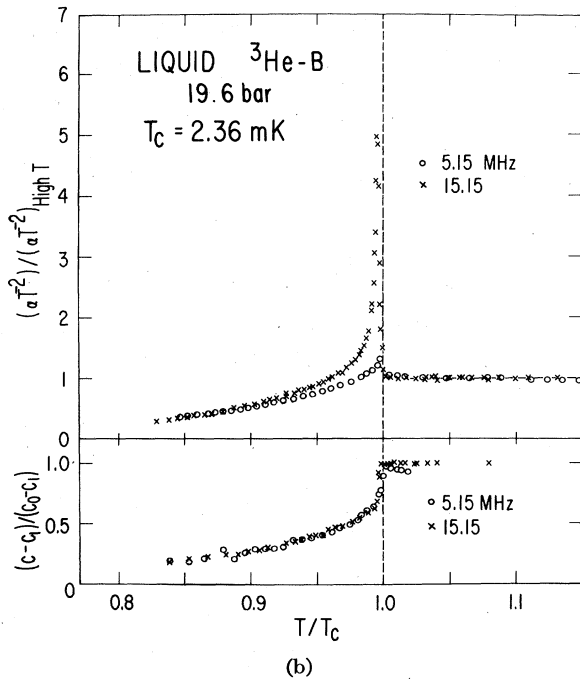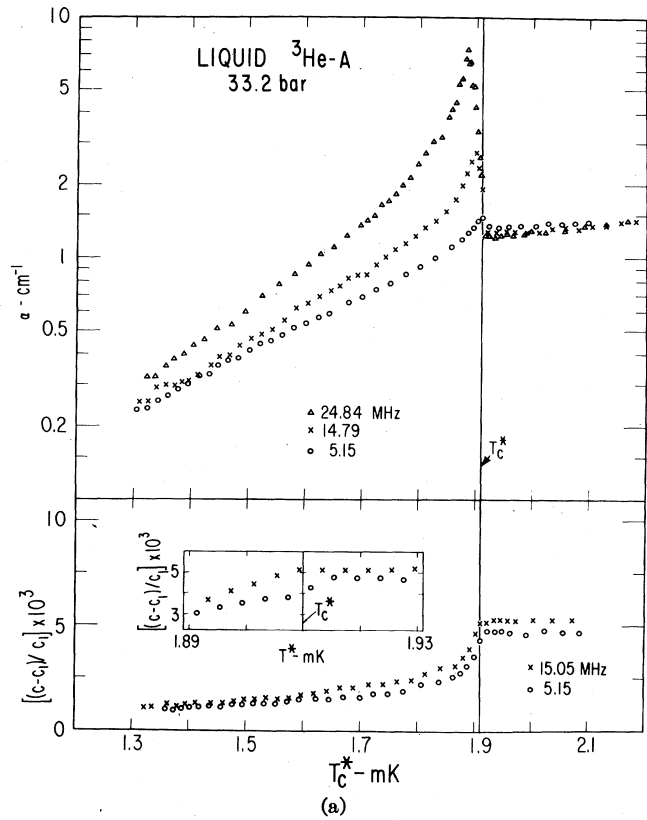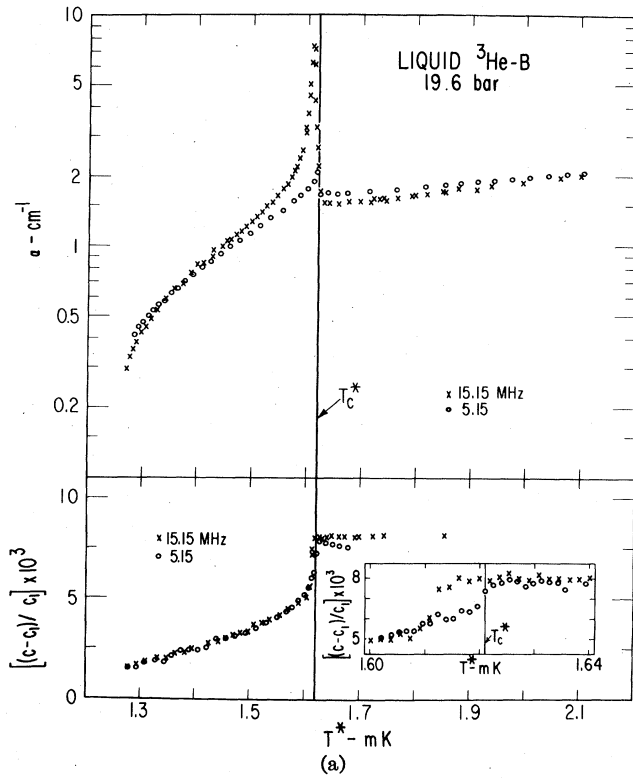
FIG. 41. (a) The logarithm of the amplitude attenuation coefficient α and the fractional velocity change relative to the first sound velocity c_1 for liquid ^{3}He-A and normal Fermi liquid at 33.2 bar for 24.84 MHz ($\triangle$), 14.79 MHz ($\times$), and 5.15 MHz ($\bigcirc$) as a function of the magnetic temperature T^* of a powdered CMN thermometer. $c_1 = 417$ m/sec. (b) The reduced amplitude attenuation coefficient $(\alpha T^{-2})/(\alpha T^{-2})_{\text{high }T}$ and reduced velocity difference $(c - c_1)/(c_0 - c_1)$ as a function of reduced temperature T/T_c for ^{3}He-A at 33.2 bar, for which $T_c = 2.59$ mK; ($\bigcirc$): 5.15 MHz; ($\times$): 15.15 MHz; ($\triangle$): 24.84 MHz. After Paulson, Johnson, and Wheatley (1973a).
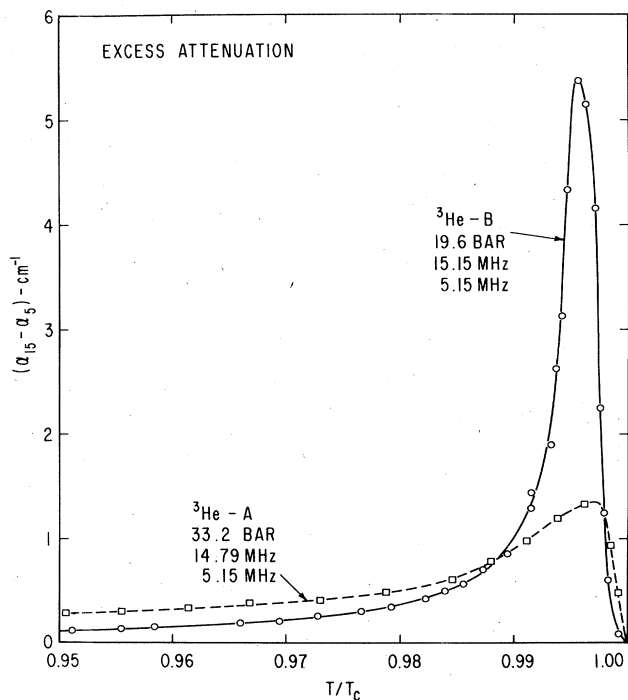
FIG. 42. Excess frequency-dependent amplitude attenuation coefficient of 15.15 MHz over 5.15 MHz ultrasound in ^{3}He-B at 19.6 bar and of 14.79 MHz over 5.15 MHz ultrasound in ^{3}He-A at 33.2 bar as a function of T/T_c near the critical temperature. From measurements by Paulson, Johnson, and Wheatley (1973a).

There is also strong evidence that as the attenuation coefficient α is rising below T_c it does so in the B phase less rapidly just below T_c, and then more rapidly close to the peak while in A phase the changes are more rapid just below T_c. Regarding the 5 MHz data as primarily reflecting a frequency-independent attenuation, one finds that the difference in α for 15 and 5 MHz has a rather small temperature width for the B phase but a much larger one for the A phase: half the excess attenuation occurs within 0.7% of T_c and the low temperature tail is weak for the B phase while half the excess attenuation lies within 2.6% of T_c and the low temperature tail is extended for the A phase. However, it is interesting that the area

$$\int_0^1 (\alpha_{15} - \alpha_5) d(T/T_c)$$

is very nearly 0.04 cm^{-1} for both phases. The half-width at half-maximum of the B phase peak in excess attenuation is less than $0.004 T_c$. (3) For 25 MHz the attenuation at the peak in the B phase was too large to measure, but in the A phase measurements were possible and it was found crudely that both the fractional temperature displacement $(T_{max} - T_c) T_c$ and the fractional attenuation $(\alpha_{max} - \alpha_0)/\alpha_0$ increase somewhat more rapidly than the square of the frequency. The 25 MHz attenuation also has a shoulder below the main peak and near $T/T_c \simeq 0.975$. (4) At 15 MHz the nature of the velocity change just below T_c was qualitatively different between B and A phases. In the B phase and as T decreased below T_c the velocity did not start to drop until below the temperature of the attenuation peak, while in the A phase the velocity started to drop at T_c. However, in the B phase, once the velocity did drop the

velocities of 5 and 15 MHz sound were indistinguishable, while in the A phase, and for 5 and 15 MHz, relative velocities seemed somewhat different for $T/T_c > 0.9$, though this is not a strong statement, and continued increasing right into T_c^*.

Contributions to the theory of ultrasonic attenuation have been made by Wolfle (1973), by Ebisawa and Maki (1974), by Maki (1974a), and by Serene (1973). The frequency-independent attenuation has not yet been discussed theoretically, most attention having been directed toward the frequency-dependent attenuation peaks. The frequency-dependent attenuation is attributed both to absorption of an ultrasonic phonon by a Cooper pair and to absorption into collective modes of the order parameter. In the theory there is considerable anisotropy predicted for the ABM phase as well as several peaks. A long tail in excess attenuation at temperatures below the peaks is predicted. For the BW phase the theory predicts both a relatively weak peak just below T_c due to pair-breaking and a "δ-function" absorption into a collective mode at a somewhat lower temperature where there is no further attenuation due to pair-breaking. These theories assume no collisions between quasiparticles.

The experiments on ^{3}He-A of Paulson et al. (1973a) were performed in zero field in an open volume roughly 8 mm in diameter and 5 mm high so one might expect that many orientations of possible domains were present. Random orientation plus the effect of collisions and difficulties in measurement may explain why detailed peak structures are not observed experimentally. However, it is significant that the integral

$$\int_0^1 \langle\alpha\rangle_{ABM}{}^{25} d(T/T_c),$$

where $\langle\alpha\rangle_{ABM}{}^{25}$ is the spatially averaged excess attenuation calculated by Serene (private communication) for the ABM phase at 25 MHz, gives a value of 0.14 cm^{-1}, in reasonable agreement with the experimentally determined area of 0.17 cm^{-1} under the curve of the excess of 25 MHz over 5 MHz attenuation as a function of T/T_c in the A phase. Furthermore, the general dependence of excess attenuation on temperature is not qualitatively incorrect and the dependence on frequency is encouraging.

The theory applied to the BW phase at 15 MHz (J. Serene, private communication) predicts a strong maximum attenuation at $1 - T/T_c = 0.004$ with a total area under the curve of excess attenuation vs T/T_c of 0.0093 cm^{-1}, only 15% of this figure coming from pair-breaking. While the excess attenuation peak at 15 MHz in the B phase is indeed quite narrow (half-width at half-maximum for 15 MHz of $0.004 T_c$) and the peak lies at $1 - T/T_c = 0.004_5$, the area under the excess attenuation curve is about 4 times the value predicted assuming that the B phase is the BW phase. Hence the frequency-dependent excess ultrasonic attenuation in ^{3}He-B does not quantitatively support its identification as a BW phase. It may be significant that the experimental value for

$$\int_0^1 (\alpha_{15} - \alpha_5)_{exptl} d(T/T_c)$$

for the B phase at 19.6 bar is essentially the same as that for the A phase at 33.2 bar.

A surprising phenomenon observed by Lawson et al.

(1974) at melting pressure and only in ³He-A is a fluctuation in time of ultrasonic attenuation with a very long correlation time (20–25 sec). For 10 MHz sound at some temperature between the A and B transitions they found that these fluctuations corresponded to a fluctuation in the amplitude attenuation coefficient of $2.0 \times 10^{-3}H^2$ cm^{-1} (kG)$^{-2}$. In a field of 10 kG the fluctuations are very large indeed! But in zero field no fluctuations are observed. Lawson et al. also indicate that they feel the ultrasonic attenuation fluctuations may be related to susceptibility fluctuations observed by Osheroff (1973).

XI. SUPERCOOLING, SUPERHEATING, AND THE PHASE DIAGRAM NEAR THE PCP

In his measurements with a compressional cooling cell Osheroff (1973) found that the B feature, corresponding to the $A \rightarrow B$ transition, on the pressurization curve was readily supercooled by substantial amounts, while the B' feature, corresponding to the $B \rightarrow A$ transition, could take place slowly at a higher temperature and was quite reproducible. It is quite common to be able to move the AB phase boundary around in a controlled way in a compressional cooling cell. The supercooling behavior was one of the early reasons for suspecting that the AB transition was first order; this was certainly true when the AB line of thermal resistance discontinuities was discovered in the liquid by Greytak, Johnson, Paulson, and Wheatley (1973). For the purpose of thermodynamic observations along the AB line it is essential to be able to produce and identify a reversible transition; either $A \rightarrow B$ or $B \rightarrow A$ will do. It would appear that the $B \rightarrow A$ transition is reversible, or nearly so, in a compressional cooling cell. Likewise in the early static magnetization measurements of Paulson, Johnson, and Wheatley (1973b) in an apparatus like that of Fig. 3 with $H_0 = 49$ G the $B \rightarrow A$ transition was slower and more reproducible than the $A \rightarrow B$ transition, but neither was clearly reversible. However, in the later static magnetism measurements of Paulson, Kojima, and Wheatley (1974b) in $H_0 = 378$ G and 480 G the $A \rightarrow B$ transition could be reversed while the $B \rightarrow A$ transition always superheated and then occurred suddenly. Even under these conditions the $A \rightarrow B$ transition strongly supercooled the first time the transition was made from temperatures considerably above T_c. However, once the $A \leftrightarrows B$ transition had been made several times the $A \rightarrow B$ transition could be reversed in the sense shown on Fig. 8(a). This is actually quite reasonable since in the apparatus, Fig. 3, the field H_0 was confined to the "static magnetism" appendix. For H_0 large enough, the temperature of the AB transition in H_0 is far enough below that for the AB transition in low field regions in the main cell that, on cooling, the B phase certainly forms first, supercooled or not, in the main cell. Then the interface between the B and A phases simply rises in the appendix as the liquid cools and the $A \rightarrow B$ transition as observed magnetically occurs. There is no nucleation problem and no irreversibility so far as liquid in the appendix at H_0 is concerned. However, once the appendix is filled with the B phase and the temperature drift is reversed to warming, the transition should occur first in the appendix. But now there is no bulk A phase available for nucleation and the $B \rightarrow A$ transition superheats. The observation of superheating calls into question the hypothesis that the A phase coats all solid boundaries, even when in the bulk

the B phase is stable (Ambegaokar, DeGennes, and Rainer, 1974). More details of the experiments are given by Kleinberg, Johnson, Webb, and Wheatley (1974).

Aside from its intrinsic interest, the question of supercooling and superheating of the AB transition is very important as it affects our knowledge of the thermodynamic T_{AB} line near the PCP. This line and its relation to the line T_c reflect importantly the relative thermal properties of the A, B, and Normal phases in the vicinity of the PCP (Leggett, 1974b). We have already seen, Fig. 10, that near the PCP even a field of 60 G has a profound effect on the T_{AB} line, deflecting it away from the T_c line as pressure is reduced.

The parallel ringing method of Webb, Kleinberg, and Wheatley (1974a) provided an excellent opportunity to study the AB transition near the PCP in fields much lower than those possible with the static magnetism observations. The principal motivation was to investigate the $A \rightleftarrows B$ transitions as close to T_c as possible as the pressure is varied near the PCP. Parallel ringing was observable if the residual field H_0 following incremental field turnoff was zero, but in this case the ringing was not degraded only if $(1 - T/T_c) > 0.01$. Thus, for $H_0 = 0$ the temperature region of greatest interest did not yield useful data. But for $H_0 = 5$ G it was possible to measure as long as $(1 - T/T_c) > 0.001$, so all measurements were carried out in this field.

It is easily possible to distinguish between the presence of the A and B phases using parallel ringing both since the B phase ringing frequency is 1.9 times that for the A phase at the same temperature near T_c and since the B phase signals frequently are degraded in quality compared with those in the A phase. In the measurements the observed A phase ringing frequencies f_A were related to reduced temperatures by means of the formula (Webb, Kleinberg, and Wheatley, 1974a)

$$1 - T/T_c = (f_A/19\,\text{kHz})^2 \times 10^{-2}, \tag{11.1}$$

which is sufficiently accurate for the small pressure and temperature range of present interest. The results of the 5-G measurements are shown in Fig. 42, where frequencies in the A phase have been converted to reduced temperature differences by means of Eq. (11.1). To obtain the data shown on this figure cooling proceeded very slowly into the A phase, while photographic observations of the A phase ringing were made. Such observations were continued until the $A \rightarrow B$ transition occurred. The temperature drift was then reversed and observations continued until A phase ringing was again observed. This procedure was continued to look for systematic trends. In Fig. 42 the * symbols refer to $A \rightarrow B$ transitions for which cooling occurred from an initial temperature greater than T_c. The $\triangle$ symbols refer to subsequent $A \rightarrow B$ transitions following $B \rightarrow A$ transitions, which are indicated by ∇ symbols. For $P > 21.5$ bar there was a very substantial supercooling observed the first time the $A \rightarrow B$ transition occurred, but on subsequent $A \rightarrow B$ transitions rather consistent results were obtained. The corresponding $B \rightarrow A$ transitions were always consistent. Also, included on Fig. 43 are three T_{AB} observations, indicated by ■ symbols, made in the heat flow measurements of Greytak et al. (1973). These were obtained in

FIG. 44. The pressure P_c of the second-order transition in zero field as a function of the magnetic temperature T_c^* as measured by Greytak, Johnson, Paulson, and Wheatley (1973). The intersection of the straight lines near a pressure of 21.2 bar is schematic only.
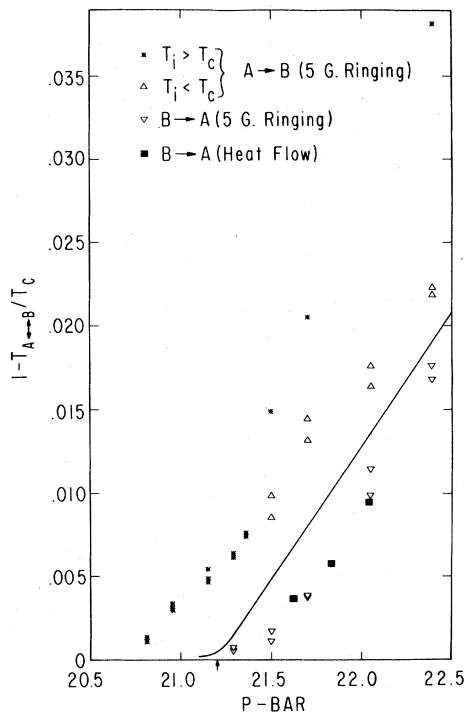
FIG. 43. Reduced temperature difference of the AB transition from the second-order transition as measured by parallel ringing in a 5-G field and by heat flow in zero field as a function of pressure near the PCP. Points marked (*) are $A \rightarrow B$ transitions determined by ringing with initial temperature greater than T_c while ($\triangle$) refer to $A \rightarrow B$ transitions with initial temperatures less than T_c. The (∇) are $B \rightarrow A$ transitions determined by ringing and the ($\blacksquare$) are $B \rightarrow A$ transitions determined by heat flow. The solid line is calculated from thermodynamic properties assuming the pressure of the PCP to be 21.2 bar ($\uparrow$ on axis). After Kleinberg, Johnson, Webb, and Wheatley (1974).

a static field less than a few tenths of a gauss following cooling to rather low temperatures; so it is both reasonable and encouraging, from the standpoint of experimental consistency, that they fall in with the $B \rightarrow A$ transitions observed using parallel ringing in a 5-G field.

In spite of the consistency of the $B \rightarrow A$ transitions and the $A \rightarrow B$ transitions (after the first time) there is no way at present to distinguish which, if either, of the transitions reflects thermodynamic equilibrium. It was not possible in low fields to start the transition in either direction and then to reverse it, as was possible in the high field case. Indeed we suspect, but cannot prove, that the thermodynamic transition lies between the $A \rightarrow B$ and $B \rightarrow A$ transition lines, and for the following reasons. The gross features of the T_{AB} line over the full field and pressure range are consistent with a rather simple form for the difference in the heat capacity per unit volume of the A and B phases, as given in Eq. (4.2). Near the pressure P_{PCP} of the polycritical point the quantity $\Delta C(P)$ in Eq. (4.2) is given by

$$\Delta C(P) = 0.37(P - P_{PCP}) \text{ erg/cm}^3 \text{ mK bar} \qquad (11.2)$$

and the quantity α is 70 erg/cm^3 mK. This description of the thermal properties may be too simplified to be applied to the present problem, but assuming its validity the reduced temperature difference of the thermodynamic AB transition $t_{AB} \equiv (1 - T_{AB}/T_c)$ should be given to lowest order in
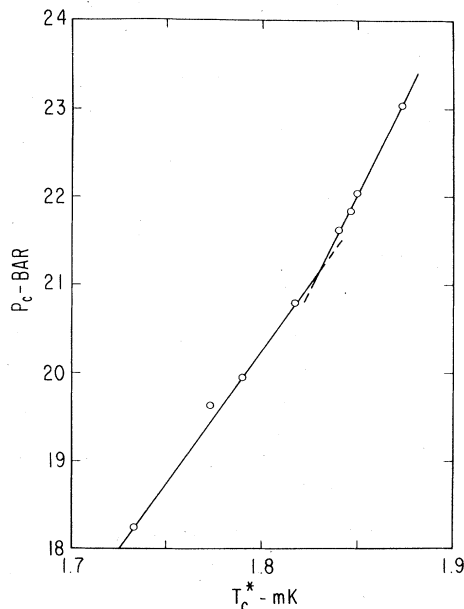
field H_0 by Eq. (4.6). At the pressure of the polycritical point $\Delta C = 0$, so we find for $P = P_{PCP}$ and $H_0 = 5$ G, using known data for χ_N and T_c (see Appendix), that $t_{AB} = 0.0004$. Examination of Fig. 43 then suggests that since $t_{B \rightarrow A}$ for P = 21.3 bar is greater than 0.0004 the pressure of the PCP lies below this pressure. If we choose, arbitrarily, the pressure of the PCP to be 21.2 bar then t_{AB} as derived using Eq. (4.6) is the solid line drawn between the $A \rightarrow B$ and $B \rightarrow A$ transition lines. If the PCP were located at 21.2 bar, then we see from Fig. 43 that in a field of 5 G very substantial supercooling of the A phase would have occurred 0.4 bar below this PCP. Alternatively, the PCP might be lower than 21.2 bar, but if the equation (4.2) is accurate the pressure of the PCP could not be less than 21.0 bar if the t_{AB} line from Eq. (4.6) is to lie to the right of the $A \rightarrow B$ line. We conclude that the equilibrium t_{AB} line near the PCP is not known at all well and that its precise location and shape near the PCP are at present an open question.

In view of the uncertainties about the t_{AB} line and the suggestion above that the pressure of the PCP probably lies below the 21.5 bar figure suggested by Paulson, Kojima, and Wheatley (1974a) on the basis of a linear extrapolation of the $B \rightarrow A$ line to $(1 - T_{AB}/T_c) = 0$, it may be appropriate to show in Fig. 44 the second-order transition line on a magnetic temperature scale as obtained by Greytak et al. (1973). It was obtained by observing the centers of the specific heat transition as a function of pressure. Such observations are subject to a rather uncertain error which may be several microdegrees and which would be influenced by changes in thermal conduction within the sample. It should not be implied that the existence of a discontinuity in dP_c/dT_c^* in the vicinity of 21.2 bar has been proved, but these data suggest that something of substance may be happening to the $P_c - T_c^*$ line near that pressure. There may be just a relatively sharp bend in the second-order line
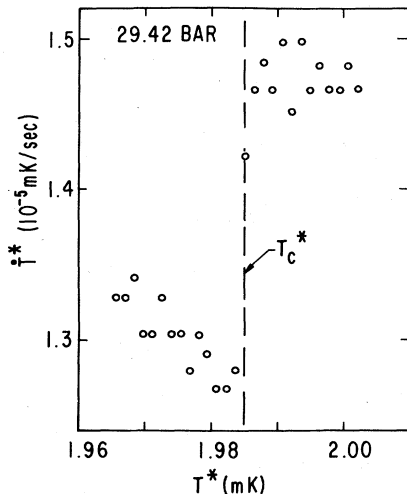
FIG. 45. The dependence of the time rate of change $\dot{T}^*$ of magnetic temperature on magnetic temperature T^* near the second-order transition T_c^* for a mixture of CMN and ³He at 29.42 bar. From unpublished measurements of Webb, Kleinberg, and Wheatley (1974).

only coincidentally related to the PCP. But on the other hand, the bend in the second-order line and the PCP may be related, in which case measurements of the T_c line itself might give information on the PCP. The data in Fig. 44 are presented on the magnetic temperature scale with which they were obtained since transfer to a provisional absolute scale would tend to blur the effect. However, evidence from measurement of parallel ringing frequencies (Webb, Kleinberg, and Wheatley, 1974a) suggests that the magnetic temperature scale itself does not have a sharp bend which could produce this effect. If the effect is spurious, then it would have been caused most probably by changes in the temperature distribution within the cell related to differences in the heat flow characteristics of the A and B phases.

Returning briefly to the general question of supercooling and superheating it is indeed remarkable that the carefully documented behavior at melting pressure in a compressional cooling cell (Osheroff, 1973) are so different from those observed at lower pressures in a CMN cell. At melting pressure supercooling is the rule while there is no tendency to superheat; on the contrary the $B \rightarrow A$ transition appears to be reversible. Osheroff presented quantitative data on the supercooling phenomenon in his compressional cooling cell. The supercooling temperature $T_{A \rightarrow B}$ was correlated with the immediately previous maximum temperature T_{max} to which the cell had been carried above the equilibrium temperature T_{AB}. Some pairs of observations taken from his thesis (1973a) and converted to reduced temperature differences using Appendix A are $[(T_{AB} - T_{A \rightarrow B})/T_c,$ $(T_{max} - T_{AB})/T_c] = [0, 0]$, $[0.0139, 0.0097]$, $[0.0172, 0.0142]$, $[0.0247, 0.0248]$, and $[0.0328, 0.0469]$. There is a tendency to saturate the supercooling effect.

At lower pressure both superheating and supercooling occur but superheating is the rule. This is documented in detail by Kleinberg, Paulson, Webb, and Wheatley (1974) but the data are too extensive to present here. Below the PCP pressure superheating of the $B \rightarrow A$ transition in a 378 G field was typically over half the temperature interval to T_c while above the PCP pressure the superheating was less. The superheating did show a history dependence. Hence

in supercooling/superheating behavior we find another qualitative difference between a property observed at melting pressure and at lower pressures. In this case the difference may be traceable to the presence of solid in the cell. It has also been suggested (Osheroff, private communication) that the difference is concerned specifically with the presence of CMN. However, it is difficult to see how the presence of CMN elsewhere in the cell can *prevent* formation of A phase in the epoxy walled magnetization tower where the measurements are made.

We also note that Ahonen et al. (1974b), who cooled ³He in a copper/copper powder cell by nuclear demagnetization and who have made measurements at 27 bar and below, state that they have never observed superheating in bulk liquid. However, they offer no proof that their $B \rightarrow A$ transition is reversible. We note in this connection that Kleinberg et al. (1974) report very reproducible $B \rightarrow A$ transitions which were nevertheless superheated.

XII. PRECISE INDICATORS OF T_c

The line of second-order transitions (P_c, T_c) is of considerable thermodynamic importance and may even hold some surprises near the PCP if it can be measured accurately. It is also important technically for the role it has played and is expected to play in thermometry as providing a foundation for a temperature scale that can be used by various experimental groups. Since pressure can be measured with great precision and accuracy what is needed is a precise indicator of T_c.

A traditional means to detect T_c is shown in Fig. 45, taken from unpublished work by Webb, Kleinberg, and Wheatley (1974). For a cell like that shown in Fig. 3 a plot of the time rate of change of magnetic temperature vs the magnetic temperature itself shows a rather sharp change near T_c. For the case shown, the transition center can be established to better than 10^{-3} mK, giving a precision of about 1 part in 2000. For CMN cells the transition becomes more difficult to see as the pressure is lowered. The transition is also broadened and possibly displaced by heat leak since one is observing the average temperature of the entire cell. The principal advantage of this type of measurement is that it will be possible to measure T_c^* in any experiment since all experiments should have some precise means for measuring temperature.

A second means for identifying T_c^* is shown in Fig. 46, where the attenuation coefficient of 5 MHz collisionless ultrasound, from measurements of Paulson, Johnson, and Wheatley (1973a), is shown as a function of the average magnetic temperature of the CMN powder in the cell. The line marked T_c^* is the center of the thermal transition as determined above. Although closely spaced attenuation measurements have never been attempted, it would appear that the drop in attenuation on warming through T_c for a small enough frequency takes place in a very small temperature range, about 10^{-3} of the temperature for the case shown. An advantage of this method is that the transition occurs in bulk, but of course in this case the ³He in the sound cell must be placed in excellent thermal contact with a suitable thermometer capable of precise measurements. We suspect that this indicator of T_c coupled with a magnetically shielded electron paramagnetic thermometer will be the best combination.
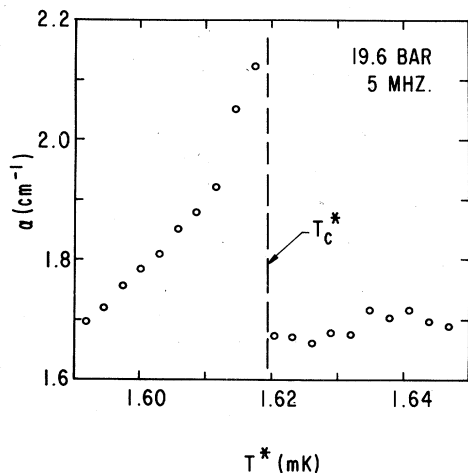
FIG. 46. Dependence of the amplitude attenuation coefficient of 5 MHz collisionless sound in zero field on magnetic temperature near T_c^* for a pressure of 19.6 bar. After Paulson, Johnson, and Wheatley (1973a).

FIG. 47. Dependence of the time constant τ of the spurious magnetic background in a magnetometer on magnetic temperature near T_c^* for a steady field of 50 G and a pressure of 33 bar. This time constant characterizes the longest relaxation time for magnetization changes following a sudden change of field parallel to itself. From unpublished measurements of Webb, Kleinberg, and Wheatley (1974).

A third rather baffling but very precise indicator of the transition was found in unpublished work of Webb, Kleinberg, and Wheatley (1974) in which an incremental field was suddenly switched off and the subsequent ringing and decay of magnetization observed by a SQUID magnetometer. It was found that a non-³He contribution to the magnetometer output decayed with a period of several seconds. The source of the magnetism was unknown, had a diamagnetic sign, but nevertheless was strongly suppressed in a field of 300 G compared, say, to 50 G. Measurements of the relaxation time τ for this magnetism following turnoff of an incremental field are shown in Fig. 47. The time τ suddenly decreases at T_c, contact to this background magnetism suddenly getting better as T increases through T_c. This phenomenon may be related to that found at melting pressure by Johnson et al. (1973) in the thermal contact to CMN powder. In their measurements the time constant for thermal equilibrium between CMN powder and ³He starts to *increase* at the A feature (T_c) and then starts to *decrease* rapidly at the B' feature (T_{AB}). It is now certain that these effects are unrelated to thermal effects in the CMN which take place at a lower temperature. No effect of the AB transition on heat transfer was seen by Webb et al. (1974a) but both experiments suggest a reduced magnetic coupling to the "walls" in the transition from normal to A fluid.

A fourth indicator of the transition useful in substantial magnetic fields is the perpendicular resonance shift. An example of experimental data of Osheroff and Anderson (1974b) at melting pressure is given in Fig. 39, where the pressure corresponding to T_{c1} is determined to less than 0.1 mbar, corresponding to an uncertainty in the location of T_{c1} of less than 1 in 10^8.

XIII. CERTAIN EXPERIMENTS ON ³He IN RESTRICTED GEOMETRIES

One lesson which we have learned is that even experiments performed "in bulk" probably should have employed a better geom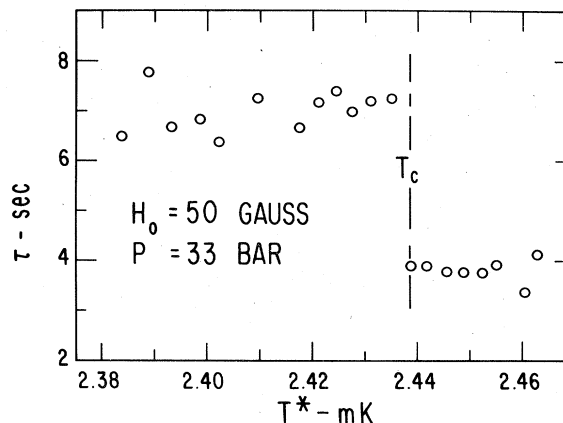etry, since it appears likely that even when superfluid ³He is confined to vessels of macroscopic dimensions the boundaries still may play an important role. Thus for experiments on fourth sound to be readily interpretable a "superleak" consisting of plane parallel passages is superior to the usual packed powder. At this stage one might say generally that a plane parallel geometry is preferred as a means to define carefully and simply the conditions of measurement.

We have already described experiments on fourth sound and on the specific heat of liquid ³He in the restricted geometry of a packed powder. In the case of specific heat, the second-order transition of ³He in the powder occurred at the same temperature as the jump in ultrasonic attenuation in bulk (Paulson, Johnson, and Wheatley, 1973a) and the specific heat itself is in good agreement with that observed by Halperin, Buhrman, and Richardson (1973) in bulk ³He in a compressional cooling cell. But for certain experiments geometry has had a really profound effect, either by reason of the smallness of the pores to which the ³He has been confined or by reason of the nature of the experiment, or both.

In one experiment Dundon, Stolfa, and Goodkind (1973) studied the specific heat of ³He in the pores of sintered copper powder. The approximate copper particle size was 1 μm. The powder was compressed to 0.45 of bulk density. Cooling was by nuclear demagnetization of copper wires and thermometry was by NMR on the copper. Specific heat of ³He was inferred by adding heat to the copper and measuring the total heat capacity with and without ³He and taking the difference. The authors argue that the temperature of the ³He is within 0.2 mK of that of the copper. The results, which lack a certain crispness of definition, are the following. The specific heat is not reproducible. In two cases (20 and 29 atm) a specific heat maximum is observed in the range 2–2.5 mK. But in another measurement at 29 atm a relatively large specific heat peak is seen in the region of 1–2 mK followed by excess specific heat up to 3 mK. This behavior was incipiently observed at lower pressures also. The authors found on integrating their specific heat data appropriately that the entropy in the

normal Fermi liquid region was larger than expected. The authors suggest that in this confined geometry the ³He-A may be supercooled to very low temperatures, accounting for the higher temperature peaks observed at 20 and 29 atm; but that if ³He-B is formed on cooling then ³He-A is not subsequently reformed on warming, accounting for the lower temperature peak in the other data. Certainly the excess entropy of normal liquid is a major problem. Furthermore the pore size may not be greatly different from that used in specific heat and fourth sound measurements. These results are very interesting but should be confirmed with more precise observations.

Ahonen, Haikala, and Krusius (1974a) made perpendicular NMR measurements in fields of 50–100 G on ³He confined to the pores of 99.95% pure Pt powder. The powder, packed to 30% of metallic density, was comprised of grains with size sharply peaked at 8 μm and with a lower limit of 3 μm. They suggest a pore size of $\approx$ 12 μm. The mixture of ³He and platinum powder was cooled to 1.6 mK using nuclear demagnetization of copper. They find that the temperature T_c is marked by the beginning of a rapid decrease in T_1 as T decreases, T_1 being given by $T_1 = 400 \ \mu$sec T^2 mK^{-2} in the normal liquid. Below T_c and for pressures above $\approx$ 21 atm they find that the amplitude of the resonance decreases in a nonreproducible way as T decreases but that the frequency does not shift, as it does in bulk ³He-A (Osheroff, Gully, Richardson, and Lee, 1972b). At a lower temperature, identified as T_{AB}, the resonance amplitude suddenly drops to zero. At pressures below $\approx$ 21 atm they find that the resonance amplitude rapidly but reproducibly approaches zero as T decreases below T_c. On a reduced temperature scale the effect is essentially pressure independent, the amplitude A obeying the empirical law $A/A_N = \exp[-60(1 - T/T_c)]$, where A_N is the amplitude in normal liquid. The amplitude is reduced to 10% of normal value at $(1 - T/T_c) \simeq 0.04$. Thus the drop in perpendicular absorption is rapid but readily measurable. The authors indicate that they have ruled out saturation, line broadening, or undetected shifts.

The above work on perpendicular NMR in ³He in platinum powder has subsequently been continued at higher fields with very interesting results (Ahonen, Haikala, Krusius, and Lounasmaa, 1974c; Krusius, private communication). In the A phase they find both a shifted and an unshifted line. The latter depends more on temperature than field, seems to be the continuation of the normal liquid line, and abruptly disappears usually when $T < T_{AB}$ and while the shifted line can be seen. This unshifted line reappears on warming well above T_{AB} and only after the shifted line is present. The amplitude of the shifted line is strongly field dependent. The authors suggest that the pores of their powder are coated with ³He-A with a normal liquid core and that a transition $N \rightarrow B$ and $B \rightarrow N$ takes place in the cores of the pores. In the B liquid an unshifted resonance line was observed with a temperature dependence like the bulk liquid but with an amplitude which is strongly field dependent: below 90 G no signal was detected while from 320 to 550 G all the liquid contributed to the integrated resonance absorption. The authors suggest that the rapid decay of magnetization described in the preceding paragraph is a manifestation of size effects as treated theoretically by Brinkman, Smith, Osheroff, and Blount (1974a), while the complete development of absorption above 320 G

reflects the inability of the textures to bend in the pores. Thus while a field of 90 G is wholly incapable of orienting the textures in the pores of the powder, a field of 320 G would effect complete orientation.

These NMR experiments are remarkable in that whereas they show no major effect on either the T_c or the T_{AB} lines, they do show a profoundly altered magnetic resonance behavior. This would suggest that the thermal properties of the liquid are not strongly affected by confinement in the small pores, but that the spin properties are profoundly altered.

In the absence of detailed calculations from theory and further experiments, especially of static instead of dynamic magnetism, it is difficult to see how Ahonen et al. (1974a) in their 90-G measurements could have missed at least some indication of a line broadening or a line shifting effect as would follow from (8.29) as Ω_B (hundreds of kilohertz at low T) develops from 0 near T_c and α increases from 0° near T_c. Given the field inhomogeneity of 6×10^{-4} from their paper the linewidth in normal liquid should have been no more than a few tenths of a kilohertz, and indeed a changing line shape is commonly observed in the A phase. Hence, at least from the standpoint of motivating further experiments, the possibility of the development of a surface phase less magnetic than bulk ³He-B but thermally very similar to ³He-B should not be ruled out. Recovery of the bulk ³He-B susceptibility above 320 G would then have reflected a phase change.

XIV. RECENT DEVELOPMENTS

Important experimental developments recently available to us are included in this section. In all cases they represent results not yet published, and I am very grateful for the opportunity to present them here.

A. Specific heat at melting pressure

This has been measured using the heat pulse method by Halperin (1974). The results are shown in Figs. 48(a) and 48(b) using a reduced temperature $T^* \equiv T/T_A$, where T_A is the value of T_c at melting pressure. The reduced specific heat C^* is the molar heat capacity multiplied by T_A. The value of $C_</C_>$ from Fig. 48(a) is somewhat greater than 3, reflecting a smaller normal state heat capacity than that deduced using data of Abel et al. (1966). The value of $C_</C_>$ from Fig. 6 at melting pressure is 2.8 ± 0.1. This will increase the discrepancy between the value of β [Eq. (9.3)] and the BCS value expected in the theory of Brinkman, Serene, and Anderson. Most of the temperature dependence of the specific heat is removed and the change in specific heat at the AB transition at reduced temperature $T_B^* \equiv T_{AB}/T_c$ is displayed by multiplying C^* by T^{*-3} as in Fig. 48(b). Since $C_</C_> \approx 3$, this is support (especially for the B phase) for the ansatz used in Sec. VII for estimating the temperature dependence of the entropy of the normal fluid and thus the effective normal fluid viscosity and relative superfluid–normal fluid velocity. If the smooth line through the B phase data is extrapolated to $T^* = 1$ a crossing of specific heats as suggested in Fig. 15 appears reasonable; that is, $C_A > C_B$ at T_c but $C_A < C_B$ at T_{AB}. Also, if the specific heat of the B phase is extrapolated to zero as T^{-3} then the entropy at T_c calculated from the superfluid specific heat is not at all unreasonable: S_c/nRT_c is 4.6 K^{-1}
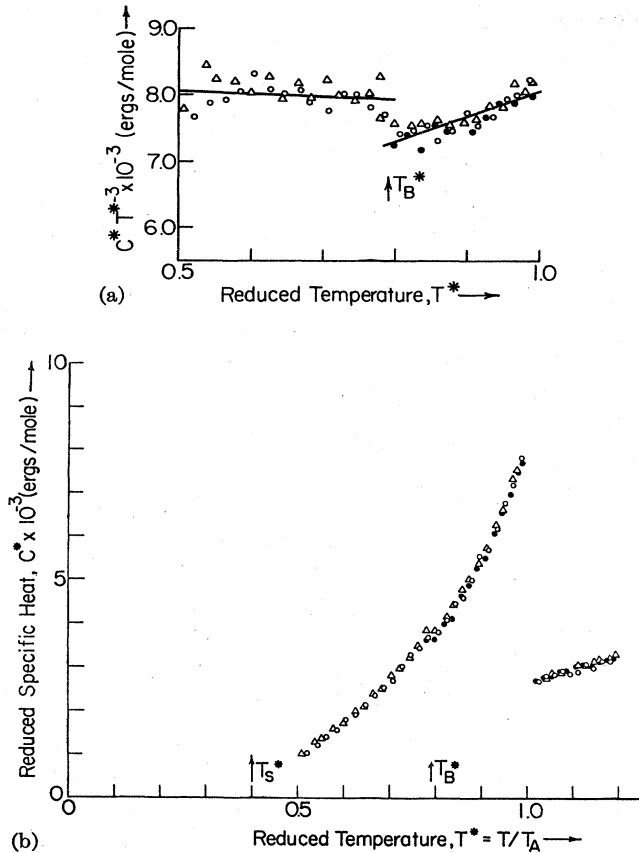
FIG. 48. (a) Reduced molar specific heat of liquid ^{3}He at melting pressure as a function of reduced temperature $T^* \equiv T/T_A$ where T_A is the temperature of the second-order transition. The reduced specific heat C^* is the actual specific heat multiplied by T_A (See Appendix A). T_B^* is the reduced temperature of the AB transition and T_S^* is the reduced temperature of the solid transition. The symbols $\triangle$, $\bigcirc$, and $\bullet$ refer to measurements in which the fraction of liquid in the cell was, respectively, 0.76, 0.79, and 0.83. (b) Reduced molar specific heat divided by the cube of the reduced temperature as a function of reduced temperature, where these quantities are defined above, for liquid ^{3}He at melting pressure. T_B^* is the reduced temperature of the AB transition. After Halperin (1974).

or 4.2 K^{-1} depending on whether T_c is taken to be 2.6 or 2.75 mK. Both values are somewhat lower than the value given in Appendix B, Table III for melting pressure. There is thus no major discrepancy in the entropy of the high pressure normal liquid, an important observation with respect to the specific heat measurements in a confined geometry by Dundon, Stolfa, and Goodkind (1973), Sec. XIII of this paper.

The discontinuity in specific heat at T_{AB} and at melting pressure is $C_A - C_B \simeq -5$ erg/cm^3 mK as deduced from Fig. 48, while a value of about -10 erg/cm^3 mK would have been obtained by extrapolating the data in Fig. 16 to melting pressure and using Eq. (4.2) with α evaluated at the pressure of the PCP. This comparison may be regarded as satisfactory inasmuch as Eq. (4.2) is no doubt inaccurate except rather near the PCP.

B. Normal viscosity near T_c at melting pressure in ^{3}He-A_1 and ^{3}He-A

Alvesalo, Collan, Loponen, Lounasmaa, and Veuro (1974b) have analyzed their vibrating wire normal viscosity

data near T_c, Fig. 37, in terms of the theory of viscosity of Shumeiko (1972) and of Soda and Fujiki (1974). Alvesalo et al. plot their data in the form

$$1 - \frac{\eta_n}{\eta_{c1}(T_{c1}/T)^2} = c_1 \frac{\Delta}{(T/T_{c1})} + c_2 \left[\frac{\Delta}{(T/T_{c1})}\right]^2, \quad (14.1)$$

where η_n is the effective normal viscosity assuming $\rho_n/\rho = T/T_{c1}$, η_{c1} is the viscosity of the normal Fermi liquid at T_{c1}, c_1 and c_2 are constants to be fitted to the data, and Δ is proportional to an average energy gap. They define Δ as being proportional to the average of $\Delta_\uparrow$ and $\Delta_\downarrow$ [Eqs. (9.10)–(9.12)] such that

$$\Delta = \frac{\frac{1}{2}(\Delta_\uparrow + \Delta_\downarrow)}{[A/(t_1 - t_2)]^{1/2}} = \frac{\beta^{1/2}}{kT_c} \frac{1}{2}(\Delta_\uparrow + \Delta_\downarrow). \quad (14.2)$$

Setting $(t_1 - t) = (T_{c1} - T)/T_{c1}$ and $(t_2 - t) = (T_{c2} - T)/T_{c1}$ in Eqs. (9.10) and (9.11) we have

$$\Delta_{A1} = \frac{1}{2}(1 - T/T_{c1})^{1/2} \quad (14.3)$$

for the A_1 phase and

$$\Delta_A = \frac{1}{2}\left[\left(1 - \frac{T_{c2}}{T_{c1}} + \frac{B}{A}\frac{T_{c2} - T}{T_{c1}}\right)^{1/2} + \left(\frac{B}{A}\frac{T_{c2} - T}{T_{c1}}\right)^{1/2}\right] \quad (14.4)$$

for the A phase. They find that the constants c_1 and c_2 are essentially the same for both A_1 and A phases. Evaluating them for the three highest fields (8940, 5960, and 2980 G) and using $B/A = 1.33$ from Osheroff and Anderson (1974) they find $c_1 = 5.4 \pm 0.2$ and $c_2 = -10.4 \pm 0.4$ as a reasonable fit to the data over the range of $\Delta/(T/T_{c1})$ from zero to 0.25. By minimizing the deviation of the experimental points from a fit to Eq. (14.1) with a variable value for B/A a value for B/A of (1.3 ± 0.15) was obtained using the 8940 G data.

The definition of Δ is somewhat arbitrary, though it would coincide with that used for the B phase in the limit of weak coupling. The data for ^{3}He-B (Sec. VII) were fit to a similar form as (14.1) with $\Delta_B \equiv (1 - T/T_c)^{1/2}$. In that case the coefficient of the Δ term in the expansion was 2.9 with an uncertain error. If in the A_1 phase we were to define the Δ without the averaging factor of $\frac{1}{2}$ then the coefficient of the Δ term would be 2.7. In the limit of zero field there is no A_1 region, and Δ in the A region is given by, using Eq. (9.12), $\Delta_A = (1 - \delta)^{-1/2}(1 - T/T_c/^{1/2}$. The only difference between this quantity and that used for the B phase involves the strong coupling parameter δ, which is $\frac{1}{4}$ at melting pressure according to Osheroff and Anderson (1974).

C. Superfluid density via fourth sound in a parallel plate geometry

Recently Kojima, Paulson, and Wheatley (1975) have completed new measurements of the propagation of fourth sound between parallel plates of epoxy with a ^{3}He thickness of 50 μ. These measurements answer some questions raised in Secs. V and VI and introduce some interesting new ones. They are shown in part in Fig. 49, along with some of the original CMN powder superleak data of Kojima et al. (1974), for which the pore size was probably about a micron.
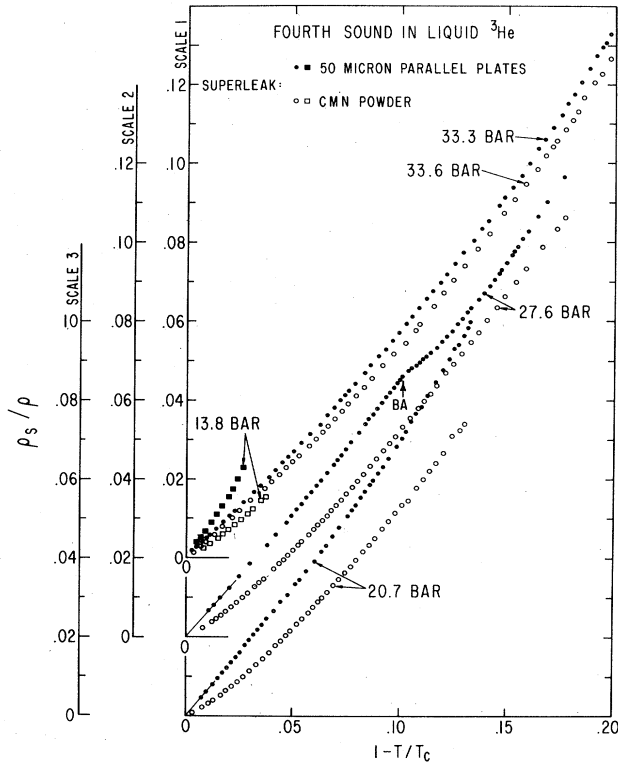
FIG. 49. Relative superfluid density in ^{3}He as a function of reduced temperature difference for both a CMN superleak (open symbols) and a superleak in which the ^{3}He is confined to plane parallel passages 50 μ across. There are three equal but shifted vertical scales: Scale 1–13.8 and 33 bar; Scale 2–27.6 bar; Scale 3–20.7 bar. The arrow labeled $B \rightarrow A$ is the temperature of the $B \rightarrow A$ transition expected from heat flow and susceptibility measurements. After Kojima, Paulson, and Wheatley (1974 and 1975).
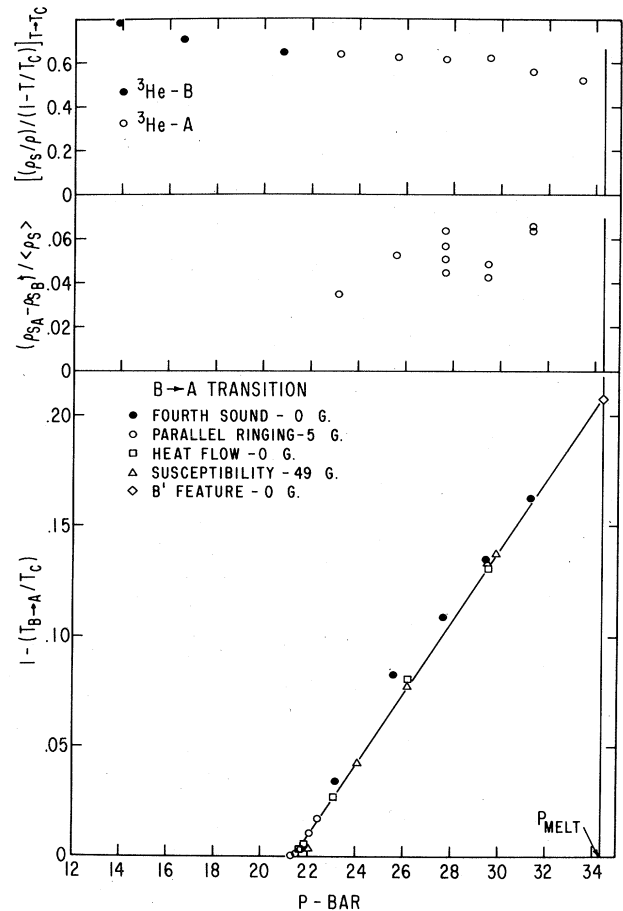

FIG. 50. Reduced temperature difference at the $B \rightarrow A$ transition, fractional increase of superfluid density at the $B \rightarrow A$ transition, and initial slope of ρ_s/ρ vs $(1 - T/T_c)$ as a function of pressure. After Kojima, Paulson, and Wheatley (1974 and 1975).

Below we refer to the CMN superleak as a "confined" geometry and the 50 μ parallel plates as an "open" geometry although they both represent a substantial confinement of the ^{3}He, but probably not on the scale of the usually accepted coherence length. To avoid confusing the data points for the four general pressure regions represented, three equal but shifted vertical scales are used. In the confined geometry ρ_s/ρ plotted against $(1 - T/T_c)$ is essentially pressure independent for $(1 - T/T_c) \gtrsim 0.03$ from 13.8 to 29.5 bar with some increase at 33.6 bar. Near T_c, ρ_s/ρ is not linear in T and tends to decrease with decreasing pressure at a given value of $(1 - T/T_c)$. No $B \rightarrow A$ transition can be seen in the data. In the open goemetry ρ_s/ρ increases as the pressure decreases, is linear in T near T_c, and a broadened $B \rightarrow A$ transition is observed (Fig. 50) at a temperature quite close to that expected from earlier data. At a pressure of 33.3 bar ρ_s/ρ in the confined geometry has the least curvature on a linear plot and is also very close to that measured in the open geometry. As the pressure is lowered the ratio of ρ_s/ρ in open to that in confined geometry increases, the effect being quite substantial at 13.8 bar, Fig. 49. One can conclude that ^{3}He in a confined geometry at any pressure in the range measured has nearly the same ρ_s/ρ at a given T/T_c, except near T_c, where ρ_s/ρ is more depressed at lower pressures, as ^{3}He-A in an open geometry at a pressure of about 33 bar (near melting pressure). That is, confinement has little effect

near melting pressure but has an increasingly large effect as the pressure is reduced below melting pressure. Thus near melting pressure the bulk ρ_s/ρ probably has been measured but at 13.8 bar this is possible but not certain.

Now that the $B \rightarrow A$ transition has been observed we have proof of superfluidity via fourth sound in both A and B phases. However, as shown in the middle section of Fig. 50, the fractional increase in ρ_s/ρ in the $B \rightarrow A$ transition is only 4%–6% and barely pressure dependent, if at all. (Note that in the vibrating wire experiments at melting pressure of Sec. VI the superfluid density was found to decrease by a large amount at the $B \rightarrow A$ transition.) On the basis of the discussion of Sec. V it is surprising that the fractional change of ρ_s is so small. It is reasonable that the average value of ρ_s changes at the $B \rightarrow A$ transition by no more than a few precent according to resonance (Fig. 31), specific heat [Fig. 48(b)], and phase diagram (Fig. 16) data. A nearly pressure-independent fractional change in ρ_s at $B \rightarrow A$ might quite reasonably be interpreted as reflecting anisotropy of the A phase or, more precisely, changes of anistropy from B to A phases. As we noted in Sec. V a 20% increase was expected in bulk if ^{3}He-A is the ABM state with orbital vector $\mathbf{l}$ perpendicular to the plates and if ^{3}He-B is the BW state and assumed to be orbitally isotropic. There is no

evidence for such high orbital anisotropy in the data, but it is not proved either that bulk properties were measured or that the A phase orbital vector was properly oriented. Regarding the first point, a 6% effect was observed at 31.3 bar, very close to 33.3 bar, where confinement had little effect on ³He-A. Regarding the second point, in the absence of electric and magnetic fields the $\mathbf{l}$ vector is thought to be oriented perpendicular to walls unless the superfluid velocity v_s is larger than about $h/2m_3d$, where $h/2m_3$ is the quantum of circulation in ³He and d is the separation between the plates (Ambegaokar, DeGennes, and Rainer, 1974; De-Gennes and Rainer, 1974). (For the present geometry $h/2m_3d = 0.13$ cm/sec) Superflow is possible in the flow of heat, but owing to the tiny plate separation most heat flows diffusively. For the maximum possible heat flows in the superleak of Kojima et al. (1975) the velocity v_s is calculated to be very much less than the critical value given above. Hence the measurement should have been detecting the perpendicular component of ρ_s in ³He-A.

In the top section of Fig. 50 is the limiting value of the slope of ρ_s/ρ on a reduced temperature difference plot near to T_c for pressures between 13.8 and 33.3 bar. These numbers are strongly dependent on the temperature scale being correct. This is the same temperature scale on which the temperature dependences of A phase ringing frequencies down to 20 bar were determined (Sec. VIII) very successfully with respect to measurements made by other groups with other methods, so perhaps some confidence can be placed on a 5%–10% level of accuracy for the conclusions of the ρ_s/ρ measurements. The quantitative conclusions are very interesting.

At 33.3 bar (near melting pressure) Kojima et al. (1975) find near T_c that $\rho_s/\rho = 0.527(1 - T/T_c)$. This result is thought to include the effect of molecular fields (Leggett, 1965) via the formula

$$1 - \frac{\rho_s}{\rho} = \frac{(1 + \frac{1}{3}F_1)f(T/T_c)}{1 + \frac{1}{3}F_1 f(T/T_c)} . \qquad (14.5)$$

The function f reflects the "bare" (but not necessarily weak coupling) properties of the fluid. Near T_c we have

$$(\rho_s/\rho)_{\text{bare}} = 1 - f = (\rho_s/\rho)(1 + \tfrac{1}{3}F_1) = 3.23(1 - T/T_c)$$

for the number given above. Now if ³He-A were in the ABM state and the experiment measured $\rho_{s\perp}/\rho$ then in weak coupling (Sec. V) we expect $1 - f = 2(1 - T/T_c)$. The ratio 3.23/2 would then reflect strong coupling, which is measured in $\langle|\Delta|^2\rangle$ by the factor

$$(C_</C_> - 1)_{\text{exptl}}/(C_</C_> - 1)_{\text{weak}}.$$

For the ABM state $(C_</C_> - 1)_{\text{weak}} = 1.43/(6/5)$, so the above ratio requires $(C_</C_>)_{\text{exptl}} = 2.9$, very close to the experiment, Sec. II. Bear in mind, of course, that the 6/5 which appeared above is the same factor which was *not* seen at the $B \to A$ transition. Next, though ρ_s/ρ for the B phase has not been measured one might guess $(\rho_s/\rho)_B \simeq 0.94(\rho_s/\rho)_A$ at this pressure and then try to calculate what $(\chi/\chi_N)_B$ would be on the basis of Eq. (14.5) above and

$$\frac{\chi_B}{\chi_N} = \frac{(1 + \frac{1}{4}Z_0)[\frac{2}{3} + \frac{1}{3}f(T/T_c)]}{1 + \frac{1}{4}Z_0[\frac{2}{3} + \frac{1}{3}f(T/T_c)]} , \qquad (14.6)$$

which allows χ_B/χ_N to be expressed as a function of $(\rho_s/\rho)_B$. In this equation one-third of the condensed pairs are taken to be nonmagnetic. The resultant curve of χ_B/χ_N vs T/T_c very nicely extrapolates into the melting pressure χ_B/χ_N data of Corrucini and Osheroff (private communication) and Osheroff (1974). Although the $B \to A$ transition did not show the 20% anisotropy change expected, most other features check out, such as the size of the strong coupling correction and the effectiveness of the molecular field corrections in relating $(\rho_s/\rho)_B$ and χ_B/χ_N.

The picture is much different at lower pressures. First of all the "bare" values of ρ_s/ρ in ³He-B obtained near T_c by $(\rho_s/\rho)(1 + F_1/3)$ are large. From the data at the top of Fig. 50 we find $(\rho_s/\rho)_{\text{bare}}/(1 - T/T_c) = 3.3_3, 3.3_9$, and 3.5_7 at, respectively, 20.7, 16.6, and 13.8 bar. For the weak coupling BW state $(\rho_s/\rho)_{\text{bare}}/(1 - T/T_c) = 2$. If we try to correct for strong coupling using the factor

$$(C_</C_> - 1)_{\text{exptl}}/(C_</C_> - 1)_{\text{weak}} = (C_</C_> - 1)/1.43$$

then, from Fig. 6, it is clear that the strong coupling correction should be nearly 1; not the 1.7 needed to explain the measurements. And it is conceivable that $(\rho_s/\rho)_B$ in this pressure range could be even larger if a 50 μ spacing does not give bulk values. If ρ_s/ρ is used to obtain $f(T/T_c)$ in Eq. (14.5) and then that $f(T/T_c)$ used in Eq. (14.6) to find χ_B one finds that the resultant values of $[(\chi_N - \chi_B)/\chi_N]/(1 - T/T_c)$ are about 25% low compared with the static measurements. In view of the essential agreement of ρ_s/ρ and dynamic χ_B/χ_N data near or at melting pressure this would appear to suggest a problem with the static magnetization data. However, the internal check of the calibration of the static measurements via diamagnetic susceptibility (Sec. III) leaves no explanation at present for the discrepancy.

The numerical values of the "strong coupling" factor as manifested both in $(\rho_s/\rho)/(1 - T/T_c)$ near T_c and in specific heat are in quite good agreement with one another for the CMN superleak, which incidentally was quite similar to the environment of the ³He for the specific heat measurements. Although the value of the strong coupling factor deduced from ρ_s/ρ measurements for the parallel plate superleak and for pressures near melting pressure is in good agreement with that for the CMN superleak, a discrepancy develops as the pressure decreases. Near the PCP and below a strong coupling factor of about 1.7 is indicated while a factor near one would be suggested by extrapolating the specific heat results in the confined CMN powder geometry. This motivates further specific heat measurements on *bulk* ³He.

XV. CRITICAL SUMMARY

In this section I shall attempt to summarize and evaluate various aspects of the diverse experiments and measurements described in this article.

1. There are at least three extraordinary phases of bulk liquid ³He. In addition to these there may be surface phases with thermal properties similar to those of the bulk phases. The pressure–temperature plane has not been explored in detail, especially above the minimum pressure of the melting curve, except just at melting pressure. The three known bulk phases are called ³He-A_1, ³He-A, and ³He-B in the

order in which they appear as the temperature is reduced at constant field. Both ³He-A and ³He-B have been proved to be superfluids using fourth sound (Secs. V and XIV) with supporting evidence at melting pressure from the motion of a vibrating wire (Sec. VI) and at lower pressures from heat flow (Sec. VII). Proof of the superfluidity of ³He-A_1 has yet to be offered.

2. Most theoretical work on superfluid ³He assumes that it can be described as a strongly coupled superfluid of BCS type, probably anisotropic in some respects, and comprised of triplet pairs. Direct quantitative evidence for strong coupling is the size of the specific heat ratio $C_</C_>$ at the transition temperature T_c, the ratio being larger at high pressure than expected for a weak coupling BCS system (Sec. II). Qualitative evidence is related to the stability of the A phase. Thermodynamic evidence for triplet pairing, apart from dynamic experiments which we assess separately, is the temperature dependence of nuclear magnetism (Sec. III). In the A phase the magnetization is temperature independent while in the B phase the magnetization does depend on temperature but extrapolates to a value $\frac{1}{4}$ to $\frac{1}{3}$ the magnetization of the normal state as $T \rightarrow 0$. Neither of the above could be explained by singlet pairing. Owing to the triplet pairing it is possible to imagine three superfluids corresponding to $\uparrow \uparrow, \downarrow \downarrow$, and triplet $\uparrow \downarrow$ pairs. ³He-A_1 is thought to be in the $\uparrow \uparrow$ (or $\downarrow \downarrow$) state; ³He-A is thought to have a mixture of $\uparrow \uparrow$ and $\downarrow \downarrow$ superfluids; and ³He-B is thought to have all three superfluid components. Thus the extraordinary phases are thought to be a mixture of normal fluid and one or more superfluids weakly coupled by a coherent nuclear dipole–dipole interaction. In this context the best evidence that ³He-A_1 has only one superfluid component is the absence of a parallel resonance (Sec. IX), in a context of the Josephson effect, while the evidence that it is a magnetic superfluid is based on both the perpendicular resonance and the small increase of magnetization (Sec. IX) as the A_1 phase develops. Strong evidence that ³He-A is a mixture of magnetic $\uparrow \uparrow$ and $\downarrow \downarrow$ fluids only is the temperature independence of the static magnetism and its near equality with the normal fluid magnetism (Sec. III). Further evidence is in parallel resonance and ringing and nonlinear phenomena which can be understood in terms of the Josephson effect (Sec. VIII). Then ³He-B contains in addition nonmagnetic $\uparrow \downarrow$ fluid to account for the temperature-dependent magnetism (Sec. III).

3. The phase diagram in zero magnetic field is characterized by a line of Ehrenfest-type second-order transitions T_c in the P–T plane and a line of first-order transitions T_{AB} which intersect the line T_c at a polycritical point PCP (Secs. I and IV). Neither the pressure of the PCP nor the form of the line T_{AB} near the PCP are known at present with certainty (Sec. XI). There may also be a sharp bend in the T_c line near the PCP. In a magnetic field of a few hundred gauss the line T_{AB} does not intersect the line T_c at all, so that ³He-A is interposed between normal liquid and ³He-B at all pressures studied. The effect of a magnetic field on the A and B phases is different since the A phase has a susceptibility nearly equal to that of the normal liquid, while the B phase has a susceptibility which decreases with decreasing T; at first linearly, then flattening out to a value 0.25 to 0.3 of the normal liquid susceptibility as $T \rightarrow 0$. The T_{AB} line and its dependence on field can be

understood rather well near the PCP if the A and B phases have the same T_c, the above magnetic properties, and a difference in specific heat per unit volume given by $C_A(T, P) - C_B(T, P) = \Delta C(P) - \alpha(1 - T/T_c)$, where α is a constant and $\Delta C(P)$ is a quantity which is zero at the PCP, greater than zero above the PCP, and less than zero below the PCP. The specific heat difference at T_c, $\Delta C(P)$, is at most a few percent of the total specific heat of either phase (Sec. IV). These properties are consistent with both A and B phases having the same l-type pairing. They also reflect the fact that while the phases are magnetically quite different they have very similar thermal properties.

4. If ordering in superfluid ³He is by BCS triplet pairs the relative orbital angular momentum of the scattering pairs must be odd. The resultant order parameter would then in general be expected to be orbitally anisotropic, except in certain special cases, among which is the Balian–Werthamer $l = 1$ pairing state, for which $| \mathbf{d}(\hat{\mathbf{k}}) |^2$ is isotropic. Orbital anisotropy may be induced by means of walls, flow, electric fields, and, via dipolar coupling, magnetic fields. What is the evidence for *orbital* isotropy or anisotropy in superfluid ³He? A number of effects in dynamic magnetism, Secs. VIII and III, have been attributed to the effects of walls and flow. At melting pressure in the A phase the apparent orbital axis has been observed to rotate substantially under the action of superfluid flow (heat flow) in fields of a few gauss, and related effects near T_c in essentially zero field are observed at lower pressures. At low fields and at melting pressure the amplitude of the shifted perpendicular resonance line in the A phase decreases with decreasing T, and this has also been interpreted in terms of disorientation of the orbital state. In the B phase profound effects of geometry on the perpendicular resonance are observed, especially at melting pressure and in a cylindrical geometry with field parallel to the cylinder axis. Qualitative changes are also observed in parallel resonance and ringing in ³He-B. There is even one zero field ringing mode known as the "wall-pinned" mode. There is other qualitative evidence for orbital anisotropy in the approximate 30% *increase* of *normal* fluid density at the $B \rightarrow A$ transition at melting pressure, as observed using a vibrating wire (Sec. VI), and the corresponding *increase* of *super*fluid density of 4%–6% at the $B \rightarrow A$ transition for fourth sound in a parallel plate geometry (Sec. XIV). The qualitative difference in the sign of the change might be explained by orbital anisotropy of superfluid or normal fluid density in the A phase if the orbital axis l were oriented perpendicular to the measuring field $\mathbf{H}$ and along the flow direction in the wire experiments and perpendicular to the flow or perpendicular to the plates in the plate experiments. The relative magnitude of the effect is not reconciled, however. Another qualitative indication of orbital anisotropy in the A phase is the linear dependence of effective viscosity on flow velocity in hydrodynamic heat flow (Sec. VII). Thus there is rather good evidence that the fluids are anistropic but the quantitative question of just how anisotropic they are is not settled. One would have thought that in the parallel plate experiments (Sec. XIV), where superfluid flow should be too slow to disorient l, the density would have increased by about 20% if ³He-A were the ABM state and if ³He-B, possibly reflecting the BW state, had an isotropic superfluid density. The small observed change in ρ_s/ρ at the $B \rightarrow A$ transition, though of reasonable sign, suggests either only a modest anisotropy for the A phase if B is

isotropic or a modest change of anisotropy. In this connection the very large value of superfluid density observed at melting pressure in the vibrating wire experients in B just below the $B \rightarrow A$ transition is remarkable. One would have thought that if B were orbitally isotropic then both ρ_s/ρ and η_n could be regarded as scalars and both would have been determined very well by the vibrating wire measurements in the vicinity of the $B \rightarrow A$ transition. But if ³He-B is not to be described by superfluid density and normal viscosity which are scalar quantities then no quantitative conclusion can be reached regarding the orbital anisotropy of the A phase from existing data. The vibrating wire experiments (Sec. VI) taken together with the fourth sound ρ_s/ρ measurements (Sec. XIV) thus open to serious question the flow properties usually assumed for the B phase.

5. The theory of Leggett serves as an underlying base for the understanding of resonance and ringing phenomena. The superfluid states are understood in terms of a triplet pairing with order parameters $d_{\uparrow\uparrow}(\hat{\mathbf{n}})$, $d_{\downarrow\downarrow}(\hat{\mathbf{n}})$, and $d_{\uparrow\downarrow}(\hat{\mathbf{n}})$ which can be related to the three components of an order parameter vector $\mathbf{d}(\hat{\mathbf{n}})$. In Leggett's theory in the superfluid state there is in addition to the usual $\gamma \mathbf{S} \times \mathbf{H}$ torque acting on the spins a coherent temperature-dependent dipolar torque $\mathbf{R}_D$ which depends on the *orientation* of $\mathbf{d}(\hat{\mathbf{n}})$. In equilibrium $\mathbf{R}_D$ is zero, but in a resonance or ringing experiment $\mathbf{d}(\hat{\mathbf{n}})$ precesses about an instantaneous effective field $(\mathbf{H} - \gamma \mathbf{S}/\chi)$. The magnitude and direction of $\mathbf{R}_D$ depend on the angular rotation of $\mathbf{d}(\hat{\mathbf{n}})$ from equilibrium. Both NMR and linear ringing experiments in ³He-A over the full pressure range of measurements suggest that $\mathbf{d}$ has the same direction $\hat{\mathbf{d}}$ for all directions $\hat{\mathbf{n}}$ around the Fermi surface and that $\mathbf{d}(\hat{\mathbf{n}}) \propto \hat{\mathbf{d}}f(\hat{\mathbf{n}})$, where $f(\hat{\mathbf{n}})$ has axial symmetry about $\hat{\mathbf{d}}$ (Sec. VIII). This corresponds to the experimental observation that $\mathbf{R}_D$ has the same magnitude for a given rotation angle θ about some axis perpendicular to $\mathbf{d}$ regardless of the direction of this axis. The ABM state has these properties. Experiments on resonance and linear ringing in ³He-B are largely consistent with a torque $\mathbf{R}_D$ which is maximum for small rotation angles of $\mathbf{d}(\hat{\mathbf{n}})$ about some axis but zero about a perpendicular axis. The BW state has these properties. Brinkman has developed a useful set of equations to describe magnetization dynamics in the BW state in which the variables are an axis $\hat{\omega}$ and an angle of rotation θ about this axis. There is little energy associated with orientation of $\hat{\omega}$, which is determined by fields and boundaries, but the coherent dipolar energy and hence $\mathbf{R}_D$ depend on θ. His equations, which are based on Leggett's, form a useful basis to discuss both normal NMR and linear ringing and very low field ringing in which motion of $\hat{\omega}$ itself is thought to take part (Secs. III and VIII).

Experiments on nonlinear parallel ringing in ³He-A can also be interpreted in terms of a Josephson effect with weakly coupled $\uparrow$ $\uparrow$ and $\downarrow$ $\downarrow$ superfluids. The same experiments should also be exactly analogous to a simple pendulum which is given impulsive blows. There is qualitative but not quantitative agreement (Sec. VIII). Similar experiments in ³He-B should be very useful in determining the dependence of coherent dipolar energy on angle of rotation of $\mathbf{d}(\hat{\mathbf{n}})$, or Brinkman's θ, but definitive work is not yet available.

Parallel NMR and parallel ringing frequencies as well as perpendicular resonance shifts in ³He-A are in very good agreement with one another. The actual frequencies and their pressure dependence are in excellent agreement with a prediction of Leggett which assumed that ³He-A is in the ABM state. The parallel NMR frequency in ³He-B at melting pressure is in excellent agreement with a value predicted for it by Leggett based on the parallel resonance frequency in ³He-A as the ABM state, on the relative susceptibility in the B phase as measured at melting pressure, on the assumption that the average square of the gap is the same in the A and B phases, and on the assumption that ³He-B is in the BW state. However, parallel ringing frequencies in ³He-B very near T_c at the pressure of the PCP and below do not show agreement with theory assuming that ³He-A is in the ABM state and ³He-B is in the BW state (Sec. VIII).

6. Most properties measured to date of the ³He-A_1 phase and the adjacent ³He-A phase in a magnetic field can be understood in terms of a Ginzberg–Landau theory involving order parameters $\Delta_\uparrow$ and $\Delta_\downarrow$ for two interpenetrating $\uparrow$ $\uparrow$ and $\downarrow$ $\downarrow$ superfluids (Sec. IX). In this theory the second-order terms include the magnetic field, and the fourth-order terms include not only a term proportional to $(\Delta_\uparrow{}^4 + \Delta_\downarrow{}^4)$ but also one, $\Delta_\uparrow{}^2\Delta_\downarrow{}^2$, coupling the two fluids and originally proposed on the basis of spin fluctuation theory. The parallel resonance frequency and perpendicular resonance shift can be calculated from Leggett's theory, assuming an axial state for the superfluid, in terms of $\Delta_\uparrow$ and $\Delta_\downarrow$. Measurements at melting pressure of the linear dependence of $T_{c_1} - T_{c_2}$ on field (as well as the relationship between $T_{c_1} - T_c$ and $T_c - T_{c_2}$) and the dependence of parallel and perpendicular resonance frequencies on temperature form a consistent picture. In order to find agreement with experiment all parameters entering into the Ginzberg–Landau theory must be regarded as adjustable; in particular the β parameter [Eq. (9.3)] cannot be set equal to its weak coupling value. The theory also predicts a change of static magnetization on cooling through the ³He-A_1 region, although an additional fluctuation theory seems necessary to deal with the experimental static magnetization results.

7. There is a great deal of evidence for the effects of bounding surfaces, flow, and magnetic fields on the superfluids, particularly for dynamic magnetic measurements in ³He-B. Measurements of ρ_s/ρ by fourth sound in confined (≈ 1 μ) and relatively open (50 μ) geometries show that confined ³He at any pressure (within a range from near melting pressure to at least 13 bar) has very nearly the same ρ_s/ρ as liquid ³He-A at pressures near melting pressure (Sec. XIV). This might suggest that even in bulk experiments solid surfaces are coated with what is effectively high pressure ³He-A. This would explain, via a nucleation theory, experiments at melting pressure (Sec. XI) where *no* superheating of the $B \rightarrow A$ transition is observed while supercooling of the $B \rightarrow A$ transition is common. However, it does not explain the result that super*heating* of the $B \rightarrow A$ transition is the rule in certain experiments at lower pressures. Furthermore there is evidence from dynamic magnetism measurements in the pores of platinum powder (Sec. XIII) that the magnetic properties of confined ³He are not just like those of high pressure liquid ³He-A. We note that a magnetic AB transition is observed for these experiments in the vicinity of the bulk AB transition. No $B \rightarrow A$ transition is observed for fourth sound in the confined geometry (Sec. V), but it is conceivable that a transi-

tion observable magnetically could take place without an appreciable change in ρ_s/ρ. These observations suggest the possibility of surface phases different in some significant way from the bulk phases which nevertheless might modify certain aspects of experiments in bulk by affecting phase nucleation or the interaction of the bulk phases with surfaces. However, we note that T_c does not seem to be affected significantly by confinement in CMN (Sec. XII). Since the coherence length is expected to be 120 Å $(1 - T/T_c)^{-1/2}$ the above modifications to ρ_s/ρ in pores of order 1 μ at $T/T_c \simeq$ 0.1 are even more remarkable.

Dynamic magnetic experiments in ³He-B, particularly of perpendicular resonance, are very geometry sensitive. This follows from Brinkman's equations by noting that when field and $\hat{\omega}$ (or texture) axes are not parallel a large resonance shift is possible. Experiments at melting pressure in a geometry with field parallel to sample cylinder axis are explained quantitatively by the Brinkman, Smith, Osheroff, and Blount theory (Secs. III and VIII). Very large fields, well over 1000 G, are needed to make H_0 and $\hat{\omega}$ essentially parallel over most of the sample. However, in similar experiments on ³He-B at lower pressures ($\approx$ 21 bar) but in a different geometry (field and cylinder axis perpendicular) essential alignment may be achieved in 100 G. The facts are unfortunately not clearly interpretable in the only cases of comparable geometry. In one the critical field separating wall and field orientation of $\hat{\omega}$ at intermediate pressures (below 25 bar) is $\approx$ 1 G in a 3 mm diam tube, while in the other parallel resonance is washed out at melting pressure in a 6 mm tube at $\approx$ 250 G (Sec. VIII). Although the interpretation of the facts is ambiguous and otherwise uncertain this is an important matter, one which can be settled experimentally, relating to the behavior of ³He near surfaces and possibly to the bending energy of the textures.

8. The interrelationship of (χ_B/χ_N) and ρ_s/ρ and the temperature dependences of these quantities are important in regard to the basic microscopic properties of the fluids, the accuracy of "molecular fields" (Secs. III and V) in eliminating certain effects of the Fermi liquid, and the general consistency of the data. Susceptibility data are available at melting pressure and at some lower pressures, especially near the pressure of the PCP (Sec. III). As pressure decreases the ratio $(C_</C_> - 1)_{\mathrm{exptl}}/(C_</C_> - 1)_{\mathrm{weak}}$, quantitatively estimating the effects of strong coupling, is about 1.6 at melting pressure and appears to be approaching approximately one at the PCP (Sec. II). Since the parameter Z_0 (Sec. III) determining the molecular field is nearly pressure independent the reduced susceptibility should decrease with reduced temperature *less* rapidly as pressure decreases below melting pressure. Quite the opposite occurs experimentally as determined in the static measurements.

Near melting pressure the "bare" superfluid relative density ρ_s/ρ in the A phase, that with the effect of molecular fields removed, is linearly dependent on $(1 - T/T_c)$ with coefficient 3.2. If ³He-A is in the ABM state and the experiments measure the perpendicular component of the superfluid density tensor the above coefficient should be 2 (as also for the BW phase). However, the strong coupling factor, preceding paragraph, is 1.6 at melting pressure so the coefficient 3.2 is explained. Further, if $(\rho_s/\rho)_B$ is taken to be 0.94 $(\rho_s/\rho)_A$ as suggested by data of Sec. XIV, then molecular field equations based on ³He-B having one-third

nonmagnetic pairs predict χ_B/χ_N from ρ_s/ρ data for $T/T_c >$ 0.8 extrapolate nicely into the melting pressure data for χ_B/χ_N for $T/T_c < 0.79$. (A very poor comparison is obtained using vibrating wire data, Sec. VI.) Hence, at melting pressure a rather consistent picture emerges, including the apparent validity of the simple molecular field corrections (at least moderately near to T_c), the approximate numerical correctness of the strong coupling effects, and consistency with the microscopic picture of ³He-A as ABM and ³He-B as BW which fits with the dynamic magnetic measurements, Sec. VIII.

In the B phase at pressures below that of the PCP the "bare" superfluid relative density near T_c is proportional to $(1 - T/T_c)$ but with coefficient 3.3–3.6, depending on pressure. Since the strong coupling factor derived both from specific heat data and from the assumption that the B phase is an isotropic state should be close to unity, the above coefficient is too large by a factor 1.7 to 1.8. All specific heat measurements below melting pressure have been made on ³He confined to the pores of CMN powder, however, with pore size comparable to that in the "confined" fourth sound measurements. A major error due to temperature scale seems ruled out from detailed agreement of resonance and ringing data on and off the melting curve. It is even conceivable that $(\rho_s/\rho)_B$ could be larger if 50 μ data are still too confined to give bulk results. A comparison of 50 μ parallel plate ρ_s/ρ data and static χ_B/χ_N data near the PCP via molecular fields, Eqs. (14.5) and (14.6), show that $[(\chi_N - \chi_B)/\chi_N]/(1 - T/T_c)$ as predicted from ρ_s/ρ is about 25% less than that measured (Sec. XIV). This discrepancy has not yet been explained.

9. Transport in the superfluid has been studied in ³He-A_1, ³He-A, and ³He-B at melting pressure using a vibrating wire (Sec. VI) and in ³He-A and ³He-B using heat flow (Sec. VII). All measurements are consistent with a very rapid drop in normal viscosity just below T_c proportional initially to $(1 - T/T_c)^{1/2}$ (Sec. XIV) followed by a temperature-independent viscosity at lower temperatures. Since all the new fluid phases may be anisotropic and the viscosity a tensor quantity probably no experiment has been interpreted correctly. This may explain why the reduced temperature-independent viscosity η_n/η_c appears greater in the heat flow experiments than it does in the wire experiments. Also a substantial increase of viscosity is observed in the wire experiments at the $B \rightarrow A$ transition at melting pressure (Sec. VI) while at lower pressures there is also an increases of viscosity at the $B \rightarrow A$ transition, but only because the A phase effective viscosity depends on flow velocity. There is essentially no change in the limit of zero flow. Critical flow velocities have been observed in both the A and B phases, the critical velocity being much lower in A than in B phase. A somewhat surprising result obtained in analysing heat flow experiments is that apparently the diffusive thermal conductivity in the B phase drops rapidly below T_c. This is qualitative only since the experiments were accounted for entirely by hydrodynamic heat flow. New experiments are required in which hydrodynamic heat flow is suppressed by a confining geometry.

10. Measurements of the propagation of collisionless ultrasound have been made at melting pressure, somewhat below melting pressure in ³He-A, and somewhat below the pressure of the PCP in ³He-B. In both A and B phases the sound velocity decreases from its zero sound value in normal

liquid rather rapidly just below T_c and appears to be approaching the velocity of first sound at lower temperatures. The attenuation below T_c has a part roughly independent of frequency which drops off below T_c and an "excess attenuation" which depends on roughly the square of the frequency. The excess attenuation in the A phase is characterized by a peak very near to T_c and then a long tail extending to lower temperatures while in the B phase it is characterized by a rather narrow peak near T_c and a much smaller low temperature tail. In the A phase the velocity starts to drop at T_c, but in the B phase the velocity stays equal to its zero sound value until the temperature of the peak of attenuation, at which temperature the velocity drops very suddenly. The theory attributes the attenuation both to pair-breaking and to absorption into collective modes of the order parameter. There is rather good agreement between the calculated area under the excess attenuation curve for the ABM state and the measured area for the A phase at 25 MHz. However, at 15 MHz the calculated area under the excess attenuation curve for the BW state is only about a fourth the measured area in the B phase. It is interesting that the areas under the experimental excess attenuation curves at 15 MHz for the A and B phases are comparable.

Near T_c the propagation of ultrasound in the A and B phases is very significantly different, and this should be especially interesting and useful in the vicinity of the PCP.

11. In many parts of this article the differences between the A and B phases have been emphasized. However, from careful measurements of specific heat at melting pressure (Sec. XIV) and from analysis of the phase diagram (Sec. IV) it is apparent that the phases are thermally very similar, heat capacity differences being only a few percent. Also actual measurements of ρ_s/ρ (Sec. XIV) show very little difference between the two phases. The profound effect of a rather small magnetic field on the relative stability of the phases owes itself to their thermal similarity.

Note in proof: Several important new experiments have recently been reported. Osheroff, Engelsberg, Brinkman, and Corruccini (1975) [D. D. Osheroff, S. Engelsberg, W. F. Brinkman, and L. R. Corruccini, Phys. Rev. Lett. **34,** 190 (1975)] have studied the NMR of ³He–B confined at melting pressure between parallel Mylar plates separated by 0.0127 cm and with the magnetic field parallel to the normal to the plates. Narrow lines are observed, unlike what was found (Secs. III and VIII) in an open tube, with frequencies which could be explained by assuming essentially the same parallel resonance frequencies as deduced earlier (Osheroff, 1974) but, at low enough fields, with $\hat{\omega}$ making an angle $\cos^{-1}(1/5)$ with $\mathbf{H}_0$ (and the normal to the plates). Studies of field dependence allowed the quantity H_BR_C (Sec. III) to be determined. The experiments are in excellent agreement with the theory of Brinkman, Smith, Osheroff, and Blount (1974), and extensions thereof, which is based on a model of ³He–B reflecting properties of the BW state.

Three new experiments on propagation of zero sound in superfluid ³He have been reported. Lawson, Bozler, and Lee (1975) [D. T. Lawson, H. M. Bozler, and D. M. Lee, Phys. Rev. Lett. **34,** 121 (1975)] have studied the attenuation of 20 MHz ultrasound near the critical temperatures

at melting pressure as a function of the angle between the propagation direction of the sound and a magnetic field. The attenuation coefficient is anisotropic, showing sharper peaks below T_{c_1} and T_{c_2} for sound direction and field parallel than at 90°. Furthermore, the fluctuations in attenuation (Sec. X) are anisotropic, being largest at 90° and least at 0° and increasing with increasing magnetic field. Roach, Abraham, Kuchnir, and Ketterson (1975) [P. R. Roach, B. M. Abraham, M. Kuchnir, and J. B. Ketterson (1975) preprint, "Sound Propagation in Superfluid ³He near the Polycritical Point"] have studied both velocity and attenuation of 20 MHz ultrasound at low field. They find in ³He–B a discontinuity in velocity in the vicinity of a strong attenuation peak just below T_c, the velocity *decreasing* with increasing temperature both just below and just above the attenuation peak. The location of the peak is in agreement with calculations of Maki (1974a) and Serene (1973) if the strong coupling factor from existing specific heat data (Sec. II) is assumed. They also report a discontinuity in both attenuation and velocity at the AB transition. Roach, Abraham, Roach, and Ketterson (1975) [P. R. Roach, B. M. Abraham, P. D. Roach, and J. B. Ketterson (1975) preprint, "Anisotropy of the Propagation of Sound in the A Phase of Superfluid ³He"] studied the dependence of both attenuation and velocity of 20 MHz ultrasound on the orientation of magnetic fields less than 27 G with respect to the sound propagation direction. No anisotropy effect is seen in the B phase but in the A phase at 26 bar anisotropy was observed and could be studied in detail both in attenuation and velocity. The size of the anisotropy was essentially saturated at 18 G in their 6 mm diam by 6 mm long sound propagation region.

ACKNOWLEDGMENTS

TABLE I. Coordinates (P_c, T_c) of second-order line in zero field (La Jolla).

P (bar)	T_{sound} (mK)	P (bar)	T_{sound} (mK)
9.5	1.9646	22.5	2.4267
10.0	1.9917	23.0	2.4364
10.5	2.0171	23.5	2.4462
11.0	2.0411	24.0	2.4562
11.5	2.0636	24.5	2.4658
12.0	2.0853	25.0	2.4748
12.5	2.1069	25.5	2.4836
13.0	2.1272	26.0	2.4925
13.5	2.1471	26.5	2.5008
14.0	2.1671	27.0	2.5088
14.5	2.1864	27.5	2.5168
15.0	2.2051	28.0	2.5245
15.5	2.2201	28.5	2.5320
16.0	2.2395	29.0	2.5392
16.5	2.2564	29.5	2.5463
17.0	2.2730	30.0	2.5532
17.5	2.2893	30.5	2.5599
18.0	2.3054	31.0	2.5660
18.5	2.3210	31.5	2.5720
19.0	2.3365	32.0	2.5775
19.5	2.3517	32.5	2.5828
20.0	2.3665	33.0	2.5878
20.5	2.3808	33.5	2.5921
21.0	2.3930	34.0	2.5970
21.5	2.4045	34.36	2.6000
22.0	2.4161		

TABLE II. Coordinates of the melting curve of ³He in zero field (Cornell).

$P - P_A$[a] (mbar)	T/T_A[b]	$P - P_A$[a]	T/T_A[b]
0	1.000	36	0.609
5	0.948	38	0.585
10	0.896	40	0.560
15	0.844	42	0.535
20	0.790	44	0.510
25	0.735	46	0.484
30	0.679	48	0.458
32	0.656	50	0.432
34	0.633		

[a] P_A is the pressure of the A feature on the pressurization curve.
[b] T_A is the absolute temperature of the A feature on the pressurization curve.

A. La Jolla

This scale has been described by Wheatley (1973). It is based in part on unpublished noise thermometry measure-

ments of Paulson, Johnson, and Wheatley (1972) of the absolute temperature of the A feature on the pressurization curve in a compressional cooling cell. It is assumed that this feature coincides with the intersection of the (P_c, T_c) second-order line with the melting curve. A temperature of (2.6 ± 0.1) mK was found for this feature, so for purposes of obtaining temperature differences precisely the (P_c, T_c) coordinates at melting pressure were taken to be 34.36 bar, 2.6000 mK.

This temperature scale is based on a provisional determination of the (P_c, T_c) curve from 9.5 bar to melting pressure which was obtained by assuming that in the normal Fermi liquid the attenuation of zero sound is proportional to the square of the absolute temperature (Abrikosov and Khalatnikov, 1957; Abel, Anderson, and Wheatley, 1966b). The scale is in no sense a CMN magnetic temperature scale. If the temperature of the A feature is different from 2.6000 mK then the whole scale would then be multiplied by a constant factor equal to $(T_A/2.6000 \text{ mK})$. In Table I we give the coordinates (P_c, T_c) currently in use in La Jolla.

B. Cornell melting pressure scale

This scale, based on work by Halperin, Rasmussen, Archie, and Richardson (1974b) has not yet been described in detail. However, one can surmise from a paper by Halperin, Archie, Rasmussen, Buhrman, and Richardson (1974a) that it is based on Clapeyron's equation in the form

$$T(dP/dT) = L/\Delta V, \tag{A1}$$

where T is absolute temperature, P is pressure, L is the latent heat of transformation from liquid to solid ³He and ΔV is the corresponding change of volume. In their work $T(dP/dT)$ is measured along the melting curve by introducing a known amount of heat L and measuring the volume change ΔV needed to maintain the pressure and hence the temperature strictly constant. The ratio of T to that for the A feature, for example, is then found by numerical

O. V. Lounasmaa, and Professor R. C. Richardson. More recently I have had useful discussions of some of this material with Dr. Osheroff at Bell and with the Cornell group, including Professor R. C. Richardson, Professor H. Hall, Professor J. Reppy, Dr. R. Combescot, Professor V. Ambegaokar, and Professor J. Wilkins.

My appreciation for the theoretical aspects of ³He has been increased by a number of theorists. Professor B. Patton introduced me to many important concepts. Professor K. Maki has contributed to my understanding of dynamic magnetic effects and of ultrasound, and I have had a very useful interaction with Professor J. Serene on propagation of ultrasound. Dr. W. F. Brinkman patiently explained several features of dynamic magnetism to me and corrected a mistaken concept of mine in perpendicular ringing.

Finally, I wish to express my appreciation to Tony Leggett, who not only has greatly aided my theoretical understanding of ³He and my appreciation of the experiments but also has read various versions of this manuscript and made helpful suggestions for its improvement.

APPENDIX A. TEMPERATURE SCALES

An absolute temperature scale is essential to progress in the temperature region of the experiments described in this paper. Without such a scale it is not possible to compare experiments done in different laboratories or indeed within the same laboratory on different occasions. Comparison with theoretical concepts and calculations is likewise not possible, on a quantitative basis, without such a scale. In this appendix we present scales in current use.

TABLE III. Experimental parameters for normal Fermi liquid ³He as $T \to 0$.

	P(bar)												
	0	3	6	9	12	15	18	21	24	27	30	33	34.36
V/n (cm³/mole)	36.84	33.87	32.07	30.76	29.71	28.86	28.13	27.56	27.06	26.58	26.14	25.71	25.54
C/nRT (K⁻¹)	3.00	3.22	3.43	3.61	3.78	3.95	4.10	4.24	4.37	4.51	4.64	4.78	4.85
c_1 (m/sec)	182.9	227.5	259.7	285.9	308.0	327.1	345.0	360.5	375.1	389.3	403.0	415.9	421.7
T^* (K)	0.359	0.305	0.277	0.256	0.238	0.224	0.212	0.205	0.198	0.191	0.185	0.179	0.177
ηT^2 (poise mK²)	1.834	1.73	1.63	1.54	1.46	1.38	1.30	1.22	1.14	1.06	0.99	0.92	0.88
κT (erg/sec cm)	34.8	29.7	25.8	22.7	20.3	18.4	16.7	15.3	14.0	12.9	11.9	11.0	10.7

TABLE IV. Formulas for the computation of derived Fermi liquid parameters.

$$m = 5.009 \times 10^{-24}\text{g} \qquad \rho = \frac{3.016\,\text{g/mole}}{(V/n)} \qquad \gamma = 2.0378 \times 10^4 \text{ (gauss sec)}^{-1}$$

$$2N(0) = \frac{(C/nRT)}{k(\pi^2/3)(V/N)} = \frac{(C/nRT)}{7.5421\,(V/n) \times 10^{-40} \text{ (erg/K) mole}}$$

$$p_F = h\left(\frac{3}{8\pi}\frac{N}{V}\right)^{1/3} = 2.7551 \times 10^{-19} \frac{\text{g cm}}{\text{sec}}\left(\frac{1 \text{ cm}^3}{\text{mole}}\right)^{1/3} (V/n)^{-1/3}$$

$$\frac{m^*}{m} = \frac{h^3}{8\pi m}\frac{2N(0)}{p_F} = 2.3110 \times 10^{-57} \frac{2N(0)}{p_F} \frac{\text{erg}^3 \text{ sec}^3}{\text{g}}$$

$$v_F = \frac{p_F}{(m^*/m)\,m} = \frac{p_F}{(m^*/m)} \frac{1}{5.009 \times 10^{-24}\text{g}}$$

$$F_0 = \frac{3m^2 c_1^2}{p_F^2}\frac{m^*}{m} - 1 = \left[7.5270 \times 10^{-47} \text{ g}^2 \frac{c_1^2}{p_F^2}\left(\frac{m^*}{m}\right)\right] - 1$$

$$F_1 = 3\left(\frac{m^*}{m} - 1\right)$$

$$Z_0 = 4\left[\frac{3kT^*(m^*/m)\,m}{p_F^2} - 1\right] = 4\left[2.0746 \times 10^{-39}\frac{\text{erg g}}{K}\frac{T^*(m^*/m)}{p_F^2} - 1\right]$$

$$\tau_\eta T^2 = \frac{\eta T^2}{(1/5)\rho v_F^2 (m^*/m)} = \frac{(\eta T^2)(V/n)}{0.6032 \text{ (g/mole) } v_F^2 (m^*/m)}$$

$$\tau_\kappa T^2 = \frac{\kappa T}{\frac{1}{3}(C_V/T)v_F^2} = \frac{(\kappa T)(V/n)}{\frac{1}{3}R(C/nRT)v_F^2} = \frac{(\kappa T)(V/n)}{2.7714 \times 10^7 \text{ (erg/mole K) } (C/nRT)v_F^2}$$

$$\chi_N = \frac{1.362 \times 10^{-8}\,K}{T^*}\frac{37.0 \text{ cm}^3/\text{mole}}{(V/n)}$$

TABLE V. Derived quantities for the normal Fermi liquid.

	P(bar)												
	0	3	6	9	12	15	18	21	24	27	30	33	34.36
$2N(0)$ [10^{38}(erg cm³)⁻¹]	1.08	1.26	1.42	1.56	1.69	1.82	1.93	2.04	2.14	2.25	2.35	2.46	2.52
$p_F(10^{-20}$ g cm/sec)	8.28	8.52	8.67	8.79	8.89	8.98	9.06	9.12	9.18	9.23	9.28	9.34	9.36
$v_F(10^3$ cm/sec)	5.48	4.97	4.58	4.29	4.05	3.84	3.67	3.52	3.40	3.27	3.16	3.05	3.00
m^*/m	3.01	3.42	3.78	4.09	4.38	4.67	4.93	5.17	5.39	5.63	5.86	6.10	6.22
F_0	10.07	17.39	24.51	31.55	38.58	45.62	52.83	59.78	66.81	74.38	82.13	90.17	94.13
F_1	6.04	7.27	8.34	9.27	10.15	11.01	11.79	12.51	13.18	13.90	14.58	15.31	15.66
Z_0	−2.69	−2.80	−2.84	−2.88	−2.90	−2.92	−2.94	−2.94	−2.95	−2.95	−2.95	−2.96	−2.95
$\tau_\eta T^2$ (10^{-6} sec mK²)	1.24	1.15	1.09	1.04	1.00	0.96	0.91	0.87	0.82	0.78	0.73	0.69	0.66
$\tau_\kappa T^2$ (10^{-6} sec mK²)	0.51	0.46	0.41	0.38	0.35	0.33	0.31	0.29	0.27	0.26	0.24	0.23	0.22
χ_N (10^{-8})	3.81	4.88	5.67	6.38	7.09	7.75	8.38	8.92	9.42	9.91	10.42	10.93	11.17

TABLE VI. Useful parameters for ³He.

						P(bar)							
	0	3	6	9	12	15	18	21	24	27	30	33	34.36[d]
$a \equiv (V/N)^{1/3}$ (Å)[a]	3.94	3.83	3.76	3.71	3.67	3.63	3.60	3.58	3.56	3.53	3.51	3.50	3.49
$\dfrac{g_D{}'}{k_B} \equiv \dfrac{2\pi\gamma^2\hbar^2}{3a^3 k_B}$ $(10^{-7}$ K$)$[b]	1.145	1.246	1.316	1.372	1.420	1.462	1.500	1.531	1.559	1.587	1.614	1.641	1.652
$T_{F_{\text{eff}}} \equiv \dfrac{3}{4}\dfrac{(N/V)}{N(0)k_B}$ (K)[c]	1.64	1.53	1.44	1.36	1.30	1.25	1.21	1.16	1.13	1.09	1.07	1.03	1.02

[a] The quantity a is an average atomic spacing.
[b] $g_D{}'/k_B$ is an average dipolar coupling energy per atom.
[c] $T_{F_{\text{eff}}}$ is an effective Fermi temperature.
[d] Melting pressure.

ⁱntegration to be

$$\frac{T}{T_A} = \exp\left[\int_{P_A}^{P}\left(T\frac{dP}{dT}\right)^{-1} dP\right]. \tag{A2}$$

They find that the reduced temperature difference from T_A is then given by

$$\frac{T_A - T}{T_A} = 1.00 \times 10^{-2}\left(\frac{P - P_A}{1 \text{ mbar}}\right)$$

$$+\, 2.1 \times 10^{-5}\left(\frac{P - P_A}{1 \text{ mbar}}\right)^2. \tag{A3}$$

This equation gives values of T/T_A deviating from the experimental points by less than half a percent for $(P - P_A) < 35$ mbar. In Table II we give values of T/T_A as a function of $(P - P_A)$ kindly supplied by Richardson (private communication). According to the Cornell data, also kindly provided by Richardson, one has $T_A = (2.75 \pm 0.11)$ mK; $T_{B'} = (2.18 \pm 0.09)$ mK; and the critical temperature of the solid transition is (1.10 ± 0.05) mK. The pressure difference $P_{B'} - P_A$ is 20.04 mbar for zero external field according to Osheroff's measurements (private communication) and 19.90 mbar according to Halperin's measurements (private communication to Osheroff). If we take $T_A = 2.6000$ mK as assumed in the La Jolla scale then for the average of these measurements we find, using Eq. (A3), that $T_{B'} = 2.059$ mK in zero field.

Evidently the temperature of the A feature has some uncertainty, although the La Jolla and Cornell measurements do agree within their stated errors. In view of this uncertainty it is probably desirable to continue representing data on the superfluid in terms of a reduced temperature.

APPENDIX B. PROPERTIES OF THE NORMAL FERMI LIQUID

In this appendix we give provisional properties of the normal Fermi liquid in the vicinity of $T = 0$. Smoothed and interpolated values of the principal experimental parameters as a function of pressure are given in Table III. Formulas for the computation of derived properties are given in Table IV, and the corresponding derived quantities

are given in Table V. Some other useful parameters for liquid ³He are given in Table VI.

For molar volumes we have used the tabulation of Wheatley (1966) and the measurements of Grilly (1971). The most doubtful quantity at intermediate pressures is the limiting value of (C/nRT), which is based on the measurements of Abel, Anderson, Black, and Wheatley (1966) at 0.28 and 27 atm and the higher temperature data at intermediate pressures of Anderson, Reese, and Wheatley (1963). New measurements over the full pressure range are badly needed. In this connection we note that recent specific heat measurements at melting pressure made at Cornell (private communication from R. C. Richardson) suggest that the 27 atm measurements of Abel et al. above may be high by about 10%. Although we can find no reason at present to doubt the accuracy of the measurements of Abel et al. which were thought to be much better than 10%, this difference should be taken into account in using the Fermi liquid properties given in Tables III and V. For the velocity of first sound we have used the recent unpublished low temperature measurements of Paulson, Johnson, and Wheatley (1973), early low temperature velocity measurements of Abel, Anderson, and Wheatley (1961), and more recent measurements of Abraham, Chung, Eckstein, Ketterson, and Roach (1972). For the magnetic temperature T^* we have used the limiting value as $T \to 0$ of C/χ, where C is the Curie constant and χ the susceptibility, as given by Ramm, Pedroni, Thompson, and Meyer (1970). The limiting $T \to 0$ values of ηT^2 were obtained from low pressure (Bertinat, Betts, Brewer, and Butterworth, 1974) and melting pressure (Alvesalo et al., 1974a,b) wire damping measurements and from the ultrasonic attenuation measurements of Paulson, Johnson, and Wheatley (1974, unpublished) with heavy weight placed on the wire damping measurements. The limiting $T \to 0$ values of κT are based on the zero pressure measurement of Abel, Johnson, Wheatley, and Zimmermann (1967) and the measurements of thermal resistance ratios under pressure of Greytak, Johnson, Paulson, and Wheatley (1973, unpublished). Significant parts of the tables are based on tabulations worked out by Paulson (1974). Derivation of Fermi liquid parameters from experimental data is discussed by Wheatley (1966). The accuracy of derived parameters is not indicated. Corruccini, Osheroff, Lee, and Richardson (1972) measured Z_1 at 0 pressure and at 27 bar. At these two pressures they found Z_1 to be, respectively, -0.6 ± 1.2 and $+0.8 \pm 2.4$.

REFERENCES

Abel, W. R., A. C. Anderson, and J. C. Wheatley, 1961, Phys. Rev. Lett. **7**, 299.

——, A. C. Anderson, W. C. Black, and J. C. Wheatley, 1965, Physics (Long Island City, L.I.) **1**, 337.

——, A. C. Anderson, W. C. Black, and J. C. Wheatley, 1966a, Phys. Rev. **147**, 111.

——, A. C. Anderson, and J. C. Wheatley, 1966b, Phys. Rev. Lett. **17**, 74.

——, R. T. Johnson, J. C. Wheatley, and W. Zimmermann, 1967, Phys. Rev. Lett. **18**, 737.

Abraham, B. M., D. Chung, Y. Eckstein, J. B. Ketterson, and P. R. Roach, 1972, J. Low Temp. Phys. **6**, 521.

Abrikosov, A. A., and I. M. Khalatnikov, 1957, Zh. Eksp. Teor. Fiz. **33**, 110 [Sov. Phys.—JETP **6**, 84 (1958)].

Ahonen, A. I., M. T. Haikala, and M. Krusius, 1974a, Phys. Lett. **47A**, 215.

——, M. T. Haikala, M. Krusius, and O. V. Lounasmaa, 1974b, Phys. Rev. Lett. **33**, 628.

——, M. T. Haikala, M. Krusius, and O. V. Lounasmaa, 1974c, Phys. Rev. Lett. **33**, 1595.

Alvesalo, T. A., Yu. D. Anufriyev, H. K. Collan, O. V. Lounasmaa, and P. Wennerström, 1973, Phys. Rev. Lett. **30**, 962.

——, H. K. Collan, M. T. Loponen, and M. C. Veuro, 1974a, Phys. Rev. Lett. **32**, 981.

——, H. K. Collan, M. T. Loponen, O. V. Lounasmaa, and M. C. Veuro, 1974b, J. Low Temp. Phys. (to be published).

Ambegaokar, V., and N. D. Mermin, 1973, Phys. Rev. Lett. **30**, 81.

——, P. G. De Gennes, and D. Rainer, 1974, Phys. Rev. A **9**, 2676.

Anderson, A. C., W. Reese, and J. C. Wheatley, 1963, Phys. Rev. **130**, 495.

Anderson, P. W., 1973, Phys. Rev. Lett. **30**, 368.

——, and P. Morel, 1961, Phys. Rev. **123**, 1911.

——, and W. F. Brinkman, 1973, Phys. Rev. Lett. **30**, 1108.

Anufriyev, Yu, 1965, Zh. Eksp. Teor. Fiz. Pis'ma Red. **1**,1 [Sov. Phys.—JETP Lett. **1**, 155].

——, T. A. Alvesalo, H. K. Collan, N. T. Opheim, and P. Wennerström, 1973, Phys. Lett. **43A**, 175.

Avenel, O., P. M. Berglund, R. G. Gylling, N. E. Phillips, A. Vetleseter, and M. Vuorio, 1973, Phys. Rev. Lett. **31**, 76.

Balian, R., and N. R. Werthamer, 1963, Phys. Rev. **131**, 1553.

Bardeen, J., L. N. Cooper, and J. R. Schrieffer, 1957, Phys. Rev. **108**, 1175.

Barter, C., R. G. Meisenheimer, and D. P. Stevenson, 1960, J. Chem. Phys. **64**, 1312.

Bertinat, M. P., D. S. Betts, D. F. Brewer, and G. J. Butterworth, 1974, J. Low Temp. Phys. **16**, 479.

Bishop, J. H., A. C. Mota, and J. C. Wheatley, 1972, in *Low Temperature Physics-LT 13*, Vol. 1, edited by K. D. Timmerhaus, W. J. O'Sullivan and E. F. Hammel (Plenum, New York, 1974), p. 406.

Black, M. A., H. E. Hall, and K. Thompson, 1971, J. Phys. C (Proc. Phys. Soc. Lond.) **4**, 129.

Bozler, H. M., M. E. R. Bernier, W. J. Gully, R. C. Richardson, and D. M. Lee, 1974, Phys. Rev. Lett. **32**, 875.

Brewer, D. F., and D. O. Edwards, 1961, Phil. Mag. **6**, 775.

Brinkman, W. F., Phys. Lett. **49A**, 411.

——, and P. W. Anderson, 1973, Phys. Rev. A **8**, 2732.

——, H. Smith, D. D. Osheroff, and E. I. Blount, 1974, Phys. Rev. Lett. **33**, 624.

——, J. Serene, and P. W. Anderson, 1974, Phys. Rev. A **10**, 2386.

Brueckner, K. A., T. Soda, P. W. Anderson, and P. Morel, 1960, Phys. Rev. **118**, 1442.

Bukshpan, I., Y. Eckstein, and J. Landau, 1973, Phys. Rev. A **8**, 3093.

Combescot, R., 1974, "On the Superfluid Density in ³He," preprint.

——, and H. Ebisawa, 1974, Phys. Rev. Lett. **33**, 810 (1974).

Czerwonko, J., 1967, Acta Phys. Pol. **32**, 335.

Corruccini, L. R., D. D. Osheroff, D. M. Lee, and R. C. Richardson, 1972, J. Low Temp. Phys. **8**, 227.

De Gennes, P. G., 1973, Phys. Lett. **44A**, 271.

——, 1974, *Physics of Liquid Crystals* (Oxford, London).

——, and D. Rainer, 1974, Phys. Lett. **46A**, 429.

Dorfman, Ya. G., 1965, *Diamagnetism and the Chemical Bond* (American Elsevier, New York), p. 33.

Dundon, J. M., D. L. Stolfa, and J. M. Goodkind, 1973, Phys. Rev. Lett. **30**, 843.

Ebisawa, H., and K. Maki, 1974, Prog. Theor. Phys. **51**, 337.

Emery, V. J., and A. M. Sessler, 1960, Phys. Rev. **119**, 43.

Engelsberg, S., W. F. Brinkman, and P. W. Anderson, 1974, Phys. Rev. A **9**, 2592.

Giffard, R. P., R. A. Webb, and J. C. Wheatley, 1971, J. Low Temp. Phys. **6**, 533.

Gorter, C. J., and J. H. Mellink, 1949, Physica **15**, 285.

Greytak, T. J., R. T. Johnson, D. N. Paulson, and J. C. Wheatley, 1973, Phys. Rev. Lett. **31**, 452.

Grilly, E. R., 1971, J. Low Temp. Phys. **4**, 615.

Gully, W. J., D. D. Osheroff, D. T. Lawson, R. C. Richardson, and D. M. Lee, 1973, Phys. Rev. A **8**, 1633.

Hall, H. E., C. Kiewiet, and J. D. Reppy, 1974, unpublished.

Halperin, W. P., 1974, thesis, Cornell University, unpublished.

——, R. A. Buhrman, D. M. Lee, and R. C. Richardson, 1973a, Phys. Lett. **45A**, 233.

——, R. A. Buhrman, and R. C. Richardson, 1973b, Bull. Am. Phys. Soc. **18**, 642.

——, C. N. Archie, F. B. Rasmussen, R. A. Buhrman, and R. C. Richardson, 1974a, Phys. Rev. Lett. **32**, 927.

——, F. Rasmussen, C. N. Archie, and R. C. Richardson, 1974b, unpublished.

Johnson, R. T., R. Rosenbaum, O. G. Symko, and J. C. Wheatley, 1969, Phys. Rev. Lett. **22**, 449.

——, D. N. Paulson, C. B. Pierce, and J. C. Wheatley, 1973, Phys. Rev. Lett. **30**, 207.

——, R. L. Kleinberg, R. A. Webb, and J. C. Wheatley, 1974, J. Low Temp. Phys. **18**, 501.

Kleinberg, R. L., D. N. Paulson, R. A. Webb, and J. C. Wheatley, 1974, J. Low Temp. Phys. **17**, 521 (1974).

Kojima, H., D. N. Paulson, and J. C. Wheatley, 1974, Phys. Rev. Lett. **32**, 141.

——, D. N. Paulson, and J. C. Wheatley, 1975, unpublished.

Kriss, M., and I. Rudnick, 1973, J. Low Temp. Phys. **3**, 339.

Landau, L. D., 1956, Zh. Eksp. Teor. Fiz. **30**, 1058 [Sov. Phys.—JETP **3**, 920 (1957)].

——, 1957, Zh. Eksp. Teor. Fiz. **32**, 59 [Sov. Phys.—JETP **5**, 101 (1957)].

Lawson, D. T., W. J. Gully, S. Goldstein, R. C. Richardson, and D. M. Lee, 1973, Phys. Rev. Lett. **30**, 541.

——, W. J. Gully, S. Goldstein, R. C. Richardson, and D. M. Lee, 1974, J. Low Temp. Phys. **15**, 169.

Leggett, A. J., 1965, Phys. Rev. A **140**, 1869.

——, 1972, Phys. Rev. Lett. **29**, 1227.

——, 1973, Phys. Rev. Lett. **31**, 352.

——, 1974a, Ann. Phys. **85**, 11.

——, 1974b, Prog. Theor. Phys. **51**, 1275.

——, and M. Vuorio, 1970, J. Low Temp. Phys. **3**, 359.

London, F., and P. R. Zilsel, 1948, Phys. Rev. **74**, 1148.

Lounasmaa, O. V., 1974, Contemp, Phys. **15**, 353.

Maki, K., 1974a, J. Low Temp. Phys. **16**, 465.

——, 1974b, "General Gauge Invariance and Spin Waves in the B Phase of Superfluid ³He," preprint.

——, 1974c, "Longitudinal Resonance in the B phase of Superfluid ³He," preprint.

——, and T. Tsuneto, 1974, Prog. Theo. Phys. **52**, 773.

——, and T. Tsuneto, 1975, Phys. Rev. **B1** (in press).

——, and C.-R. Hu, 1975, J. Low Temp. Phys. **18**, 337.

——, and H. Ebisawa, 1975, "Dynamic Susceptibility in the A phase of Superfluid ³He in Hydrodynamic Regime," submitted to Phys. Rev.

Mills, D. L., and M. T. Beal-Monod, 1974, Phys. Rev. A **10**, 2473.

Osgood, E. B., and J. M. Goodkind, 1967, Phys. Rev. Lett. **18**, 894.

Osheroff, D. D., 1973, thesis, Cornell University, unpublished.

——, 1974, Phys. Rev. Lett. **33**, 1009.

——, R. C. Richardson, and D. M. Lee, 1972a, Phys. Rev. Lett. **28**, 885.

——, W. J. Gully, R. C. Richardson, and D. M. Lee, 1972b, Phys. Rev. Lett. **29**, 920.

——, and W. F. Brinkman, 1974, Phys. Rev. Lett. **32**, 584.

——, and P. W. Anderson, 1974, Phys. Rev. Lett. **33**, 686.

Patton, B. R., 1974, Phys. Lett. **47A**, 459.

Paulson, D. N., 1974, thesis, University of California (San Diego), unpublished.

——, R. T. Johnson, and J. C. Wheatley, 1973a, Phys. Rev. Lett. **30**, 829.

——, R. T. Johnson, and J. C. Wheatley, 1973b, Phys. Rev. Lett. **31**, 746.

——, H. Kojima, and J. C. Wheatley, 1974a, Phys. Rev. Lett. **32**, 1098.

——, H. Kojima, and J. C. Wheatley, 1974b, Phys. Lett. **47A**, 457.

Peshkov, V. P., 1964, Zh. Eksp. Teor. Fiz. **46**, 1510 [Sov. Phys.—JETP **19**, 1023 (1964)].

Pitaevskii, L. P., 1959, Zh. Eksp. Teor. Fiz. **37**, 1794 [Sov. Phys.—JETP **10**, 1267 (1960)].

Pomeranchuk, I., 1950, Zh. Eksp. Teor. Fiz. **20**, 919.

Ramm, H., P. Pedroni, J. R. Thompson, and H. Meyer, 1970, J. Low Temp. Phys. **2**, 539.

Saslow, W. M., 1973, Phys. Rev. Lett. **31**, 870.

Serene, J., 1973, thesis, Cornell University, unpublished.

Shapiro, K. A., and I. Rudnick, 1965, Phys. Rev. A **137**, 1385.

Shumeiko, V. S., 1972, Zh. Eksp. Teor. Fiz. **63**, 621. [Sov. Phys.—JETP **36**, 330 (1973)].

Sites, J. R., D. D. Osheroff, R. C. Richardson, and D. M. Lee, 1969, Phys. Rev. Lett. **23**, 836.

Soda, T., and K. Fujiki, 1974, Prog. Theo. Phys. **52**, 1405.

Stokes, G. G., 1922, *Mathematical and Physical Papers* (Cambridge University, London) Vol. III, p. 38.

Straty, G. C., and E. D. Adams, 1969, Rev. Sci. Instrum. **40**, 1393.

Takagi, S., 1974a, Prog. Theo. Phys. **51**, 1998.

——, 1974b, "On the NMR Near the ^{3}He–A-Normal Transition," preprint.

Thouless, D. J., 1960, Ann. Phys. **10**, 553.

Vuorio, M., 1974, J. Phys. C. (Solid State Physics) **7**, L5.

Vvedenskii, V. L., 1972, Zh. Eksp. Teor. Fiz. **16**, 358 [Sov. Phys.—JETP Lett. **16**, 254 (1972)].

Webb, R. A., R. P. Giffard, and J. C. Wheatley, 1973a, J. Low Temp. Phys. **13**, 383.

——, T. J. Greytak, R. T. Johnson, and J. C. Wheatley, 1973b, Phys. Rev. Lett. **30**, 210.

——, R. L. Kleinberg, and J. C. Wheatley, 1974a, Phys. Rev. Lett. **33**, 145.

——, R. L. Kleinberg, and J. C. Wheatley, 1974b, Phys. Lett. **48A**, 421.

Wheatley, J. C., 1966, in *Quantum Fluids*, edited by D. F. Brewer, (North-Holland, Amsterdam), p. 183.

——, 1968, Phys. Rev. **165**, 304.

——, 1973, Physica **69**, 218.

Wolfle, P., 1973, Phys. Rev. Lett. **30**, 1169.

Yanof, A. W., and J. D. Reppy, 1974, Phys. Rev. Lett. **33**, 631, and 1030 (Erratum).

——, E. Smith, D. M. Lee, R. C. Richardson, and J. D. Reppy, 1974, Bull. Am. Phys. Soc. **19**, 435.